Nonequilibrium mode-coupling theory for uniformly sheared underdamped systems

Koshiro Suzuki*
Analysis Technology Development Center, Canon Inc., 30-2 Shimomaruko 3-chome, Ohta-ku, Tokyo 146-8501, Japan

Hisao Hayakawa
Yukawa Institute for Theoretical Physics, Kyoto University, Kitashirakawa Oiwake-cho, Kyoto 606-8502, Japan
(Received 27 April 2012; revised manuscript received 13 December 2012; published 4 January 2013)

Nonequilibrium mode-coupling theory (MCT) for uniformly sheared underdamped systems is developed, starting from the microscopic thermostated Sllod equation and the corresponding Liouville equation. Special attention is paid to the translational invariance in the sheared frame, which requires an appropriate definition of the transient time correlators. The derived MCT equation satisfies the alignment of the wave vectors and is manifestly translationally invariant. Isothermal condition is implemented by the introduction of current fluctuation in the dissipative coupling to the thermostat. This current fluctuation grows in the α relaxation regime, which generates a pronounced relaxation of the yield stress compared to the overdamped case. This result fills the gap between the molecular dynamics simulation and the overdamped MCT reported previously. The response to a perturbation of the shear rate demonstrates an inertia effect which is not observed in the overdamped case. Our theory turns out to be a nontrivial extension of the theory by Fuchs and Cates [J. Rheol. **53**, 957 (2009)] to underdamped systems. Since our starting point is identical to that of Chong and Kim [Phys. Rev. E **79**, 021203 (2009)], the contradictions between Fuchs-Cates and Chong-Kim are resolved.

DOI: 10.1103/PhysRevE.87.012304 PACS number(s): 64.70.P−, 61.20.Lc, 83.50.Ax, 83.60.Fg

I. INTRODUCTION

Liquids under shear are attracting continuous interest, not only because of the importance of their application to industry, but also because of their significance to the study of nonequilibrium statistical physics as ideal but experimentally accessible systems. Among them, special attention has been paid to dense supercooled liquids in the vicinity of the glass transition, i.e., glassy materials, due to the difficulty of understanding them and their peculiarity compared with conventional systems which exhibit thermodynamic phase transitions.

Although not yet perfect, the mode-coupling theory (MCT) presents remarkable success in its application to glassy materials such as colloidal suspensions [1–3]. Probably the most striking feature of the MCT is that it predicts a two-step relaxation phenomenon (β relaxation followed by α relaxation) [4,5] of the intermediate scattering function (i.e., density time correlator) in the vicinity of a critical packing fraction φ_c, which is referred to as the "MCT transition point." This two-step relaxation is thoroughly investigated, and it is established that the MCT is able to explain, e.g., the following properties: (i) the square-root cusp anomaly of the temperature dependence of the plateau height of the density time correlator (called the nonergodic parameter; NEP) [6], (ii) the power-law time dependence with von Schweidler exponents of the density time correlator around the β relaxation [7–9], and (iii) the time-temperature superposition principle realized by the Kohlrausch-Williams-Watts-type behavior of the density time correlator at the α relaxation [10]. On the other hand, the MCT is marred with the problem that the NEP can survive for temperatures below the critical temperature T_c, while it decays to zero in actual glassy states [4,11]. Moreover, φ_c is about 10% smaller than the experimental value. To overcome these difficulties, successive studies beyond the conventional MCT have been carried out eagerly as well, e.g., (i) field-theoretic formulations [12–16], (ii) inclusion of higher-order correlations [17–19], and (iii) estimation of the dynamic correlation length [20].

The framework of the MCT itself is generic, and extensions to other materials such as dense granular materials [21–23] have also been attempted. In particular, the MCT is able to incorporate the effect of shear and its resulting demolition of the "cage effect."

The introduction of shear into the MCT has been worked out in the pioneering papers by Fuchs and Cates (FC) [24] and Miyazaki and Reichman [25], both of which have been formulated for sheared systems immersed in solvents, such as colloidal suspensions. The weak point of the approach in Ref. [25], which was followed by Ref. [21], has been pointed out by Chong and Kim (CK) [26]. They argued that the approach of Refs. [21,25], where the *steady-state* structure factor (or, equivalently, the radial distribution function) is plugged in as an input, and then the steady-state shear stress is calculated as an output, is inconsistent, since they should be treated on the same footing. Rather, the *equilibrium* structure factor should be plugged in as an input, which is the case for Ref. [24]. (This scheme [27] is referred to as "integration through transient" (ITT) (Ref. [28].)

In this spirit, CK [26] have constructed the MCT for a sheared system associated with a thermostat, where the Sllod equation [27,29] is chosen as a microscopic starting point. In contrast to the theory of FC [24,28,30], where a Brownian system governed by the Smoluchowski operator is the starting point, the Sllod equation is governed by the Liouville operator (Liouvillian), and the momentum variables are left unintegrated, i.e., it is an *underdamped* system.

Besides this issue, apparent discrepancies between the resulting equations of CK [26] and FC [24,28,30] have been

*suzuki.koshiro@canon.co.jp

noticed. For instance, the "initial decay rate" of the Debye relaxation, which exhibits the conventional Taylor dispersion, is time dependent in FC [24,28,30], while it is not in CK [26]. Probably the most notable difference is that there appears an additional memory kernel in CK [26], in addition to the conventional one which also appears commonly in other MCTs. As is well known, and is also argued in CK [26], these discrepancies cannot be the result of the difference between underdamped and overdamped systems, since they exhibit quite similar behavior for long-time dynamics, at least for the density time correlator [31–33]. These contradictions were apparent, at least at the formal level, but as far as we know, no reconciliation has been proposed so far.

In this paper, we reformulate the MCT for uniformly sheared *underdamped* systems and resolve the contradictions mentioned above. We point out that the definition of the time correlators of CK [26] should be modified to satisfy the translational invariance in the sheared frame and fulfill the requirement of physical correlations between the Fourier modes of the fluctuations. This modification leads to complexities, which are absent in the formulation of CK [26], due to the noncommutativity and the non-Hermiticity of the Liouvillians. The path which handles these complexities closely follows that of FC [30], which we believe to be the most sensible so far [34].

The crucial difference between our formulation and CK's is the introduction of the isothermal condition, which is implemented at the level of the Mori-type equations. This is realized by incorporating current fluctuations into the dissipative coupling to the thermostat, accompanied by the introduction of a multiplier. The resulting equation for the time correlators formally corresponds to that of FC [30] in the overdamped limit, but the effect of the inertia or the fluctuating coupling to the thermostat renders this correspondence to be highly nontrivial. In fact, the growth of the fluctuating coupling in the α-relaxation regime generates a pronounced relaxation of the yield stress compared to the overdamped case. This result fills the gap between the molecular dynamics (MD) simulation and the overdamped MCT reported previously [35]. Hence, our framework appears to be a nontrivial extension of FC [30] to underdamped systems. The significance of the underdamped formulation is also demonstrated by its application to the calculation of the response to a perturbation of the shear rate, where the inertia effect is clearly observed.

The paper is organized as follows. In Sec. II, we briefly review the microscopic starting points. In Sec. III, special attention is paid to the translational invariance in the sheared frame and the physically sensible definition of the time correlators. Adjoint Liouvillians are introduced, which turns out to be natural in the treatment of sheared systems. In Sec. IV, Mori-type equations are derived by the application of the projection operator formalism, first without the isothermal condition. After that, the isothermal condition is formulated, and the Mori-type equation where this condition is implemented is derived. In Sec. V, the mode-coupling approximation is worked out, and a closed equation for the time correlators (MCT equation) is derived. In Sec. VI, a general formula of time correlators for steady-state quantities is presented, and specific forms of the dissipative coupling and the multiplier are discussed. A formula for the steady-state shear stress in this formulation is derived. In Sec. VII, the result of the numerical calculation is shown for the density time correlator and the steady-state shear stress, where the current fluctuation in the coupling to the thermostat plays an important role in the α relaxation. The results of the CK theory [26] and the overdamped limit are also shown and are compared to the above result. In addition, the response to a perturbation of the shear rate is shown. Section VIII is provided for discussion. There, we first compare our work with the major preceding works. We hope that issues which were previously confusing are clarified. Then the physical significance of the present formulation and the possibility of its extension are discussed. Finally, in Sec. IX, we summarize our results and conclude the paper. An application to the response theory (Appendix A), a comparison of Mori-type equations in the underdamped and overdamped cases (Appendix B), and technical details (Appendixes C and D) are collected in the Appendixes.

II. MICROSCOPIC STARTING POINTS

Here we briefly summarize our microscopic starting points, i.e., the Sllod equation, the Liouville equation, and the steady-state formula. Our treatment closely follows that of CK [26], so the details in common are to be referred to Ref. [26]. The crucial difference, however, is that our formulation is intended to satisfy the isothermal condition, which is presented in Sec. IV D. Attention is paid to this issue.

A. Sllod equation

We deal with an assembly of N equivalent spheres with diameter d and mass m, interacting with themselves and a thermostat in a volume V. The interaction between the spheres is assumed to be a two-body soft-core potential force. Uniform shear is imposed on this system, where the shear velocity is given by $\boldsymbol{v}_{\rm sh} = \boldsymbol{\kappa} \cdot \boldsymbol{r}$. Here, $\boldsymbol{\kappa}$ is the shear rate tensor, which is assumed to be of the form $\boldsymbol{\kappa}_{\mu\nu} = \dot{\gamma}\delta_{\mu x}\delta_{\nu y}$ in this paper, where the shear rate is denoted $\dot{\gamma}$. $\boldsymbol{r}$ is the spatial coordinate, and Greek indices λ, μ, ν, etc., denote spatial components $\{x,y,z\}$ in the remainder. We introduce the distance of the two shear boundaries, L, for later convenience. Then the shear velocities at the boundaries are $v_0^{(\pm)} \equiv \pm\dot{\gamma}L/2$ for $y = \pm L/2$, respectively. The Newtonian equation of motion for the ith sphere ($i = 1,2,\ldots,N$) is given by the following Sllod equation [27,29]:

$$\dot{\boldsymbol{r}}_i(t) = \frac{\boldsymbol{p}_i(t)}{m} + \boldsymbol{\kappa} \cdot \boldsymbol{r}_i(t), \tag{1}$$

$$\dot{\boldsymbol{p}}_i(t) = \boldsymbol{F}_i(t) - \boldsymbol{\kappa} \cdot \boldsymbol{p}_i(t) - \alpha(\boldsymbol{\Gamma})\,\boldsymbol{p}_i(t). \tag{2}$$

Here, $\{\boldsymbol{r}_i(t), \boldsymbol{p}_i(t)\}$ is the position and the momentum of the ith sphere at time t, and $\boldsymbol{\Gamma}(t) \equiv \{\boldsymbol{r}_i(t), \boldsymbol{p}_i(t)\}_{i=1}^N$ is the phase-space coordinate. In Eq. (1), $\boldsymbol{p}_i(t)$ is defined as a relative momentum in the sheared frame and is referred to as the *peculiar* or the *thermal* momentum. $\boldsymbol{F}_i(t) \equiv -\partial U/\partial \boldsymbol{r}_i(t) = -\sum_j \partial u(r_{ij}(t))/\partial \boldsymbol{r}_{ij}(t)$ is the conservative force acting on the ith sphere from other spheres, U is the total potential, $u(r_{ij}(t))$ is the two-body potential, $\boldsymbol{r}_{ij}(t) \equiv \boldsymbol{r}_i(t) - \boldsymbol{r}_j(t)$ is the relative position, and $r_{ij}(t) \equiv |\boldsymbol{r}_{ij}(t)|$ is the relative distance between

the ith and the jth spheres, respectively. The parameter $\alpha(\mathbf{\Gamma})$ represents the strength of the coupling of spheres to the thermostat, which in general implicitly depends on time through its dependence on $\mathbf{\Gamma}(t)$. Note that $\alpha(\mathbf{\Gamma})$ has been assumed to be a constant in Ref. [26]. It is possible to prevent the system from heating up and to control the kinetic temperature to be a constant by tuning the coupling $\alpha(\mathbf{\Gamma})$, in which case $\alpha(\mathbf{\Gamma})$ should be regarded as a multiplier, rather than an independent physical parameter. A well-known example can be found in MD, which is the Gaussian isokinetic thermostat [27]. This thermostat is distinguished by its generality and its importance, which has the explicit time dependence

$$\alpha(t) = \frac{\sum_i \left[\boldsymbol{F}_i(t)\cdot\boldsymbol{p}_i(t) - \dot\gamma\, p_i^x(t)p_i^y(t)\right]}{\sum_j \boldsymbol{p}_j(t)\cdot\boldsymbol{p}_j(t)}, \tag{3}$$

which can be derived from the condition $\frac{d}{dt}\sum_i \boldsymbol{p}_i(t)^2 = 0$. The specific form of $\alpha(\mathbf{\Gamma})$ in the MCT with the isothermal condition is discussed in Sec. VI B. Note that Eqs. (1) and (2) reduce to Newtonian equations if we introduce the viscous force $\boldsymbol{F}_i^{(\mathrm{vis})}(t) \equiv -\alpha(\mathbf{\Gamma})m(\dot{\boldsymbol{r}}_i(t) - \boldsymbol{\kappa}\cdot\boldsymbol{r}_i(t))$, except for the instant onset of the shear.

B. Liouville equation

The Liouville equation for a phase-space variable $A(\mathbf{\Gamma}(t))$ reads

$$\begin{aligned}\frac{d}{dt}A(\mathbf{\Gamma}(t)) &= \dot{\mathbf{\Gamma}}(\mathbf{\Gamma}(t))\cdot\left.\frac{\partial A(\mathbf{\Gamma})}{\partial\mathbf{\Gamma}}\right|_{\mathbf{\Gamma}=\mathbf{\Gamma}(t)}\\ &= e^{i\mathcal{L}t}i\mathcal{L}A(\mathbf{\Gamma}(0)) = i\mathcal{L}A(\mathbf{\Gamma}(t)),\end{aligned} \tag{4}$$

where the action of the Liouvillian $i\mathcal{L}$ is defined as

$$i\mathcal{L}A(\mathbf{\Gamma}(0)) \equiv \dot{\mathbf{\Gamma}}(\mathbf{\Gamma})\cdot\left.\frac{\partial A(\mathbf{\Gamma}')}{\partial\mathbf{\Gamma}'}\right|_{\mathbf{\Gamma}'=\mathbf{\Gamma}}. \tag{5}$$

Here, and henceforth, the abbreviated notation $\mathbf{\Gamma} \equiv \mathbf{\Gamma}(0)$ is adopted. The formal solution of Eq. (4) is given by $A(\mathbf{\Gamma}(t)) = e^{i\mathcal{L}t}A(\mathbf{\Gamma})$. Note that, in Eqs. (4) and (5), the Liouvillian is assumed not to bear explicit time dependence. This is compatible with a time-independent shear, which we consider in this paper.

On the other hand, the Liouville equation for the nonequilibrium distribution function $\rho(\mathbf{\Gamma},t)$ reads

$$\frac{\partial\rho(\mathbf{\Gamma},t)}{\partial t} = -\left[\dot{\mathbf{\Gamma}}\cdot\frac{\partial}{\partial\mathbf{\Gamma}} + \Lambda(\mathbf{\Gamma})\right]\rho(\mathbf{\Gamma},t) = -i\mathcal{L}^\dagger\rho(\mathbf{\Gamma},t), \tag{6}$$

where

$$i\mathcal{L}^\dagger \equiv \dot{\mathbf{\Gamma}}\cdot\frac{\partial}{\partial\mathbf{\Gamma}} + \Lambda(\mathbf{\Gamma}) = i\mathcal{L} + \Lambda(\mathbf{\Gamma}) \tag{7}$$

is the adjoint Liouvillian, and

$$\Lambda(\mathbf{\Gamma}) \equiv \frac{\partial}{\partial\mathbf{\Gamma}}\cdot\dot{\mathbf{\Gamma}} \tag{8}$$

is the volume contraction factor of the phase space. The formal solution of Eq. (6) is $\rho(\mathbf{\Gamma},t) = e^{-i\mathcal{L}^\dagger t}\rho(\mathbf{\Gamma},0)$. In general, $\Lambda(\mathbf{\Gamma}) \neq 0$ for nonequilibrium systems, and hence the Liouvillian is non-Hermitian. In our case, $\Lambda(\mathbf{\Gamma})$ is

$$\begin{aligned}\Lambda(\mathbf{\Gamma}) &= \sum_i\left(\frac{\partial}{\partial\boldsymbol{r}_i}\cdot\dot{\boldsymbol{r}}_i + \frac{\partial}{\partial\boldsymbol{p}_i}\cdot\dot{\boldsymbol{p}}_i\right)\\ &= -3N\alpha(\mathbf{\Gamma}) - \sum_i\frac{\partial\alpha(\mathbf{\Gamma})}{\partial\boldsymbol{p}_i}\cdot\boldsymbol{p}_i\\ &\simeq -3N\alpha(\mathbf{\Gamma}),\end{aligned} \tag{9}$$

where the last approximate equality holds in the thermodynamic limit. This is verified for our specific choice of $\alpha(\mathbf{\Gamma})$ in Sec. VI B.

Let us decompose the Liouvillian as follows for convenience:

$$i\mathcal{L} = i\mathcal{L}_0 + i\mathcal{L}_{\dot\gamma} + i\mathcal{L}_\alpha, \tag{10}$$

$$i\mathcal{L}_0 \equiv \sum_i\left(\frac{\boldsymbol{p}_i}{m}\cdot\frac{\partial}{\partial\boldsymbol{r}_i} + \boldsymbol{F}_i\cdot\frac{\partial}{\partial\boldsymbol{p}_i}\right), \tag{11}$$

$$i\mathcal{L}_{\dot\gamma} \equiv \sum_i\left(\boldsymbol{r}_i\cdot\boldsymbol{\kappa}^T\cdot\frac{\partial}{\partial\boldsymbol{r}_i} - \boldsymbol{p}_i\cdot\boldsymbol{\kappa}^T\cdot\frac{\partial}{\partial\boldsymbol{p}_i}\right), \tag{12}$$

$$i\mathcal{L}_\alpha \equiv -\alpha(\mathbf{\Gamma})\sum_i\boldsymbol{p}_i\cdot\frac{\partial}{\partial\boldsymbol{p}_i}. \tag{13}$$

As can be easily seen, $i\mathcal{L}_0$, $i\mathcal{L}_{\dot\gamma}$, and $i\mathcal{L}_\alpha$ are the time-evolution generators of the conservative force, shearing, and the thermostat, respectively. We consider a situation where the system is initially in equilibrium with temperature T, and at time $t = 0$ a uniform shear with shear rate $\dot\gamma$ and a thermostat with strength $\alpha(\mathbf{\Gamma})$ are turned on.

The Liouvillian obeys the following adjoint relation inside the integral with respect to the phase-space coordinates,

$$\int d\mathbf{\Gamma}\,[i\mathcal{L}A(\mathbf{\Gamma})]\,B(\mathbf{\Gamma}) = -\int d\mathbf{\Gamma}\,A(\mathbf{\Gamma})[i\mathcal{L}^\dagger B(\mathbf{\Gamma})], \tag{14}$$

whose repeated use leads to

$$\int d\mathbf{\Gamma}[e^{i\mathcal{L}t}A(\mathbf{\Gamma})]B(\mathbf{\Gamma}) = \int d\mathbf{\Gamma}\,A(\mathbf{\Gamma})[e^{-i\mathcal{L}^\dagger t}B(\mathbf{\Gamma})]. \tag{15}$$

Equation (14) can be easily shown by partial integration. The adjoint relation, Eq. (14), and the definition of the adjoint Liouvillian, Eq. (7), lead to the following important relation, which indicates the action of the Liouvillian *inside the time correlators*:

$$\begin{aligned}\langle[i\mathcal{L}A(\mathbf{\Gamma}(t))]B(\mathbf{\Gamma})^*\rangle &= -\langle A(\mathbf{\Gamma}(t))[i\mathcal{L}B(\mathbf{\Gamma})]^*\rangle\\ &\quad + \langle A(\mathbf{\Gamma}(t))B(\mathbf{\Gamma})^*\Omega(\mathbf{\Gamma})\rangle,\end{aligned} \tag{16}$$

where $\Omega(\mathbf{\Gamma})$ is the work function,

$$\Omega(\mathbf{\Gamma}) \equiv -\beta\dot\gamma\sigma_{xy}(\mathbf{\Gamma}) - 2\beta\alpha(\mathbf{\Gamma})\delta K(\mathbf{\Gamma}). \tag{17}$$

Here, $\sigma_{xy}(\mathbf{\Gamma}) \equiv \sum_i(p_i^x p_i^y/m + y_i F_i^x)$ and $\delta K(\mathbf{\Gamma}) \equiv K(\mathbf{\Gamma}) - 3Nk_BT/2$ are the zero-wave-vector limit of the shear stress and the fluctuation of the kinetic energy $K(\mathbf{\Gamma}) \equiv \sum_i \boldsymbol{p}_i^2/(2m)$, respectively, and $\beta \equiv 1/(k_BT)$. The derivation of Eq. (17) is reported in Appendix C 1. The ensemble average $\langle\cdots\rangle$ in Eq. (16) is defined for a phase-space variable $A(\mathbf{\Gamma}(t))$ as

$$\langle A(\mathbf{\Gamma}(t))\rangle \equiv \int d\mathbf{\Gamma}\,\rho_{\mathrm{ini}}(\mathbf{\Gamma})A(\mathbf{\Gamma}(t)), \tag{18}$$

where $\rho_{\rm ini}(\mathbf{\Gamma})$ is the initial Maxwell-Boltzmann distribution, and the definition of Eq. (18) corresponds to the "Heisenberg picture" [27], which we adopt in this work.

Finally, we state here a steady-state formula for a phase-space variable $A(\mathbf{\Gamma}(t))$,

$$\langle A\rangle_{\rm SS} = \langle A(\mathbf{\Gamma})\rangle - \beta\dot\gamma\int_0^\infty dt\langle A(\mathbf{\Gamma}(t))\sigma_{xy}(\mathbf{\Gamma})\rangle - 2\beta\int_0^\infty dt\langle A(\mathbf{\Gamma}(t))\alpha(\mathbf{\Gamma})\delta K(\mathbf{\Gamma})\rangle, \tag{19}$$

where

$$\langle A\rangle_{\rm SS} \equiv \lim_{t\to\infty}\langle A(\mathbf{\Gamma}(t))\rangle \tag{20}$$

is the ensemble average in a nonequilibrium steady state. Refer to Appendix C 1 for the derivation of Eq. (19).

III. TRANSLATIONAL INVARIANCE IN THE SHEARED FRAME

So far we have repeated the formulation by CK [26], aside from the introduction of the dependence on the phase-space variables $\mathbf{\Gamma}$ of the dissipative coupling to the thermostat, $\alpha(\mathbf{\Gamma})$. In this section, a detailed discussion is devoted to the translational invariance in the sheared frame and to the definition of the time correlators. This discussion clearly indicates a crucial mistake in the Fourier transform of the phase-space variables by CK.

A. Fourier transform

A crucial feature of the sheared system is that the translational invariance is preserved only in the sheared frame. Hence, in order to examine the implications of the translational invariance, we must move on to this frame. As derived in Appendix C 2, Eq. (C22), the wave vector of the Fourier transform in the sheared frame is Affine deformed from that of the experimental frame (we refer to it as the "advected wave vector" in the following):

$$A_{\boldsymbol{q}(-t)}(\tilde t) = \int d^3\tilde{\boldsymbol{r}}\,A(\tilde{\boldsymbol{r}},\tilde t)e^{i\boldsymbol{q}(-t)\cdot\tilde{\boldsymbol{r}}}, \tag{21}$$

$$\boldsymbol{q}(t) \equiv \boldsymbol{q} - \boldsymbol{q}\cdot\boldsymbol{\kappa}t. \tag{22}$$

Here, $\tilde t \equiv t$ and $\tilde{\boldsymbol{r}} \equiv \boldsymbol{r} - (\boldsymbol{\kappa}\cdot\boldsymbol{r})\,t$ are the temporal and spatial coordinates in the sheared frame, respectively. We adopt the definition of the advected wave vector of FC [30], which differs from the conventional one, $\boldsymbol{q}(t) \equiv \boldsymbol{q} + \boldsymbol{q}\cdot\boldsymbol{\kappa}t$ [21,25,26]. The reason for this choice is explained later. The values of the phase-space variables are equivalent, irrespective of the frames, so the following equality holds:

$$A_{\boldsymbol{q}(-t)}(\tilde t) = A_{\boldsymbol{q}}(t). \tag{23}$$

The time evolution of the Fourier transform in the sheared frame is generated by $i\mathcal{L}_0$, $i\mathcal{L}_\alpha$, and $i\mathcal{L}_{\dot\gamma_p}$, where $i\mathcal{L}_{\dot\gamma_p}$ is the momentum part of $i\mathcal{L}_{\dot\gamma}$:

$$\frac{\partial}{\partial\tilde t}A_{\boldsymbol{q}(-t)}(\tilde t) = i\tilde{\mathcal{L}}A_{\boldsymbol{q}(-t)}(\tilde t), \tag{24}$$

$$i\tilde{\mathcal{L}} \equiv i\mathcal{L}_0 + i\mathcal{L}_\alpha + i\mathcal{L}_{\dot\gamma_p}, \tag{25}$$

$$i\mathcal{L}_{\dot\gamma_p} \equiv -\sum_i \boldsymbol{p}_i\cdot\boldsymbol{\kappa}^T\cdot\frac{\partial}{\partial\boldsymbol{p}_i}. \tag{26}$$

The derivation is reported in Appendix C 2. Note that the action of the coordinate part of $i\mathcal{L}_{\dot\gamma}$, which we denote

$$i\mathcal{L}_{\dot\gamma_r} \equiv \sum_i \boldsymbol{r}_i\cdot\boldsymbol{\kappa}^T\cdot\frac{\partial}{\partial\boldsymbol{r}_i}, \tag{27}$$

is already incorporated in the advected wave vector. This fact has been pointed out by Hayakawa and Otsuki (HO) [21]. We refer to $i\mathcal{L}_{\dot\gamma_r}$ as the "advection Liouvillian," since it generates an advection of the wave vectors of plane waves, $e^{-i\mathcal{L}_{\dot\gamma_r}t}e^{i\boldsymbol{q}\cdot\boldsymbol{r}} = e^{i\boldsymbol{q}(t)\cdot\boldsymbol{r}}$.

B. Adjoint Liouvillians inside the time correlators

We have seen above that the Fourier transform separates the Liouvillian $i\mathcal{L}$ into $i\tilde{\mathcal{L}}$ and the advection Liouvillian $i\mathcal{L}_{\dot\gamma_r}$. Hence it is convenient to decompose the adjoint relation, Eq. (16), into those for $i\tilde{\mathcal{L}}$ and $i\mathcal{L}_{\dot\gamma_r}$ and define the corresponding adjoint Liouvillians, $i\tilde{\mathcal{L}}^\dagger$ and $i\mathcal{L}^\dagger_{\dot\gamma_r}$. As for $i\tilde{\mathcal{L}}$, it is

$$\langle[i\tilde{\mathcal{L}}A(\mathbf{\Gamma}(t))]B(\mathbf{\Gamma})^*\rangle = -\langle A(\mathbf{\Gamma}(t))[i\tilde{\mathcal{L}}^\dagger B(\mathbf{\Gamma})]^*\rangle, \tag{28}$$

$$i\tilde{\mathcal{L}}^\dagger \equiv i\tilde{\mathcal{L}} - \tilde\Omega, \tag{29}$$

where

$$\tilde\Omega(\mathbf{\Gamma}) \equiv -\beta\dot\gamma\sigma^{\rm (kin)}_{xy}(\mathbf{\Gamma}) - 2\beta\alpha(\mathbf{\Gamma})\delta K(\mathbf{\Gamma}) \tag{30}$$

is the modified work function, which includes only the kinetic part of the shear stress,

$$\sigma^{\rm (kin)}_{xy} \equiv \sum_i \frac{p_i^x p_i^y}{m}. \tag{31}$$

As for $i\mathcal{L}_{\dot\gamma_r}$, it is

$$\langle[i\mathcal{L}_{\dot\gamma_r}A(\mathbf{\Gamma}(t))]B(\mathbf{\Gamma})^*\rangle = -\left\langle A(\mathbf{\Gamma}(t))\left[i\mathcal{L}^\dagger_{\dot\gamma_r}B(\mathbf{\Gamma})\right]^*\right\rangle, \tag{32}$$

$$i\mathcal{L}^\dagger_{\dot\gamma_r} \equiv i\mathcal{L}_{\dot\gamma_r} + \beta\dot\gamma\sigma^{\rm (pot)}_{xy}, \tag{33}$$

where the repeated use of Eq. (32) results in

$$\langle[e^{i\mathcal{L}_{\dot\gamma_r}t}A(\mathbf{\Gamma}(t))]B(\mathbf{\Gamma})^*\rangle = \langle A(\mathbf{\Gamma}(t))[e^{-i\mathcal{L}^\dagger_{\dot\gamma_r}t}B(\mathbf{\Gamma})]^*\rangle. \tag{34}$$

Here, $\sigma^{\rm (pot)}_{xy}$ is the potential part of the shear stress,

$$\sigma^{\rm (pot)}_{xy} \equiv \sum_i y_i F_i^x. \tag{35}$$

Note that the adjoint Liouvillians $i\tilde{\mathcal{L}}^\dagger$ and $i\mathcal{L}^\dagger_{\dot\gamma_r}$ are well defined *only inside the time correlators* and are not to be confused with the adjoint Liouvillian $i\mathcal{L}^\dagger$, which is defined in Eq. (7) as an independent operator.

C. General time correlators

In nonequilibrium statistical mechanics, time correlators play an essential role. Hence, we figure out the implications of the translational invariance on the time correlators. An immediate consequence of the translational invariance in the

sheared frame is

$$A(\tilde{\boldsymbol{r}},\tilde{t}) = A(\tilde{\boldsymbol{r}} + \boldsymbol{a}(t),\tilde{t}), \tag{36}$$

$$A_{\boldsymbol{k}}(\tilde{t}) = e^{i\boldsymbol{k}\cdot\boldsymbol{a}(t)} A_{\boldsymbol{k}}(\tilde{t}), \tag{37}$$

where $\boldsymbol{a}(t) \equiv (\dot{\gamma} t L, L, 0)$. Here, L is the distance between the two shear boundaries, which is introduced in Sec. II A. Equation (37) leads to the following "selection rule" of the wave vectors of the one-point and two-point functions in the sheared frame:

$$\langle A_{\boldsymbol{k}}(\tilde{t})\rangle = \langle A_{\boldsymbol{k}=0}(\tilde{t})\rangle \delta_{\boldsymbol{k},0}, \tag{38}$$

$$\langle A_{\boldsymbol{k}}(\tilde{t}) B^*_{\boldsymbol{q}}(0)\rangle = \langle A_{\boldsymbol{q}}(\tilde{t}) B^*_{\boldsymbol{q}}(0)\rangle \delta_{\boldsymbol{k},\boldsymbol{q}}. \tag{39}$$

Application of the equivalence of the Fourier transforms in the experimental and the sheared frames, i.e., Eq. (23), to Eq. (39) results in the following selection rule in the experimental frame:

$$\langle A_{\boldsymbol{k}(t)}(t) B^*_{\boldsymbol{q}}(0)\rangle = \langle A_{\boldsymbol{q}(t)}(t) B^*_{\boldsymbol{q}}(0)\rangle \delta_{\boldsymbol{k},\boldsymbol{q}}. \tag{40}$$

Here, the Fourier transform with the advected wave vector $A_{\boldsymbol{q}(t)}(t)$ is explicitly written in terms of the Liouvillians as

$$\begin{aligned} A_{\boldsymbol{q}(t)}(t) &= \sum_i e^{i\mathcal{L}t} A_i(\boldsymbol{\Gamma}(0)) e^{i\boldsymbol{q}(t)\cdot\boldsymbol{r}_i} \\ &= \sum_i e^{i\mathcal{L}t} A_i(\boldsymbol{\Gamma}(0)) e^{-i\mathcal{L}_{\dot{\gamma}r}t} e^{i\boldsymbol{q}\cdot\boldsymbol{r}_i}, \end{aligned} \tag{41}$$

where $A_i(\boldsymbol{\Gamma}(t))$ is the Fourier coefficient, which is defined in Eq. (C9).

One might think that the two-point function, Eq. (40), involves an ambiguity; it might seem that another choice, e.g., $\langle A_{\boldsymbol{q}}(t) B^*_{\boldsymbol{q}(-t)}(0)\rangle$, is equally valid. Actually, this was the choice made by CK [26] and FC [24,28]. However, the two expressions $\langle A_{\boldsymbol{q}(t)}(t) B^*_{\boldsymbol{q}}(0)\rangle$ and $\langle A_{\boldsymbol{q}}(t) B^*_{\boldsymbol{q}(-t)}(0)\rangle$ are in fact inequivalent, due to the noncommutativity and the non-Hermiticity of the Liouvillians. We prove this statement below. First, with the use of Eq. (41), $\langle A_{\boldsymbol{q}(t)}(t) B^*_{\boldsymbol{q}}(0)\rangle$ can be written in the following form:

$$\begin{aligned} &\langle A_{\boldsymbol{q}(t)}(t) B^*_{\boldsymbol{q}}(0)\rangle \\ &= \left\langle \left[\sum_i e^{i\mathcal{L}t} A_i(\boldsymbol{\Gamma}(0)) e^{-i\mathcal{L}_{\dot{\gamma}r}t} e^{i\boldsymbol{q}\cdot\boldsymbol{r}_i} \right] \sum_j B_j(\boldsymbol{\Gamma}(0))^* e^{-i\boldsymbol{q}\cdot\boldsymbol{r}_j} \right\rangle. \end{aligned} \tag{42}$$

Similarly, $\langle A_{\boldsymbol{q}}(t) B^*_{\boldsymbol{q}(-t)}(0)\rangle$ can be written as follows:

$$\begin{aligned} &\langle A_{\boldsymbol{q}}(t) B^*_{\boldsymbol{q}(-t)}(0)\rangle \\ &= \left\langle \left[\sum_i e^{i\mathcal{L}t} A_i(\boldsymbol{\Gamma}(0)) e^{i\boldsymbol{q}\cdot\boldsymbol{r}_i} \right] \sum_j B_j(\boldsymbol{\Gamma}(0))^* e^{i\mathcal{L}_{\dot{\gamma}r}t} e^{-i\boldsymbol{q}\cdot\boldsymbol{r}_j} \right\rangle. \end{aligned} \tag{43}$$

Even when the advection Liouvillian $i\mathcal{L}_{\dot{\gamma}r}$ commutes with $A_i(\boldsymbol{\Gamma}(0))$ and $B_j(\boldsymbol{\Gamma}(0))$, which is the case of interest in the MCT, where these variables are the density and the current-density fluctuations, Eqs. (42) and (43) are not equivalent. This can be seen by the use of the adjoint relation of the Liouvillians, Eq. (34), and the relations $[i\mathcal{L}_{\dot{\gamma}r}, i\mathcal{L}] \neq 0$ and $i\mathcal{L}_{\dot{\gamma}r} \neq i\mathcal{L}^\dagger_{\dot{\gamma}r}$. It can also be foreseen from Eqs. (42) and (43) that different definitions of the two-point functions lead to different physical consequences.

We assert that the specific definition, Eq. (40), is the physically sensible choice. It states that a fluctuation at time $t = 0$ with a wave vector $\boldsymbol{q} = \boldsymbol{q}(0)$ is correlated at time t with a fluctuation with a wave vector $\boldsymbol{q}(t)$, exclusively. Note that the definition of the advected wave vector, Eq. (22), is chosen for its compatibility with the intuitive picture described above. This definition is essentially coincident with the one adopted in the previous studies [21,25,30], although it appears to be $\langle A_{\boldsymbol{q}(-t)}(t) B^*_{\boldsymbol{q}}(0)\rangle$ in Refs. [21,25]. This superficial discrepancy with Eq. (40) is due to the different definition of the advected wave vector, $\boldsymbol{q}(t) \equiv \boldsymbol{q} + \boldsymbol{q}\cdot\boldsymbol{\kappa} t$.

IV. MORI-TYPE EQUATIONS

In liquid theory, slowly varying (i.e., long-wavelength and low-frequency) conserved variables are of interest. Conventionally these are the density fluctuation and the current-density (momentum) fluctuation. In MCT for sheared thermostated systems, the formula for the steady-state quantities is formulated in terms of a time correlator for density fluctuations (density time correlator). In this section, we introduce the time correlators of interest and derive the Mori-type equations [36] for them by applying the projection operator formalism. First, we derive the Mori-type equations without the isothermal condition. Then we formulate the isothermal condition by introducing a multiplier for this constraint. Finally, we derive corrections to the Mori-type equations, where the multiplier is introduced.

A. Time correlators of interest

Density and current-density fluctuations at equilibrium are denoted in Fourier space as

$$n_{\boldsymbol{q}} \equiv \sum_i e^{i\boldsymbol{q}\cdot\boldsymbol{r}_i} - N\delta_{\boldsymbol{q},0}, \tag{44}$$

$$j^\lambda_{\boldsymbol{q}} \equiv \sum_i \frac{p^\lambda_i}{m} e^{i\boldsymbol{q}\cdot\boldsymbol{r}_i} \quad (\lambda = x,y,z), \tag{45}$$

respectively. The spatial dimension is assumed to be 3, in accordance with the numerical calculation which is carried out in Sec. VII. The corresponding time correlators of interest, of the form of Eq. (40), are as follows:

$$\Phi_{\boldsymbol{q}}(t) \equiv \frac{1}{N}\langle n_{\boldsymbol{q}(t)}(t) n_{\boldsymbol{q}}(0)^*\rangle, \tag{46}$$

$$H^\lambda_{\boldsymbol{q}}(t) \equiv \frac{i}{N}\langle j^\lambda_{\boldsymbol{q}(t)}(t) n_{\boldsymbol{q}}(0)^*\rangle. \tag{47}$$

Here, $\Phi_{\boldsymbol{q}}(t)$ is the density time correlator, and $H^\lambda_{\boldsymbol{q}}(t)$ is referred to as the density-current cross time correlator. As already mentioned, the Fourier coefficient $A_i(\boldsymbol{\Gamma}(0))$ in Eq. (41) is $A_i(\boldsymbol{\Gamma}(0)) = 1$ for the density fluctuation and $A_i(\boldsymbol{\Gamma}(0)) = p^\lambda_i/m$ for the current-density fluctuation; hence they commute with $i\mathcal{L}_{\dot{\gamma}r}$, respectively. This leads to the following expression for the density and current-density fluctuations at time t:

$$\xi_{\boldsymbol{q}(t)}(t) = e^{i\mathcal{L}t} e^{-i\mathcal{L}_{\dot{\gamma}r}t} \xi_{\boldsymbol{q}} = e^{i\mathcal{L}t} \xi_{\boldsymbol{q}(t)} = U(t)\xi_{\boldsymbol{q}}, \tag{48}$$

where

$$\xi_{\boldsymbol{q}(t)} \equiv e^{-i\mathcal{L}_{\dot{\gamma}r}t}\xi_{\boldsymbol{q}}, \tag{49}$$

$$U(t) \equiv e^{i\mathcal{L}t}e^{-i\mathcal{L}_{\dot{\gamma}r}t}. \tag{50}$$

Here, ξ is either of the hydrodynamic variables, n or j, and $U(t)$ is the time-evolution operator for ξ in Fourier space. Note that $U(t)$ is non unitary since the Liouvillians are non-Hermitian. Then Eqs. (46) and (47) are expressed, respectively, as

$$\Phi_{\boldsymbol{q}}(t) = \frac{1}{N}\langle [U(t)n_{\boldsymbol{q}}]n^*_{\boldsymbol{q}}\rangle, \tag{51}$$

$$H^{\lambda}_{\boldsymbol{q}}(t) = \frac{i}{N}\langle \left[U(t)j^{\lambda}_{\boldsymbol{q}}\right]n^*_{\boldsymbol{q}}\rangle. \tag{52}$$

B. Continuity equations

Now we derive the equations of motion for Eqs. (51) and (52). The time derivative of $U(t)$ is

$$\frac{d}{dt}U(t) = e^{i\mathcal{L}t}\left(i\mathcal{L} - i\mathcal{L}_{\dot{\gamma}_r}\right)e^{-i\mathcal{L}_{\dot{\gamma}_r}t} = e^{i\mathcal{L}t}i\tilde{\mathcal{L}}e^{-i\mathcal{L}_{\dot{\gamma}_r}t}, \tag{53}$$

where $i\tilde{\mathcal{L}}$ is defined in Eq. (25). The action of $i\tilde{\mathcal{L}}$ on $n_{\boldsymbol{q}}$ is obtained from Eqs. (11), (13), and (26) as

$$i\tilde{\mathcal{L}}n_{\boldsymbol{q}} = i\boldsymbol{q}\cdot\boldsymbol{j}_{\boldsymbol{q}}. \tag{54}$$

From Eqs. (52)–(54) we obtain

$$\begin{aligned}\frac{d}{dt}\Phi_{\boldsymbol{q}}(t) &= \frac{1}{N}\left\langle\left[\frac{d}{dt}U(t)n_{\boldsymbol{q}}\right]n^*_{\boldsymbol{q}}\right\rangle \\ &= \frac{1}{N}\langle\left[e^{i\mathcal{L}t}i\tilde{\mathcal{L}}n_{\boldsymbol{q}(t)}\right]n^*_{\boldsymbol{q}}\rangle = \boldsymbol{q}(t)\cdot\boldsymbol{H}_{\boldsymbol{q}}(t).\end{aligned} \tag{55}$$

On the other hand, the action of $i\tilde{\mathcal{L}}$ on $\boldsymbol{j}_{\boldsymbol{q}}$ cannot be written in a concise form as simply as Eq. (54):

$$\begin{aligned}\frac{d}{dt}H^{\lambda}_{\boldsymbol{q}}(t) &= \frac{i}{N}\left\langle\left[\frac{d}{dt}U(t)j^{\lambda}_{\boldsymbol{q}}\right]n^*_{\boldsymbol{q}}\right\rangle \\ &= \frac{i}{N}\langle\left[e^{i\mathcal{L}t}i\tilde{\mathcal{L}}j^{\lambda}_{\boldsymbol{q}(t)}\right]n^*_{\boldsymbol{q}}\rangle.\end{aligned} \tag{56}$$

A conventional way to handle Eq. (56) is to deform it into a Mori-type equation [36]. This task is conducted in Sec. III C by the application of the projection operator formalism.

C. Projection operator formalism

We have introduced the time correlators, Eqs. (46) and (47), in a physically sensible way that a fluctuation at time $t = 0$ with a wave vector $\boldsymbol{q}$ is correlated at time t with a fluctuation with a wave vector $\boldsymbol{q}(t)$. We refer to this feature as the "*alignment of the wave vectors*" in this paper. Even if the wave vectors of the time correlators are aligned, this feature is not necessarily preserved in their entire continuity equations. As for the density time correlator $\Phi_{\boldsymbol{q}}(t)$, this is positive, as can be seen from Eq. (55). In deriving a Mori-type equation for the cross time correlator $H^{\lambda}_{\boldsymbol{q}}(t)$, we demand the alignment of the wave vectors as a principle.

For this purpose, we introduce the *time-dependent* projection operator [30],

$$\mathcal{P}(t)X \equiv \sum_{\boldsymbol{k}}\frac{\langle Xn^*_{\boldsymbol{k}(t)}\rangle}{NS_{k(t)}}n_{\boldsymbol{k}(t)} + \sum_{\boldsymbol{k}}\frac{\langle Xj^{\lambda *}_{\boldsymbol{k}(t)}\rangle}{Nv_T^2}j^{\lambda}_{\boldsymbol{k}(t)}, \tag{57}$$

and its complementary operator,

$$\mathcal{Q}(t) \equiv 1 - \mathcal{P}(t). \tag{58}$$

Here, X is an arbitrary phase-space variable in Fourier space and the normalization factors are determined from the equal-time (equilibrium) correlators, $\langle n_{\boldsymbol{q}}n^*_{\boldsymbol{q}'}\rangle = NS_q\delta_{\boldsymbol{q},\boldsymbol{q}'}$ and $\langle j^{\lambda}_{\boldsymbol{q}}j^{\mu}_{\boldsymbol{q}'}\rangle = Nv_T^2\delta^{\lambda\mu}\delta_{\boldsymbol{q},\boldsymbol{q}'}$, where S_q is the static structure factor [36] and $v_T \equiv \sqrt{k_BT/m}$ is the thermal velocity. These operators preserve the desired properties: (i) idempotency, $\mathcal{P}(t)^2 = \mathcal{P}(t)$, $\mathcal{Q}(t)^2 = \mathcal{Q}(t)$; (ii) orthogonality, $\mathcal{P}(t)\mathcal{Q}(t) = \mathcal{Q}(t)\mathcal{P}(t) = 0$; and (iii) Hermiticity,

$$\langle[\mathcal{P}(t)A_{\boldsymbol{q}(t)}(t)]B_{\boldsymbol{q}}(0)^*\rangle = \langle A_{\boldsymbol{q}(t)}(t)[\mathcal{P}(t)B_{\boldsymbol{q}}(0)]^*\rangle, \tag{59}$$

$$\langle[\mathcal{Q}(t)A_{\boldsymbol{q}(t)}(t)]B_{\boldsymbol{q}}(0)^*\rangle = \langle A_{\boldsymbol{q}(t)}(t)[\mathcal{Q}(t)B_{\boldsymbol{q}}(0)]^*\rangle. \tag{60}$$

In addition, we further introduce a "rescaled static projection operator" [30],

$$\bar{\mathcal{P}}_tX = \sum_{\boldsymbol{k}}\frac{\langle Xn^*_{\boldsymbol{k}}\rangle}{NS_{k(t)}}n_{\boldsymbol{k}} + \sum_{\boldsymbol{k}}\frac{\langle Xj^{\lambda *}_{\boldsymbol{k}}\rangle}{Nv_T^2}j^{\lambda}_{\boldsymbol{k}}, \tag{61}$$

whose *raison d'être* is explained later. Although Eq. (61) is a projection operator onto the subspace spanned by the static density and current-density fluctuations $\{n_{\boldsymbol{k}}, \boldsymbol{j}_{\boldsymbol{k}}\}$, it involves a dependence on time through the advected index of $S_{k(t)}$, so we appended a subscript t. One can easily verify, by the use of Eq. (34), the following relation between $\mathcal{P}(t)$ and $\bar{\mathcal{P}}_t$,

$$\mathcal{P}(t) = e^{-i\mathcal{L}_{\dot{\gamma}r}t}\bar{\mathcal{P}}_te^{i\mathcal{L}^{\dagger}_{\dot{\gamma}r}t}, \tag{62}$$

where the adjoint of the advection Liouvillian $i\mathcal{L}^{\dagger}_{\dot{\gamma}r}$ is defined in Eq. (33).

Now we derive a Mori-type equation for Eq. (56) by inserting the projection operators as follows:

$$\begin{aligned}\frac{d}{dt}U(t) &= e^{i\mathcal{L}t}\left[\mathcal{P}(t) + \mathcal{Q}(t)\right]i\tilde{\mathcal{L}}e^{-i\mathcal{L}_{\dot{\gamma}r}t} \\ &= e^{i\mathcal{L}t}[e^{-i\mathcal{L}_{\dot{\gamma}r}t}\bar{\mathcal{P}}_te^{i\mathcal{L}^{\dagger}_{\dot{\gamma}r}t} + \mathcal{Q}(t)]i\tilde{\mathcal{L}}e^{-i\mathcal{L}_{\dot{\gamma}r}t} \\ &= e^{i\mathcal{L}t}e^{-i\mathcal{L}_{\dot{\gamma}r}t}[\bar{\mathcal{P}}_te^{i\mathcal{L}^{\dagger}_{\dot{\gamma}r}t} + e^{i\mathcal{L}_{\dot{\gamma}r}t}\mathcal{Q}(t)]i\tilde{\mathcal{L}}e^{-i\mathcal{L}_{\dot{\gamma}r}t} \\ &= U(t)[\bar{\mathcal{P}}_te^{i\mathcal{L}^{\dagger}_{\dot{\gamma}r}t}i\tilde{\mathcal{L}}e^{-i\mathcal{L}_{\dot{\gamma}r}t} + e^{i\mathcal{L}_{\dot{\gamma}r}t}\mathcal{Q}(t)i\tilde{\mathcal{L}}e^{-i\mathcal{L}_{\dot{\gamma}r}t}].\end{aligned} \tag{63}$$

The formal solution of Eq. (63) is given as

$$U(t) = U_0(t,0) + \int_0^t dsU(s)\bar{\mathcal{P}}_se^{i\mathcal{L}^{\dagger}_{\dot{\gamma}r}s}i\tilde{\mathcal{L}}e^{-i\mathcal{L}_{\dot{\gamma}r}s}U_0(t,s), \tag{64}$$

where $U_0(t,t')$ is the solution of the homogeneous equation. $U_0(t,t')$ can be written in terms of the time-ordered exponential, $\exp_{\rightarrow}[\int_{t'}^t dsX(s)] \equiv 1 + \sum_{n=1}^{\infty}\int_{t'}^t ds_1\cdots\int_{t'}^{s_{n-1}} ds_nX(s_n)\cdots X(s_1)$, as follows:

$$U_0(t,t') = \exp_{\rightarrow}\left[\int_{t'}^t dse^{i\mathcal{L}_{\dot{\gamma}r}s}\mathcal{Q}(s)i\tilde{\mathcal{L}}e^{-i\mathcal{L}_{\dot{\gamma}r}s}\right]. \tag{65}$$

From Eqs. (63) and (64), the time derivative of the current-density fluctuation, which appears in Eq. (56), can be decomposed into the "correlated part" and the "uncorrelated part":

$$\frac{d}{dt}U(t)j^{\lambda}_{\boldsymbol{q}} = U(t)\bar{\mathcal{P}}_t e^{i\mathcal{L}^{\dagger}_{\dot{\gamma}_r}t} i\tilde{\mathcal{L}} j^{\lambda}_{\boldsymbol{q}(t)} + U_0(t,0)e^{i\mathcal{L}_{\dot{\gamma}_r}t}\mathcal{Q}(t)i\tilde{\mathcal{L}}j^{\lambda}_{\boldsymbol{q}(t)} + \int_0^t ds\, U(s)\bar{\mathcal{P}}_s e^{i\mathcal{L}^{\dagger}_{\dot{\gamma}_r}s} i\tilde{\mathcal{L}} e^{-i\mathcal{L}_{\dot{\gamma}_r}s} U_0(t,s) \times e^{i\mathcal{L}_{\dot{\gamma}_r}t}\mathcal{Q}(t)i\tilde{\mathcal{L}}j^{\lambda}_{\boldsymbol{q}(t)}. \tag{66}$$

Here, the first term on the right-hand side (r.h.s.) is the correlated part and the second and third terms are the uncorrelated part. Applying Eq. (61) to Eq. (66), and then substituting Eq. (66) to Eq. (56), we obtain the Mori-type equation. Following the derivation in Appendix C 3, we obtain

$$\frac{d}{dt}H^{\lambda}_{\boldsymbol{q}}(t) = -v_T^2\frac{q(t)^{\lambda}}{S_{q(t)}}\Phi_{\boldsymbol{q}}(t) - \alpha_0 H^{\lambda}_{\boldsymbol{q}}(t) - [\boldsymbol{\kappa}\cdot\boldsymbol{H}_{\boldsymbol{q}}(t)]^{\lambda} + \frac{i}{N}\left\langle R^{\lambda}_{\boldsymbol{q}(t)}(t)n^{*}_{\boldsymbol{q}}\right\rangle - \int_0^t ds\, L^{\lambda}_{\boldsymbol{q}}(t,s)\Phi_{\boldsymbol{q}}(s) - \int_0^t ds\, M^{\lambda\mu}_{\boldsymbol{q}}(t,s)H^{\mu}_{\boldsymbol{q}}(s), \tag{67}$$

where we have introduced

$$R^{\lambda}_{\boldsymbol{q}(t)}(t) \equiv U_0(t,0)e^{i\mathcal{L}_{\dot{\gamma}_r}t}R^{\lambda}_{\boldsymbol{q}(t)}, \tag{68}$$

$$R^{\lambda}_{\boldsymbol{q}(t)} \equiv \mathcal{Q}(t)i\tilde{\mathcal{L}}j^{\lambda}_{\boldsymbol{q}(t)}, \tag{69}$$

$$iL^{\lambda}_{\boldsymbol{q}}(t,s) \equiv \frac{1}{NS_{q(t)}}\left\langle\left[i\tilde{\mathcal{L}}\tilde{U}_0(t,s)R^{\lambda}_{\boldsymbol{q}(t)}\right]n^{*}_{\boldsymbol{q}(s)}\right\rangle, \tag{70}$$

$$M^{\lambda\mu}_{\boldsymbol{q}}(t,s) \equiv -\frac{1}{Nv_T^2}\left\langle\left[i\tilde{\mathcal{L}}\tilde{U}_0(t,s)R^{\lambda}_{\boldsymbol{q}(t)}\right]j^{\mu *}_{\boldsymbol{q}(s)}\right\rangle, \tag{71}$$

$$\tilde{U}_0(t,s) \equiv e^{-i\mathcal{L}_{\dot{\gamma}_r}s}U_0(t,s)e^{i\mathcal{L}_{\dot{\gamma}_r}t}. \tag{72}$$

Here, $R^{\lambda}_{\boldsymbol{q}(t)}(t)$ is the "random force," whose time evolution is given by the projected time-evolution operator, $U_0(t,0)$. Two types of memory kernels appear, $L^{\lambda}_{\boldsymbol{q}}(t,s)$ and $M^{\lambda\mu}_{\boldsymbol{q}}(t,s)$, due to the projection onto the current-density and the density fluctuations, respectively. The correction of the friction coefficient α_0 due to the introduction of the isothermal condition is discussed in Sec. IV E.

Note that the random force, Eq. (68), is not orthogonal to the density fluctuation at this stage. An additional requirement leads to the orthogonality, which is discussed in Eqs. (88) and (89) in Sec. V. Note also that the memory kernels possess two time arguments, in contrast to those which appear in CK. This issue is also discussed in Sec. V.

D. Isothermal condition

So far we have derived the Mori-type equations without the isothermal condition, which is the condition necessary to hold the kinetic temperture unchanged. In this section, we attempt to implement the isothermal condition. The derivation of the resulting Mori-type equations is performed in Sec. IV E.

At the level of the Sllod equation, it is known that the isothermal condition is satisfied by the specific choice of $\alpha(t)$ given by Eq. (3), which is referred to as the Gaussian isokinetic thermostat. In principle, the Mori-type equations derived from the corresponding Liouville equation, with $\alpha(\boldsymbol{\Gamma})$ given by Eq. (3), no longer contain any multiplier, and the invariance of the kinetic temperature is assured automatically. However, this choice of $\alpha(\boldsymbol{\Gamma})$ leads to difficulty in deriving the Mori-type equations, since the integral of a rational function with Gaussian weight is difficult to perform explicitly.

This motivates us to implement the isothermal condition *at the level of the Mori-type equations*, which is attained by requiring the time derivative of the *average kinetic temperature* to vanish. Note that this scheme requires the time derivative of the kinetic temperature, not necessarily itself but at least its average, to vanish. In this scheme, we avoid to fully incorporate the fluctuations as in Eq. (3) and attempt to incorporate them partially, compensating it with a *multiplier* at the level of the Mori-type equations. We denote this multiplier, which corresponds to the multiplier of the Liouville equation $\alpha(\boldsymbol{\Gamma})$, as $\lambda_{\alpha}(t)$ in the remainder.

By differentiating the generalized Green-Kubo formula for the kinetic temperature, we obtain

$$\frac{d}{dt}\langle T(\boldsymbol{\Gamma}(t))\rangle = \frac{2}{3Nk_B}\langle K(\boldsymbol{\Gamma}(t))\Omega(\boldsymbol{\Gamma})\rangle = -\frac{2\beta}{3Nk_B}\{\dot{\gamma}G_{K,\sigma}(t) + 2G_{K,\alpha\delta K}(t)\}, \tag{73}$$

where

$$G_{K,\sigma}(t) \equiv \langle [U(t)K(\boldsymbol{\Gamma})]\sigma_{xy}(\boldsymbol{\Gamma})\rangle \tag{74}$$

and

$$G_{K,\alpha\delta K}(t) \equiv \langle [U(t)K(\boldsymbol{\Gamma})]\alpha(\boldsymbol{\Gamma})\delta K(\boldsymbol{\Gamma})\rangle\,. \tag{75}$$

Hence, the isothermal condition at the level of the Mori-type equations reads

$$\dot{\gamma}G_{K,\sigma}(t) + 2G_{K,\alpha\delta K}(t) = 0. \tag{76}$$

In order to satisfy this constraint, we introduce $\lambda_{\alpha}(t)$ in $G_{K,\alpha\delta K}(t)$, the result of which we denote $G^{(\lambda)}_{K,\alpha\delta K}(t)$, and recast Eq. (76) as

$$\dot{\gamma}G_{K,\sigma}(t) + 2G^{(\lambda)}_{K,\alpha\delta K}(t) = 0. \tag{77}$$

However, from Eq. (75), we can see that the definition of $G^{(\lambda)}_{K,\alpha\delta K}(t)$ is nontrivial, since the effect of the time evolution of the multiplier appears in $U(t)$, rather than $\alpha(\boldsymbol{\Gamma})$. This leads us to define a "renormalized" time-evolution operator $U_R(t)$, where

$$U_R(t) \equiv \lambda_{\alpha}(t)U(t), \tag{78}$$

and define $G^{(\lambda)}_{K,\alpha\delta K}(t)$ as

$$G^{(\lambda)}_{K,\alpha\delta K}(t) \equiv \langle [U_R(t)K(\boldsymbol{\Gamma})]\alpha(\boldsymbol{\Gamma})\delta K(\boldsymbol{\Gamma})\rangle = \lambda_{\alpha}(t)G_{K,\alpha\delta K}(t). \tag{79}$$

Here, $\lambda_{\alpha}(t)$ factors out, since it is not a phase-space variable. Then, if $G_{K,\alpha\delta K}(t) \neq 0$, choosing the multiplier as

$$\lambda_{\alpha}(t) = -\frac{\dot{\gamma}}{2}\frac{G_{K,\sigma}(t)}{G_{K,\alpha\delta K}(t)} \tag{80}$$

assures the isothermal condition, Eq. (77), to be satisfied. Note that, while $\alpha(\boldsymbol{\Gamma})$ is expressed in terms of the phase-space

variables $\mathbf{\Gamma}$, $\lambda_\alpha(t)$ is expressed in terms of time correlators at time t, when the constraint, Eq. (77), is satisfied. Concrete examples of $\alpha(\mathbf{\Gamma})$ and $\lambda_\alpha(t)$ are discussed in Sec. VI B.

E. Isothermal Mori-type equations

Now we figure out how the multiplier $\lambda_\alpha(t)$ enters into the Mori-type equations. The identification of the complete correction is possible but rather lengthy. Furthermore, most of the modifications vanish in the mode-coupling approximation, which we discuss in Sec. V. Hence, we only focus on the modification which survives the mode-coupling approximation, which is for the friction term $\alpha_0 H^\lambda_{\boldsymbol{q}}(t)$ in Eq. (67). As shown in Appendix C 3, this term arises from the correlated part in Eq. (66), which is explicitly

$$\begin{aligned}&\left\langle\left[U(t)\bar{\mathcal{P}}_t e^{i\mathcal{L}^\dagger_{\dot\gamma r}t} i\mathcal{L}_\alpha j^\lambda_{\boldsymbol{q}(t)}\right]n^*_{\boldsymbol{q}}\right\rangle\\&\quad=\left\langle\left[U(t)\bar{\mathcal{P}}_t e^{i\mathcal{L}^\dagger_{\dot\gamma r}t}\alpha(\mathbf{\Gamma})i\mathcal{L}_p j^\lambda_{\boldsymbol{q}(t)}\right]n^*_{\boldsymbol{q}}\right\rangle.\end{aligned}\tag{81}$$

Here, we extract $\alpha(\mathbf{\Gamma})$ and define the remaining part as $i\mathcal{L}_p \equiv -\sum_i \boldsymbol{p}_i\cdot\partial/\partial\boldsymbol{p}_i$. We introduce $\lambda_\alpha(t)$ here as done in Eq. (78), which leads to

$$\left\langle\left[U_R(t)\bar{\mathcal{P}}_t e^{i\mathcal{L}^\dagger_{\dot\gamma r}t}\alpha(\mathbf{\Gamma})i\mathcal{L}_p j^\lambda_{\boldsymbol{q}(t)}\right]n^*_{\boldsymbol{q}}\right\rangle=\lambda_\alpha(t)\alpha_0,\tag{82}$$

where the explicit form of $\alpha(\mathbf{\Gamma})$, which is specified in Sec. VI B, Eq. (112), is utilized. Hence, the Mori-type equation with the isothermal condition is

$$\begin{aligned}\frac{d}{dt}H^\lambda_{\boldsymbol{q}}(t)=&-v_T^2\frac{q(t)^\lambda}{S_{q(t)}}\Phi_{\boldsymbol{q}}(t)-\lambda_\alpha(t)\alpha_0 H^\lambda_{\boldsymbol{q}}(t)-[\boldsymbol{\kappa}\cdot\boldsymbol{H}_{\boldsymbol{q}}(t)]^\lambda\\&+\frac{i}{N}\left\langle R^\lambda_{\boldsymbol{q}(t)}(t)n^*_{\boldsymbol{q}}\right\rangle-\int_0^t ds L^\lambda_{\boldsymbol{q}}(t,s)\Phi_{\boldsymbol{q}}(s)\\&-\int_0^t ds M^{\lambda\mu}_{\boldsymbol{q}}(t,s)H^\mu_{\boldsymbol{q}}(s).\end{aligned}\tag{83}$$

The fact that $\lambda_\alpha(t)$ does not appear in the memory kernels in the mode-coupling approximation can be verified in Sec. V, where the resulting memory kernels turn out to be independent of α_0. In addition, as shown in Sec. V, the vanishing of $\langle R^\lambda_{\boldsymbol{q}(t)}(t)n^*_{\boldsymbol{q}}\rangle$ is not affected by $\alpha(\mathbf{\Gamma})$, and hence $\lambda_\alpha(t)$ does not appear here either.

In principle, the Mori-type equations which follow from the choice, Eq. (3), of $\alpha(\mathbf{\Gamma})$ contain no multiplier and are expected to satisfy the isothermal condition, Eq. (76), automatically. On the other hand, the Mori-type equations, Eqs. (55) and (83), which follow from $\alpha(\mathbf{\Gamma})$ of Eq. (112) contain a multiplier $\lambda_\alpha(t)$, and the isothermal condition, Eq. (77), is explicitly satisfied if $\lambda_\alpha(t)$ is chosen as Eq. (120), which is derived in Sec. VI B. We expect that the physical equivalence is achieved for these two schemes. The Mori-type equations of the underdamped and overdamped [30] cases are compared and discussed in Appendix B.

V. MODE-COUPLING APPROXIMATION

We have derived an isothermal Mori-type equation for the cross time correlator $H^\lambda_{\boldsymbol{q}}(t)$, Eq. (83), in the previous section. However, this is not a closed equation for the time correlators $\Phi_{\boldsymbol{q}}(t)$ and $H^\lambda_{\boldsymbol{q}}(t)$, unless the memory kernels are expressed in terms of them. For this purpose, we introduce a *time-dependent* second projection operator [30], which extracts the dynamics correlated with the slowly varying pair-density modes:

$$\mathcal{P}_2(t)X\equiv\sum_{\boldsymbol{k}>\boldsymbol{p}}\frac{\left\langle X n^*_{\boldsymbol{k}(t)}n^*_{\boldsymbol{p}(t)}\right\rangle}{N^2 S_{k(t)}S_{p(t)}}n_{\boldsymbol{k}(t)}n_{\boldsymbol{p}(t)}.\tag{84}$$

The normalization factor is determined by the factorization approximation of the equal-time (equilibrium) four-point function of the density fluctuations, $\langle n_{\boldsymbol{k}(t)}n_{\boldsymbol{p}(t)}n^*_{\boldsymbol{k}'(t)}n^*_{\boldsymbol{p}'(t)}\rangle\simeq\langle n_{\boldsymbol{k}(t)}n^*_{\boldsymbol{k}'(t)}\rangle\langle n_{\boldsymbol{p}(t)}n^*_{\boldsymbol{p}'(t)}\rangle=\delta_{\boldsymbol{k},\boldsymbol{k}'}\delta_{\boldsymbol{p},\boldsymbol{p}'}N^2S_{k(t)}S_{p(t)}(\boldsymbol{k}>\boldsymbol{p},\boldsymbol{k}'>\boldsymbol{p}')$. The second projection operator, Eq. (84), is idempotent and Hermitian, similar to the projection operator, Eq. (57).

In underdamped MCT, there exists a potential next-to-leading second projection operator, which projects the dynamics onto the density-current modes [37]. However, it can be shown that this projection is negligible compared to the projection onto the pair-density modes, at least for time-reversible thermostated systems [38]. Hence, the choice of Eq. (84) is assured. Note that this feature does not always hold, e.g., for granular systems, where the projection onto the density-current modes plays an essential role [23,37].

There is one subtle issue we should handle in order for the application of Eq. (84) to work [39]. The operator which appears in the memory kernels defined in Eqs. (70) and (71), $i\tilde{\mathcal{L}}\tilde{U}_0(t,s)R^\lambda_{\boldsymbol{q}(t)}$, can be deformed as follows,

$$\begin{aligned}&i\tilde{\mathcal{L}}\tilde{U}_0(t,s)R^\lambda_{\boldsymbol{q}(t)}\\&\quad=i\tilde{\mathcal{L}}[1+\Sigma(s)]\,e^{-i\mathcal{L}^\dagger_{\dot\gamma r}s}U_0(t,s)e^{i\mathcal{L}_{\dot\gamma r}t}\mathcal{Q}(t)R^\lambda_{\boldsymbol{q}(t)},\end{aligned}\tag{85}$$

where Eq. (72), the idempotency of $\mathcal{Q}(t)$, and the identity

$$e^{-i\mathcal{L}_{\dot\gamma r}t}=[1+\Sigma(t)]\,e^{-i\mathcal{L}^\dagger_{\dot\gamma r}t}\tag{86}$$

is applied. Here,

$$\Sigma(t)\equiv\beta\dot\gamma\int_0^t ds e^{i\mathcal{L}^\dagger_{\dot\gamma r}s}\sigma^{(\mathrm{pot})}_{xy}e^{-i\mathcal{L}_{\dot\gamma r}s}\tag{87}$$

is the accumulated elastic energy due to shear, where $\sigma^{(\mathrm{pot})}_{xy}$ is the potential part of the shear stress introduced in Eq. (35). As discussed in FC [30], the shear-induced term $\Sigma(t)$ is an obstacle for the application of the second projection operator and the factorization approximation. We assume here $\Sigma(t)\simeq 0$, whose validation is discussed in FC [30]. At least, this assumption is valid in the weak-shear regime, since $\Sigma(t)$ is proportional to $\dot\gamma$.

The neglect of $\Sigma(t)$ leads to the following relation,

$$e^{-i\mathcal{L}^\dagger_{\dot\gamma r}s}U_0(t,s)=\mathcal{Q}(s)e^{-i\mathcal{L}^\dagger_{\dot\gamma r}s}U_0(t,s),\tag{88}$$

whose proof is given in Appendix C 4. The first implication of Eq. (88) is the orthogonality of the random force,

$$\begin{aligned}\left\langle R^\lambda_{\boldsymbol{q}(t)}(t)\xi^*_{\boldsymbol{q}}\right\rangle&=\left\langle\left[U_0(t,0)e^{i\mathcal{L}_{\dot\gamma r}t}R^\lambda_{\boldsymbol{q}(t)}\right]\xi^*_{\boldsymbol{q}}\right\rangle\\&=\left\langle\left[\mathcal{Q}(0)U_0(t,0)e^{i\mathcal{L}_{\dot\gamma r}t}R^\lambda_{\boldsymbol{q}(t)}\right]\xi^*_{\boldsymbol{q}}\right\rangle\\&=\left\langle\left[U_0(t,0)e^{i\mathcal{L}_{\dot\gamma r}t}R^\lambda_{\boldsymbol{q}(t)}\right]\mathcal{Q}(0)\xi^*_{\boldsymbol{q}}\right\rangle=0,\end{aligned}\tag{89}$$

where $\xi=n$ or j. The second implication is the form of the aforementioned operator described in Eq. (85),

$$i\tilde{\mathcal{L}}\tilde{U}_0(t,s)R^\lambda_{\boldsymbol{q}(t)}\simeq i\tilde{\mathcal{L}}\mathcal{Q}(s)e^{-i\mathcal{L}^\dagger_{\dot\gamma r}s}U_0(t,s)e^{i\mathcal{L}_{\dot\gamma r}t}\mathcal{Q}(t)R^\lambda_{\boldsymbol{q}(t)},\tag{90}$$

which now has the desirable feature, i.e., the projection of $U_0(t,s)$ is now complete. The memory kernels, Eqs. (70) and (71), can be rewritten, from Eq. (90), as follows:

$$iL^{\lambda}_{\boldsymbol{q}}(t,s) = \frac{1}{NS_{q(t)}}\left\langle\left[\tilde{U}_0'(t,s)R^{\lambda}_{\boldsymbol{q}(t)}\right]\mathcal{Q}(s)\left[n^*_{\boldsymbol{q}(s)}\tilde{\Omega}\right]\right\rangle, \tag{91}$$

$$M^{\lambda\mu}_{\boldsymbol{q}}(t,s) = \frac{1}{Nv_T^2}\left\langle\left[\tilde{U}_0'(t,s)R^{\lambda}_{\boldsymbol{q}(t)}\right]\Delta R^{\mu *}_{\boldsymbol{q}(s)}\right\rangle. \tag{92}$$

Here,

$$\tilde{U}_0'(t,s) \equiv \mathcal{Q}(s)e^{-i\mathcal{L}^{\dagger}_{\dot{\gamma}r}s}U_0(t,s)e^{i\mathcal{L}_{\dot{\gamma}r}t}\mathcal{Q}(t) \tag{93}$$

is the modified projected time-evolution operator,

$$\Delta R^{\mu}_{\boldsymbol{q}(s)} \equiv R^{\mu}_{\boldsymbol{q}(s)} - \mathcal{Q}(s)\left[j^{\mu}_{\boldsymbol{q}(s)}\tilde{\Omega}\right] \tag{94}$$

is the modified random force, and $\tilde{\Omega}$ is the modified work function defined in Eq. (30). The derivation of the above equations, Eqs. (91)–(94), is reported in Appendix C 5.

Now we insert the second projection operator, Eq. (84), into Eqs. (91) and (92) as $\mathcal{Q}(s)e^{-i\mathcal{L}^{\dagger}_{\dot{\gamma}r}s}U_0(t,s)e^{i\mathcal{L}_{\dot{\gamma}r}t}\mathcal{Q}(t) \simeq \mathcal{P}_2(s)\mathcal{Q}(s)e^{-i\mathcal{L}^{\dagger}_{\dot{\gamma}r}s}U_0(t,s)e^{i\mathcal{L}_{\dot{\gamma}r}t}\mathcal{Q}(t)\mathcal{P}_2(t)$, which results in the following form, i.e., products of vertex functions at times s and t, bridged by a propagator from time s to t:

$$\begin{aligned} iL^{\lambda}_{\boldsymbol{q}}(t,s) \simeq{}& \frac{1}{NS_{q(t)}}\sum_{\boldsymbol{k}'>\boldsymbol{p}'}\sum_{\boldsymbol{k}>\boldsymbol{p}}\frac{\left\langle R^{\lambda}_{\boldsymbol{q}(t)}n^*_{\boldsymbol{k}(t)}n^*_{\boldsymbol{p}(t)}\right\rangle}{N^2S_{k(t)}S_{p(t)}} \\ &\times\left\langle\left[\tilde{U}_0'(t,s)n_{\boldsymbol{k}(t)}n_{\boldsymbol{p}(t)}\right]n^*_{\boldsymbol{k}'(s)}n^*_{\boldsymbol{p}'(s)}\right\rangle \\ &\times\frac{\left\langle n_{\boldsymbol{k}'(s)}n_{\boldsymbol{p}'(s)}\mathcal{Q}(s)\left[n^*_{\boldsymbol{q}(s)}\tilde{\Omega}\right]\right\rangle}{N^2S_{k'(s)}S_{p'(s)}}, \end{aligned} \tag{95}$$

$$\begin{aligned} M^{\lambda\mu}_{\boldsymbol{q}}(t,s) \simeq{}& \frac{1}{Nv_T^2}\sum_{\boldsymbol{k}'>\boldsymbol{p}'}\sum_{\boldsymbol{k}>\boldsymbol{p}}\frac{\left\langle R^{\lambda}_{\boldsymbol{q}(t)}n^*_{\boldsymbol{k}(t)}n^*_{\boldsymbol{p}(t)}\right\rangle}{N^2S_{k(t)}S_{p(t)}} \\ &\times\langle[\tilde{U}_0'(t,s)n_{\boldsymbol{k}(t)}n_{\boldsymbol{p}(t)}]n^*_{\boldsymbol{k}'(s)}n^*_{\boldsymbol{p}'(s)}\rangle \\ &\times\frac{\langle n_{\boldsymbol{k}'(s)}n_{\boldsymbol{p}'(s)}\Delta R^{\mu *}_{\boldsymbol{q}(s)}\rangle}{N^2S_{k'(s)}S_{p'(s)}}. \end{aligned} \tag{96}$$

We can see from the above expressions that the derived forms of the memory kernels are consistent with the principle of the alignment of the wave vectors; the vertex function at time t includes as indices only the advected wave vectors with argument t, e.g., $\boldsymbol{q}(t)$, and a similar feature also holds for the propagator.

The remaining tasks are the calculation of the vertex functions and the approximation of the propagators. As for the vertex functions, the convolution approximation [36] is applied. We only show the results below, since the derivation, which is reported in Appendix C 6, is straightforward:

$$\frac{\left\langle R^{\lambda}_{\boldsymbol{q}(t)}n^*_{\boldsymbol{k}(t)}n^*_{\boldsymbol{p}(t)}\right\rangle}{N^2S_{k(t)}S_{p(t)}} = -i\frac{n}{N}\delta_{\boldsymbol{q},\boldsymbol{k}+\boldsymbol{p}}V^{\lambda}_{\boldsymbol{q}(t),\boldsymbol{k}(t),\boldsymbol{p}(t)}, \tag{97}$$

$$\frac{\left\langle n_{\boldsymbol{k}(t)}n_{\boldsymbol{p}(t)}\Delta R^{\lambda *}_{\boldsymbol{q}(t)}\right\rangle}{N^2S_{k(t)}S_{p(t)}} = i\frac{n}{N}\delta_{\boldsymbol{q},\boldsymbol{k}+\boldsymbol{p}}V^{\lambda *}_{\boldsymbol{q}(t),\boldsymbol{k}(t),\boldsymbol{p}(t)}, \tag{98}$$

$$V^{\lambda}_{\boldsymbol{q},\boldsymbol{k},\boldsymbol{p}} \equiv v_T^2(k^{\lambda}c_k + p^{\lambda}c_p), \tag{99}$$

$$\frac{\langle n_{\boldsymbol{k}(t)}n_{\boldsymbol{p}(t)}\mathcal{Q}(t)[n^*_{\boldsymbol{q}(t)}\tilde{\Omega}]\rangle}{N^2S_{k(t)}S_{p(t)}} = 0. \tag{100}$$

As for the propagator, we adopt the factorization approximation, which replaces it with the product of the projection-free propagators:

$$\begin{aligned} &\frac{1}{N^2}\langle[\tilde{U}_0'(t,s)n_{\boldsymbol{k}(t)}n_{\boldsymbol{p}(t)}]n^*_{\boldsymbol{k}'(s)}n^*_{\boldsymbol{p}'(s)}\rangle \\ &\quad\simeq \delta_{\boldsymbol{k}',\boldsymbol{k}}\delta_{\boldsymbol{p}',\boldsymbol{p}}\Phi_{\boldsymbol{k}(s)}(t-s)\Phi_{\boldsymbol{p}(s)}(t-s). \end{aligned} \tag{101}$$

The derivation of Eq. (101) is reported in Appendix C 7.

From Eqs. (95)–(101), we arrive at the final expressions for the memory kernels,

$$iL^{\lambda}_{\boldsymbol{q}}(t,s) = 0, \tag{102}$$

$$\begin{aligned} M^{\lambda\mu}_{\boldsymbol{q}}(t,s) = \frac{n}{2v_T^2}\int\frac{d^3\boldsymbol{k}}{(2\pi)^3}V^{\lambda}_{\boldsymbol{q}(t),\boldsymbol{k}(t),\boldsymbol{p}(t)}V^{\mu *}_{\boldsymbol{q}(s),\boldsymbol{k}(s),\boldsymbol{p}(s)} \\ \times\Phi_{\boldsymbol{k}(s)}(t-s)\Phi_{\boldsymbol{p}(s)}(t-s), \end{aligned} \tag{103}$$

where the summation of the wave vectors is replaced by the integral, and $\boldsymbol{p} \equiv \boldsymbol{q} - \boldsymbol{k}$. Note that the memory kernel $L^{\lambda}_{\boldsymbol{q}}$ introduced by CK [26] vanishes in our formulation. This helps us to connect our formulation with the previous ones [24,25,30]. Note also that the memory kernel in Eq. (103) cannot be expressed solely in terms of the time difference $t-s$, even after the application of the mode-coupling approximation. This is in contrast to the cases of CK [26], where the memory kernels depend only on the time difference $t-s$ at the level of the Mori-type equations.

VI. STEADY-STATE PROPERTIES

In the previous sections, we have derived a set of closed equations for the time correlators $\Phi_{\boldsymbol{q}}(t)$ and $H^{\lambda}_{\boldsymbol{q}}(t)$, i.e., Eqs. (55) and (83), where the memory kernels are given by Eqs. (102) and (103). According to the integration through transient (ITT) scheme [24,28,30], the steady-state properties are written in terms of the time correlators, with equilibrium quantities (e.g., the static structure factor) as the only inputs. We follow this scheme and derive a closed formula for the steady-state quantities. In the course of this procedure, we derive an explicit expression of the multiplier $\lambda_{\alpha}(t)$ introduced in Sec. IV D. A specific formula for the steady-state shear stress is derived in Sec. VI C.

A. Time correlators of interest

From the analog of the Green-Kubo relation, Eq. (19), time correlators of interest are of the following form:

$$G_{A,B}(t) \equiv \langle A(\boldsymbol{\Gamma}(t))B(\boldsymbol{\Gamma})\rangle = \langle[U(t)A(\boldsymbol{\Gamma})]B(\boldsymbol{\Gamma})\rangle, \tag{104}$$

$$B(\boldsymbol{\Gamma}) \equiv \sigma_{xy}(\boldsymbol{\Gamma}) \quad \text{or} \quad \alpha(\boldsymbol{\Gamma})\delta K(\boldsymbol{\Gamma}). \tag{105}$$

In this paper, we concentrate on the steady-state kinetic temperature and the shear stress; i.e., we consider the specific cases, $A(\boldsymbol{\Gamma}) = K(\boldsymbol{\Gamma})$ and $\sigma_{xy}(\boldsymbol{\Gamma})$.

Similarly to the case of static projection operators [26], we can show that the time correlator, Eq. (104), resides in the subspace orthogonal to the density and the current-density fluctuations, i.e.,

$$G_{A,B}(t) = \langle[U_0(t,0)A(\boldsymbol{\Gamma})]\,B(\boldsymbol{\Gamma})\rangle, \tag{106}$$

whose proof is given in Appendix C 8.

Now we apply the second projection operator to Eq. (106). Since $B(\mathbf{\Gamma}) = \sigma_{xy}(\mathbf{\Gamma})$ and $\alpha(\mathbf{\Gamma})\delta K(\mathbf{\Gamma})$ are zero-wave-vector quantities, it is sufficient to project onto the "zero-mode" pair-density correlator,

$$\mathcal{P}_2^0(t)X \equiv \sum_{\boldsymbol{k}>0} \frac{\langle X n^*_{\boldsymbol{k}(t)} n_{\boldsymbol{k}(t)}\rangle}{N^2 S^2_{k(t)}} n_{\boldsymbol{k}(t)} n^*_{\boldsymbol{k}(t)}, \tag{107}$$

which is a restricted form of Eq. (84). The mode-coupling approximation to Eq. (106) is then

$$\begin{aligned} G_{A,B}(t) &\simeq \left\langle \left[\mathcal{P}_2^0(0)\tilde{U}_0(t,0)\mathcal{P}_2^0(t)A(\mathbf{\Gamma})\right] B(\mathbf{\Gamma})\right\rangle \\ &= \left\langle \left[\tilde{U}_0(t,0)\mathcal{P}_2^0(t)A(\mathbf{\Gamma})\right] \mathcal{P}_2^0(0)B(\mathbf{\Gamma})\right\rangle, \end{aligned} \tag{108}$$

where the Hermiticity of the projection operator $\mathcal{P}_2^0$ is applied in the last equality. Note that $\tilde{U}_0(t,0)$, rather than $U_0(t,0)$, appears due to the insertion of $\mathcal{P}_2^0(t)$.

B. Isothermal condition in MCT

To proceed further, it is necessary to calculate the explicit form of the multiplier $\lambda_\alpha(t)$ given by Eq. (80). For this purpose, we specify the form of $\alpha(\mathbf{\Gamma})$ and explicitly calculate $G_{K,\sigma}(t)$ and $G_{K,\alpha\delta K}(t)$, which are given in the mode-coupling approximation as

$$G_{K,\sigma}(t) \simeq \left\langle \left[\tilde{U}_0(t,0)\mathcal{P}_2^0(t)K(\mathbf{\Gamma})\right] \mathcal{P}_2^0(0)\sigma_{xy}(\mathbf{\Gamma})\right\rangle, \tag{109}$$

$$G_{K,\alpha\delta K}(t) \simeq \left\langle \left[\tilde{U}_0(t,0)\mathcal{P}_2^0(t)K(\mathbf{\Gamma})\right] \mathcal{P}_2^0(0)\alpha(\mathbf{\Gamma})\delta K(\mathbf{\Gamma})\right\rangle. \tag{110}$$

In the following, we examine concrete examples of $\alpha(\mathbf{\Gamma})$ and $\lambda_\alpha(t)$. The simplest choice of $\alpha(\mathbf{\Gamma})$ is to fully neglect its $\mathbf{\Gamma}$ dependence. In this case, no fluctuations are incorporated, and $\alpha(\mathbf{\Gamma})$ is a constant, which we denote α_0. However, we illustrate here that this choice always causes a heating-up of the kinetic temperature [40]. For $\alpha(\mathbf{\Gamma}) = \alpha_0$, Eq. (110) reads

$$G_{K,\alpha\delta K}(t) = \alpha_0 \left\langle \left[\tilde{U}_0(t,0)\mathcal{P}_2^0(t)K(\mathbf{\Gamma})\right] \mathcal{P}_2^0(0)\delta K(\mathbf{\Gamma})\right\rangle, \tag{111}$$

which vanishes due to $\mathcal{P}_2^0(0)\delta K(\mathbf{\Gamma}) = 0$. This implies, together with the fact that $G_{K,\sigma}(t) \neq 0$, which is shown below, that the isothermal condition, Eq. (77), cannot be satisfied. Hence, the average kinetic temperature calculated in this way is unphysical and cannot be regarded as a steady-state temperature. Note that this case is the one adopted by CK [26].

From the above argument, it is shown that, in order to retain $G_{K,\alpha\delta K}(t)$ nonvanishing, it is at least necesssary to introduce fluctuations into $\alpha(\mathbf{\Gamma})$. The simplest choice for this is to incorporate current fluctuations as

$$\alpha(\mathbf{\Gamma}) = \frac{\alpha_0}{\frac{3}{2}Nk_BT} \sum_i \frac{\boldsymbol{p}_i^2}{2m}, \tag{112}$$

where α_0 is a constant which gives the initial strength of the dissipative coupling to the thermostat. Now we calculate the projected properties $\mathcal{P}_2^0(0)[\alpha(\mathbf{\Gamma})\delta K(\mathbf{\Gamma})]$, $\mathcal{P}_2^0(0)\sigma_{xy}(\mathbf{\Gamma})$, and $\mathcal{P}_2^0(t)K(\mathbf{\Gamma})$, which appear in Eqs. (109) and (110), with the choice of Eq. (112) for $\alpha(\mathbf{\Gamma})$. Straightforward calculation leads to

$$\mathcal{P}_2^0(0)[\alpha(\mathbf{\Gamma})\delta K(\mathbf{\Gamma})] = \alpha_0 \frac{k_BT}{N} \sum_{\boldsymbol{k}>0} \frac{n_{\boldsymbol{k}} n^*_{\boldsymbol{k}}}{S_k}, \tag{113}$$

$$\mathcal{P}_2^0(t)K(\mathbf{\Gamma}) = \frac{3}{2}k_BT \sum_{\boldsymbol{k}>0} \frac{n_{\boldsymbol{k}(t)} n^*_{\boldsymbol{k}(t)}}{S_{k(t)}}, \tag{114}$$

and

$$\mathcal{P}_2^0(t)\sigma_{xy}(\mathbf{\Gamma}) = -\frac{k_BT}{N} \sum_{\boldsymbol{k}>0} \frac{W_{\boldsymbol{k}(t)}}{S_{k(t)}} n_{\boldsymbol{k}(t)} n^*_{\boldsymbol{k}(t)}, \tag{115}$$

$$W_{\boldsymbol{k}} \equiv \frac{k_x k_y}{k} \frac{1}{S_k} \frac{\partial S_k}{\partial k}, \tag{116}$$

which are derived in Appendix C 9. From Eqs. (109), (110), and (113)–(115), $G_{K,\sigma}(t)$ and $G_{K,\alpha\delta K}(t)$ are given by

$$\begin{aligned} G_{K,\sigma}(t) = -\frac{3}{2}\frac{(k_BT)^2}{N} \sum_{\boldsymbol{k}>0}\sum_{\boldsymbol{k}'>0} \frac{1}{S_{k(t)}} \frac{W_{\boldsymbol{k}'}}{S_{k'}} \\ \times \langle [\tilde{U}_0(t,0) n_{\boldsymbol{k}(t)} n^*_{\boldsymbol{k}(t)}] n_{\boldsymbol{k}'} n^*_{\boldsymbol{k}'}\rangle \end{aligned} \tag{117}$$

and

$$\begin{aligned} G_{K,\alpha\delta K}(t) = \frac{3}{2}\alpha_0\frac{(k_BT)^2}{N} \sum_{\boldsymbol{k}>0}\sum_{\boldsymbol{k}'>0} \frac{1}{S_{k(t)}} \frac{1}{S_{k'}} \\ \times \langle [\tilde{U}_0(t,0) n_{\boldsymbol{k}(t)} n^*_{\boldsymbol{k}(t)}] n_{\boldsymbol{k}'} n^*_{\boldsymbol{k}'}\rangle, \end{aligned} \tag{118}$$

respectively. Application of the factorization approximation to the four-point function reads

$$\frac{1}{N^2}\langle [\tilde{U}_0(t,0) n_{\boldsymbol{k}(t)} n^*_{\boldsymbol{k}(t)}] n_{\boldsymbol{k}'} n^*_{\boldsymbol{k}'}\rangle \simeq [\delta_{\boldsymbol{k}',\boldsymbol{k}} + \delta_{\boldsymbol{k}',-\boldsymbol{k}}]\Phi_{\boldsymbol{k}}(t)^2, \tag{119}$$

where $n^*_{\boldsymbol{k}} = n_{-\boldsymbol{k}}$, $\Phi_{-\boldsymbol{k}}(t) = \Phi_{\boldsymbol{k}}(t)$ are applied. The derivation of Eq. (119) is shown in Appendix C 7. From Eqs. (80) and (117)–(119), the functional form of the multiplier $\lambda_\alpha(t)$ should be given by

$$\lambda_\alpha(t) = \frac{\dot\gamma}{2\alpha_0} \frac{\sum_{\boldsymbol{k}>0} \frac{1}{S_{k(t)}} \frac{W_{\boldsymbol{k}}}{S_k} \Phi_{\boldsymbol{k}}(t)^2}{\sum_{\boldsymbol{k}>0} \frac{1}{S_{k(t)} S_k} \Phi_{\boldsymbol{k}}(t)^2} \tag{120}$$

in order to satisfy the constraint, Eq. (77). This can be regarded as an analog for MCT of the Gaussian isokinetic thermostat, Eq. (3), for MD.

We note here that, with the choice of Eq. (112), the second term of $\Lambda(\mathbf{\Gamma})$ in Eq. (9) reads $\sum_i [\partial\alpha(\mathbf{\Gamma})/\partial \boldsymbol{p}_i] \cdot \boldsymbol{p}_i = 2\alpha(\mathbf{\Gamma})$. This is negligible compared to the first term of Eq. (9), which is proportional to N, in the thermodynamic limit.

C. Steady-state stress formula

We define the steady-state shear stress by the steady-state stress tensor as follows:

$$\langle\sigma\rangle_{\rm SS} \equiv -\frac{1}{V}\langle\sigma_{xy}\rangle_{\rm SS}. \tag{121}$$

From the steady-state formula, Eqs. (19) and (20), and remembering that $\langle\sigma_{xy}(\mathbf{\Gamma})\rangle = 0$, the steady-state shear stress is given by the time correlators as

$$\langle\sigma\rangle_{\rm SS} = \frac{\beta\dot\gamma}{V}\int_0^\infty dt G_{\sigma,\sigma}(t) + \frac{2\beta}{V}\int_0^\infty dt G^{(\lambda)}_{\sigma,\alpha\delta K}(t), \tag{122}$$

where the time correlators $G_{\sigma,\sigma}(t)$ and $G^{(\lambda)}_{\sigma,\alpha\delta K}(t)$ are given by

$$G_{\sigma,\sigma}(t) \equiv \langle [U(t)\sigma_{xy}(\mathbf{\Gamma})]\sigma_{xy}(\mathbf{\Gamma})\rangle \tag{123}$$

and

$$\begin{aligned} G^{(\lambda)}_{\sigma,\alpha\delta K}(t) &\equiv \langle [U_R(t)\sigma_{xy}(\mathbf{\Gamma})]\alpha(\mathbf{\Gamma})\delta K(\mathbf{\Gamma})\rangle \\ &= \lambda_\alpha(t) G_{\sigma,\alpha\delta K}(t). \end{aligned} \tag{124}$$

In Eq. (124), we have introduced the multiplier $\lambda_\alpha(t)$ by applying $U_R(t)$, Eq. (78), which is required from the arguments in Sec. IV D. In the mode-coupling approximation, $G_{\sigma,\sigma}(t)$ and $G^{(\lambda)}_{\sigma,\alpha\delta K}(t)$ are approximated as

$$G_{\sigma,\sigma}(t) \simeq \left\langle \left[\tilde{U}_0(t,0)\mathcal{P}^0_2(t)\sigma_{xy}(\mathbf{\Gamma})\right]\mathcal{P}^0_2(0)\sigma_{xy}(\mathbf{\Gamma})\right\rangle \tag{125}$$

and

$$\begin{aligned} G^{(\lambda)}_{\sigma,\alpha\delta K}(t) \simeq \lambda_\alpha(t) \big\langle &\left[\tilde{U}_0(t,0)\mathcal{P}^0_2(t)\sigma_{xy}(\mathbf{\Gamma})\right] \\ &\times \mathcal{P}^0_2(0)\left[\alpha(\mathbf{\Gamma})\delta K(\mathbf{\Gamma})\right]\big\rangle, \end{aligned} \tag{126}$$

respectively. From Eqs. (113), (115), (119), (125), and (126), Eq. (122) reads

$$\langle\sigma\rangle_{\rm SS} = \frac{k_B T}{2}\int_0^\infty dt \int \frac{d^3\boldsymbol{k}}{(2\pi)^3}\frac{W_{\boldsymbol{k}(t)}}{S_{k(t)}}\frac{\dot\gamma W_{\boldsymbol{k}} - 2\lambda_\alpha(t)\alpha_0}{S_k}\Phi_{\boldsymbol{k}}(t)^2. \tag{127}$$

We can see that a correction due to the dissipative coupling, which originates in the current fluctuation incorporated in $\alpha(\mathbf{\Gamma})$, arises to the well-known formula for the overdamped case [30]. This is in contrast to the case of $\alpha(\mathbf{\Gamma}) = \alpha_0$, where the steady-state stress formula is coincident with the overdamped case [26]. Note that this correction parallels the "cooling effect" of the kinetic temperature, which compensates the "heat-up" by the shearing and keeps the kinetic temperature unchanged from its initial equilibrium value.

VII. NUMERICAL CALCULATION

To demonstrate the validity of our formulation, we show the results of the numerical calculations in this section. As is well known, it is ineffective at present to perform grid calculations for a three-dimensional system, due to limitations of computational resources. In this work, we adopt the "isotropic approximation," which has been formulated and implemented by FC [28,30] and CK [26]. The grid calculations in two-dimensional sheared Brownian systems [41,42] show that the anisotropy is relatively small, which assures the validation of this approximation, at least in two dimensions [43]. This approximation also enables us to compare formally similar equations for the underdamped and overdamped cases, as discussed in Appendix B. The details of the formulation of the isotropic approximation are well described by CK [26], so we only report the results below and make some additional remarks in Appendix D.

Sheared systems are genuinely anisotropic, which can be seen from, e.g., the existence of the anisotropic term $-[\boldsymbol{\kappa}\cdot\boldsymbol{H}_{\boldsymbol{q}}(t)]^\lambda$ in the Mori-type equation, Eq. (83). By the application of the isotropic approximation, the anisotropic terms are neglected, which allows us to obtain a single second-order equation for the density time correlator by combining Eqs. (55) and (83). The resulting (MCT) equation is

$$\begin{aligned} \frac{d^2}{dt^2}\Phi_q(t) \simeq -v_T^2\frac{\bar q(t)^2}{S_{\bar q(t)}}\Phi_q(t) - \left[\lambda_\alpha(t)\alpha_0 - \dot\gamma\frac{\frac{2}{3}\dot\gamma t}{1+\frac{1}{3}(\dot\gamma t)^2}\right] \\ \times\frac{d}{dt}\Phi_q(t) - \int_0^t ds\,\bar M_{\bar q(s)}(t-s)\frac{d}{ds}\Phi_q(s), \end{aligned} \tag{128}$$

where the memory kernel is given by

$$\begin{aligned} &\bar M_{\bar q(s)}(t-s) \\ &= \frac{n v_T^2}{2q^2}\left[1+\frac{1}{3}(\dot\gamma t)^2\right]\int\frac{d^3\boldsymbol{k}}{(2\pi)^3}[(\boldsymbol{q}\cdot\boldsymbol{k})c_{\bar k(t)} + (\boldsymbol{q}\cdot\boldsymbol{p})c_{\bar p(t)}] \\ &\quad\times[(\boldsymbol{q}\cdot\boldsymbol{k})c_{\bar k(s)} + (\boldsymbol{q}\cdot\boldsymbol{p})c_{\bar p(s)}]\Phi_{\bar k(s)}(t-s)\Phi_{\bar p(s)}(t-s). \end{aligned} \tag{129}$$

Here, $\boldsymbol{p} \equiv \boldsymbol{q} - \boldsymbol{k}$ is assumed. The notation and the derivation of Eqs. (128) and (129) are reported in Appendix D 1. Since the multiplier $\lambda_\alpha(t)$ given by Eq. (120) is a functional of $\Phi_q(t)$, Eq. (128) is solved by iteration between $\Phi_q(t)$ and $\lambda_\alpha(t)$.

A. Time correlators

In the isotropic approximation, the MCT equation Eq. (128) is numerically solved on one-dimensional spatial and temporal grids. The spatial grid is for the wave number (modulus of the wave vector). The discretized form of the memory kernel, Eq. (129), on the spatial grid is reported in Appendix D 2. For the time integration, we adopt the algorithm in Ref. [44], which enables us to calculate robustly in long time scales by gradual coarse-graining in the temporal grid. For the units of nondimensionalization, we choose the diameter d and the mass m of the sphere for the length and mass, respectively, and $\tau_0 \equiv d/v_0$, where $v_0 \equiv v_0^{(+)} - v_0^{(-)} = \dot\gamma L$ is the relative shear velocity at the two boundaries, for the time.

The conditions of the calculation are as follows. The spatial grid is chosen as $qd = \hat q\Delta$, where $\Delta = 0.4$ is the grid spacing and $\hat q = (2m-1)/2$ $(m = 1,2,\ldots,100)$ is the discretized index. The cutoff of the wave number is $q_{\rm max}d = 39.8$. The number of temporal grids is $N_t = 256$. The time step is initially $\Delta t_0 = 10^{-6}\tau_0$, which is doubled in every $N_t/2$ steps. There are three inputs; the volume fraction $\varphi \equiv \pi n d^3/6$, the static structure factor S_q, and the shear rate $\dot\gamma$. The volume fraction is expressed in terms of the "distance" from the critical volume fraction of the MCT transition in the equilibrium MCT, $\varphi_c = 0.515\,912\,13$ [45], which is denoted $\epsilon \equiv (\varphi - \varphi_c)/\varphi_c$. This definition of the distance implies $\epsilon > 0$ for the glass phase, while $\epsilon < 0$ for the liquid phase. The value of ϵ is fixed at $\epsilon = +10^{-3}$ for the calculation of the time correlator, while it is varied for the shear stress, as reported in Sec. VII B. As for the static structure factor, the analytic solution of the Percus-Yevick equation [36] for three-dimensional hard-sphere systems is adopted, whose explicit expression in the Fourier space can be found in, e.g., Ref. [46]. The initial conditions are $\Phi_q(t=0) = S_q$ and $[\partial\Phi_q(t)/\partial t]_{t=0} = 0$.

The result of the calculation is shown in Fig. 1. Here, the wave number is fixed at $qd = 7.0$ (the first, highest peak of the static structure factor; refer to Fig. 4), while the shear rate

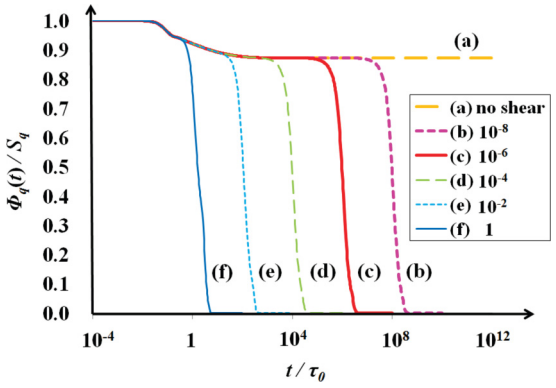

FIG. 1. (Color online) Numerical solution for the normalized density time correlator. The wave number is fixed at $qd = 7.0$ (the first, highest peak of the static structure factor), while the shear rate $\dot{\gamma}$ is varied. The lines correspond to $\dot{\gamma}\tau_0$ equal to (a) 0 (no shear), (b) 10^{-8}, (c) 10^{-6}, (d) 10^{-4}, (e) 10^{-2}, and (f) 1.

$\dot{\gamma}$ is varied. The lines correspond to $\dot{\gamma}\tau_0 = 0$ (no shear), 10^{-8}, 10^{-6}, 10^{-4}, 10^{-2}, and 1.

For comparison, we show the result for the overdamped case in Fig. 2. The MCT equation for this case is presented in Appendix B, Eq. (B8). The effective friction coefficient which appears in Eq. (B8), $\alpha_{\rm od}$, is fixed as $\alpha_{\rm od}d^2/(v_T^2\tau_0) = 0.1$. The result in Fig. 2 is qualitatively in accordance with the previous results [41,42] and almost coincident with them at the quantitative level as well.

From Figs. 1 and 2, the density time correlator decays due to shearing around the time scale $\tau_\alpha \simeq \dot{\gamma}^{-1}$ (α-relaxation time), for both the underdamped and the overdamped cases. The resemblance between the two cases can be seen not only in the α-relaxation time τ_α, but also in the NEP, which is almost coincident. These results are consistent with the observation that the long-time dynamics after the early-β-relaxation time τ_β is dominated by the memory kernel, and the instantaneous dynamics are invalid at this time scale [31–33]. The difference between the two cases can be seen at the early stage before τ_β [41]. As for the underdamped case, the density time correlator is held constant at its initial value until $t \simeq 10^{-1}\tau_0$, since the frequency of the sound wave, $\omega_q(t) \equiv$

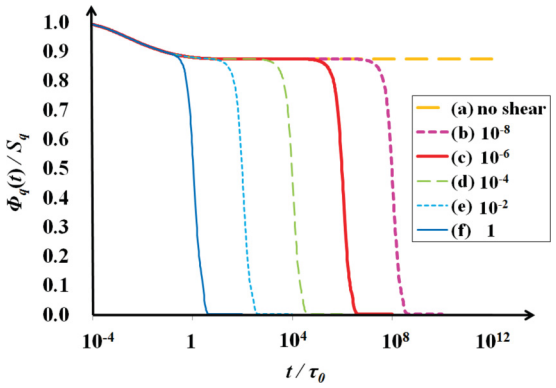

FIG. 2. (Color online) Numerical solution for the normalized density time correlator in the overdamped limit. Conditions and captions are the same as for Fig. 1.

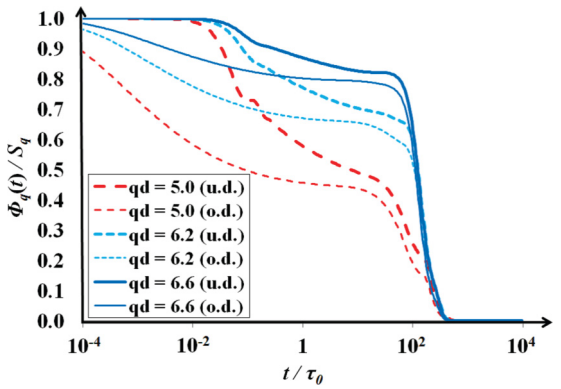

FIG. 3. (Color online) Numerical solution for the normalized density time correlator. The shear rate is fixed at $\dot{\gamma}\tau_0 = 10^{-2}$, while results for several wave numbers below the first, highest peak of the static structure factor are shown. The lines correspond to wave numbers qd of 5.0, 6.2, and 6.6. u.d., underdamped case; o.d., overdamped case.

$\sqrt{v_T^2\bar{q}(t)^2/S_{\bar{q}(t)}}$, dominates the transient behavior at this stage (for $qd = 7.0$, $\omega_q(t)^{-1} \simeq 0.27\tau_0$ at $t \ll \tau_\beta$). On the other hand, for the overdamped case, the density time correlator is already decreasing at $t \simeq 10^{-4}\tau_0$, which can be seen from its approximate solution at this stage, $\Phi_q(t) \simeq \exp[-t/\tau_{\rm od}]$, where $\tau_{\rm od} \equiv \alpha_{\rm od}S_{\bar{q}(t)}/[v_T^2\bar{q}(t)^2] = \alpha_{\rm od}/\omega_q(t)^2$ is the time scale of this damping (for $qd = 7.0$, $\tau_{\rm od} \simeq 7 \times 10^{-3}\tau_0$ at $t \ll \tau_\beta$). The emergence of two time scales is one of the significant features of the underdamped systems. In overdamped systems, there is only a single time scale which is the ratio of $\alpha_{\rm od}$ and $\omega_q(t)$, while $\lambda_\alpha(t)\alpha_0$ and $\omega_q(t)$ settle independent time scales in the underdamped case. Due to this fact, overdamped systems are scaled by a single nondimensional parameter, the Péclet number, $\mathrm{Pe} \equiv \dot{\gamma}\tau_0$, while this is not the case for the underdamped case. There are also effects of the difference on the steady-state shear stress, which is discussed in Sec. VII B.

Next, we show the results for several wave numbers in Fig. 3. The shear rate is fixed at $\dot{\gamma}\tau_0 = 10^{-2}$, and other conditions are the same as in Fig. 1. Three wave numbers below the first, highest peak of the static structure factor are chosen: $qd = 5.0$, 6.2, and 6.6. They are depicted in Fig. 4 by filled (red) circles, where the static structure factor we adopt is shown. We can see that the density time correlator is almost monotonically decreasing, except for the spike around $t \simeq 10^{-1}\tau_0$, for the underdamped case. This spike is the vestige of the oscillation of the sound wave, which is smeared out at longer time scales. In fact, there is no spike in the result for the overdamped case, which is shown in Fig. 3.

Next, we show the result for the CK theory [26] in Fig. 5, where the conditions are the same as in Fig. 3. The difference from the result of our formulation is obvious; there are significant signals of overshoot or undershoot, i.e., the normalized density time correlator exceeds 1.0 or becomes negative. For equilibrium systems, it is easy to prove that the absolute value of the normalized density time correlator is <1.0 [36] and that the density time correlator monotonically decays in the overdamped limit [2]. On the other hand, for general nonequilibrium systems, there seems to be no rigorous

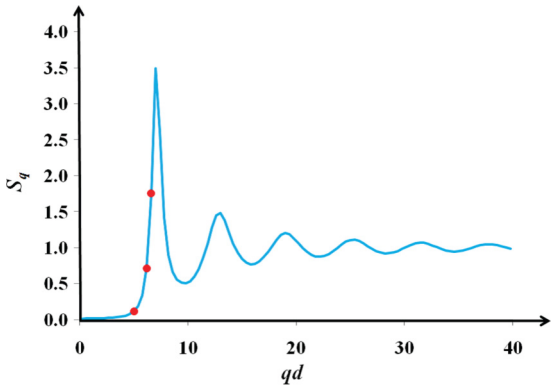

FIG. 4. (Color online) The structure factor used as an input in the calculation. The three wave numbers whose density time correlator is shown in Fig. 3 are highlighted by filled (red) circles; $qd = 5.0$, 6.2, and 6.6, from left to right. $qd = 7.0$ corresponds to the first, highest peak.

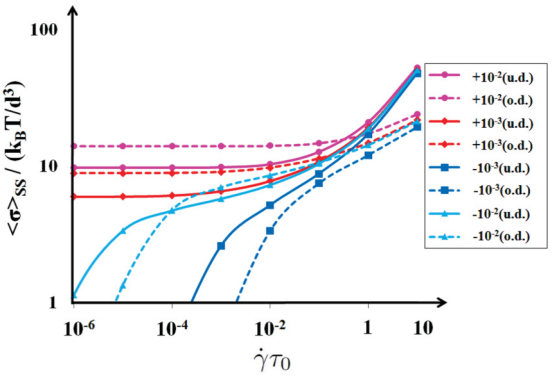

FIG. 6. (Color online) Numerical result for the steady-state shear stress, in units of $k_B T/d^3$. Solid lines represent the underdamped case; dotted lines, the overdamped case. The four lines for each case are for $\epsilon = \pm 10^{-2}, \pm 10^{-3}$, where $\epsilon \equiv (\varphi - \varphi_c)/\varphi_c$ is the distance of the volume fraction φ from the MCT transition point φ_c. u.d., underdamped case; o.d., overdamped case.

proof of the bounded property or the monotonicity of the density time correlators. However, it is natural to expect that these properties also hold as well, at least for cases with small shear. In addition, it is obvious that the overshoot or undershoot is not the result of the oscillating nature of the underdamped system. The overshoot or undershoot appears in the α-relaxation regime, where the instantaneous oscillation is already sufficiently damped. From these considerations, we conclude that the overshoot or undershoot found in CK theory [26] is an artifact of the inappropriate definition of the density time correlator. The problem of overshoot or undershoot is discussed further in Sec. VIII around Eq. (135).

B. Shear stress

Now we present the result for the steady-state shear stress in units of $k_B T/d^3$, where d is the diameter of the sphere, in Fig. 6, which is calculated from the solution of the density time correlator by Eq. (127). The conditions are the same as in Sec. VII A, aside from two exceptions. One is the strength of the thermostat in the overdamped case $\alpha_{\rm od}$, which is fixed at $\alpha_{\rm od} d^2/(v_T^2 \tau_0) = 1$ here. This value is chosen to

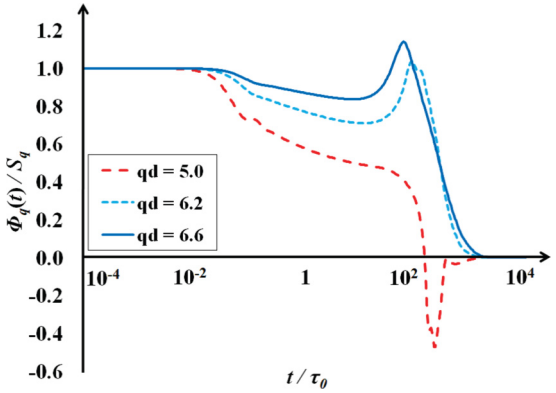

FIG. 5. (Color online) Numerical solution for the normalized density time correlator of the theory of Chong and Kim [26]. The conditions are the same as for Fig. 3.

conform with the previous work [24] which is the direct reference for our calculation. Another is the volume fraction, where four cases, $\epsilon = \pm 10^{-2}$, $\pm 10^{-3}$, are considered for underdamped and overdamped cases, respectively. The results for the underdamped case are shown by solid lines, while those for the overdamped case are shown by dotted lines.

As discussed in Sec. VII A, underdamped systems are not scaled by a single parameter, the Péclet number Pe, in contrast to overdamped systems. Hence, we choose as the horizontal axis the nondimensionalized shear rate, $\dot{\gamma}\tau_0$.

The results for the overdamped case reproduce those found in Ref. [24]. We can see from Fig. 6 that the underdamped case shows similar tendencies to the overdamped case. That is, in the liquid phase with $\epsilon < 0$, the shear stress shows the Newtonian behavior, $\sigma_{xy} \propto \dot{\gamma}$, for small shear rates. For large shear rates, the above linearity is broken, which signals "shear thinning." In the glass phase with $\epsilon > 0$, the shear stress remains finite in the limit $\dot{\gamma} \to 0$, which is nothing but the yield stress.

At the quantitative level, however, discrepancies can be observed. For high shear rates, e.g., $\dot{\gamma}\tau_0 > 1.0$, the shear stress is larger for the underdamped case. This is because the density time correlator is held constant in the short-time regime $t < 0.1\tau_0$ due to the inertia effect in the underdamped case, while it is already decreasing in the overdamped case, as previously discussed.

On the other hand, for low shear rates, the yield stress which emerges in the glass phase ($\epsilon > 0$) is smaller for the underdamped case. This is due to the analog of the "cooling effect," which is explained after Eq. (127). To prove this statement, the accumulated shear stress as a function of time, which we define by

$$\langle\sigma(t)\rangle \equiv \frac{k_B T}{2} \int_0^t ds \int \frac{d^3\boldsymbol{k}}{(2\pi)^3} \frac{W_{k(s)}}{S_{k(s)}} \times \frac{\dot{\gamma} W_{\boldsymbol{k}} - 2\lambda_\alpha(s)\alpha_0}{S_k} \Phi_{\boldsymbol{k}}(s)^2, \tag{130}$$

is shown in Fig. 7, and the multiplier $\lambda_\alpha(t)$, given by Eq. (120), is shown in Fig. 8, for the case $\epsilon = +10^{-3}$ and $\dot{\gamma}\tau_0 = 10^{-4}$,

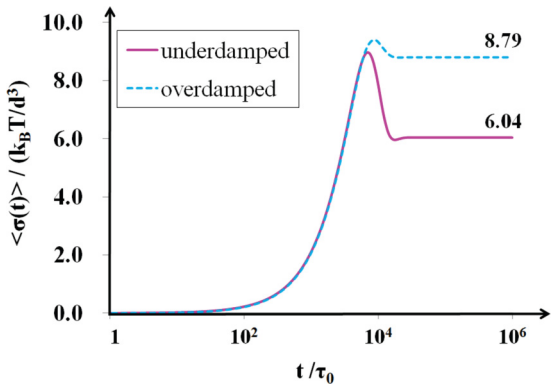

FIG. 7. (Color online) Numerical result for the accumulated steady-state shear stress $\langle\sigma(t)\rangle$, Eq. (130), in units of k_BT/d^3. The two lines are for the underdamped and overdamped cases, respectively, for $\epsilon = +10^{-3}$ and $\dot{\gamma}\tau_0 = 10^{-4}$. The steady-state value of the shear stress is indicated for each line.

respectively. In Fig. 7, the steady-state value of the shear stress is attatched to each result. We can see that the discrepancy between the underdamped and the overdamped cases arises in the α-relaxation regime, $t \sim \dot{\gamma}^{-1} = 10^4\tau_0$. It is notable that the multiplier $\lambda_\alpha(t)$ correspondingly magnifies in this regime, which suggests the growth of the current fluctuation incorporated in $\alpha(\mathbf{\Gamma})$. This implies that the growth of the current fluctuation in the dissipative coupling results in a significant relaxation of the shear stress in the underdamped case. It might also be worth noting that the density time correlators are almost coincident in the α-relaxation regime for the underdamped and overdamped cases. However, in the underdamped case, the time derivative of the density time correlator is nothing but the density-current cross time correlator, Eq. (B2), which also exhibits growth in the α-relaxation regime. This is an additional evidence that the current fluctuation incorporated in $\alpha(\mathbf{\Gamma})$ is the origin of the stress relaxation.

Now it is clear why the correction in Eq. (127) appears in the vertex function; since it originates in the current fluctuation, it cannot appear in the density time correlator, which leaves the vertex function as the only possibility. Together with the fact

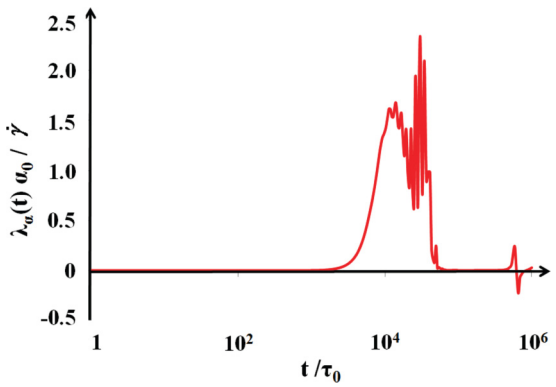

FIG. 8. (Color online) Numerical result for the mutiplier $\lambda_\alpha(t)$. We plot $\lambda_\alpha(t)\alpha_0$ in units of $\dot{\gamma}$. Conditions are the same as for Fig. 7.

that the correction is actually the multiplier, Eq. (120), which is written in terms of the density time correlator.

It is remarkable that the existence of a discrepancy between the overdamped MCT and the MD simulation, which has an inertia effect in the α-relaxation regime, has been reported [35]. Our result presented here suggests that the discrepancy is quite generic. Thus, we should be careful in comparing the results of MD with overdamped dynamics, such as Brownian dynamics or the overdamped MCT.

C. Response to a perturbation

As an application of the underdamped MCT so far constructed, we calculate the response of the density time correlator to a perturbation of the shear rate and demonstrate the significance of the underdamped formulation. We discuss a response to an instantaneous change in the shear rate $\dot{\gamma}$ at quasi–steady state which corresponds to the plateau of the density time correlator at $t = t_0$. Specifically, we consider a pulse-like perturbation of the form

$$\dot{\gamma}(t) = \dot{\gamma} + \Delta\dot{\gamma}[\Theta(t - t_0) - \Theta(t - (t_0 + \Delta t_{\dot{\gamma}}))], \quad (131)$$

where $\Delta t_{\dot{\gamma}}$ is the width of a rectangular pulse, $\Theta(t)$ is Heaviside's step function, and t_0 is of the order of the early-β-relaxation time, $t_0 \sim \tau_\beta$.

For a time-dependent external field (the shear rate in our case), the time-evolution operator is expressed in terms of a time-ordered exponential [27], and hence we cannot simply apply the MCT formulated in this paper, which is valid for a constant shear rate. However, for a pulse-like perturbation, it can be shown that the time-ordered exponential reduces to a *normal* exponential for the case of a weak and instantaneous perturbation, i.e., $\Delta\dot{\gamma}/\dot{\gamma} \ll 1$ and $\Delta t_{\dot{\gamma}}/(t - t_0) \ll 1$. In this case, the time-evolution operator $U_\rightarrow(t_0,t)$ can be expanded as

$$U_\rightarrow(t_0,t) = e^{i\mathcal{L}(\Delta\dot{\gamma})(t-t_0)} + \mathcal{O}(\Delta\dot{\gamma}^2(t - t_0)^2), \quad (132)$$

where $i\mathcal{L}(\Delta\dot{\gamma})$ is the perturbed Liouvillian, whose shear part $i\mathcal{L}_{\dot{\gamma}} \equiv \dot{\gamma} i\tilde{\mathcal{L}}_{\dot{\gamma}}$, $i\tilde{\mathcal{L}}_{\dot{\gamma}} \equiv \sum_{i=1}^N \left(y_i\partial/\partial x_i - p_i^y\partial/\partial p_i^x\right)$ is given by

$$i\mathcal{L}_{\dot{\gamma}}(\Delta\dot{\gamma}) = \tilde{\dot{\gamma}}(t) i\tilde{\mathcal{L}}_{\dot{\gamma}}, \quad (133)$$

$$\tilde{\dot{\gamma}}(t) \equiv \dot{\gamma}\left\{1 + \frac{\Delta\dot{\gamma}}{\dot{\gamma}}\frac{\Delta t_{\dot{\gamma}}}{t - t_0}\Theta(t - (t_0 + \Delta t_{\dot{\gamma}}))\right\}. \quad (134)$$

That is, we can apply the MCT formulated for a *normal* exponential, together with a time-dependent shear rate, Eq. (134).

The conditions of the calculation are as follows. The time when the perturbation is switched on, i.e., t_0, is set to the order of the early-β-relaxation time $\tau_\beta \sim 10^2\tau_0$. This choice is made by the observation that the onset of the plateau of the density time correlator is around $10^2\tau_0$, which is shown in Fig. 1. The shear rate and its magnitude of perturbation are set to $\dot{\gamma} = 10^{-4}\tau_0$ and $\Delta\dot{\gamma}/\dot{\gamma} = 0.1$, respectively. Note that the α-relaxation time is $\tau_\alpha \sim \dot{\gamma}^{-1} = 10^4\tau_0$, and hence the quasi–steady state lasts for a time interval of $99t_0$. The initial time step is set to $\Delta t_0 = 10^{-6}\tau_0$, which is doubled every 4096 steps ($N_t = 8192$). The width of the pulse is set to $\Delta t_{\dot{\gamma}} = \Delta t_0$, which is small enough compared to the time scale of the response. Hence, the shear rate Eq. (134) is pulse-like at this time scale.

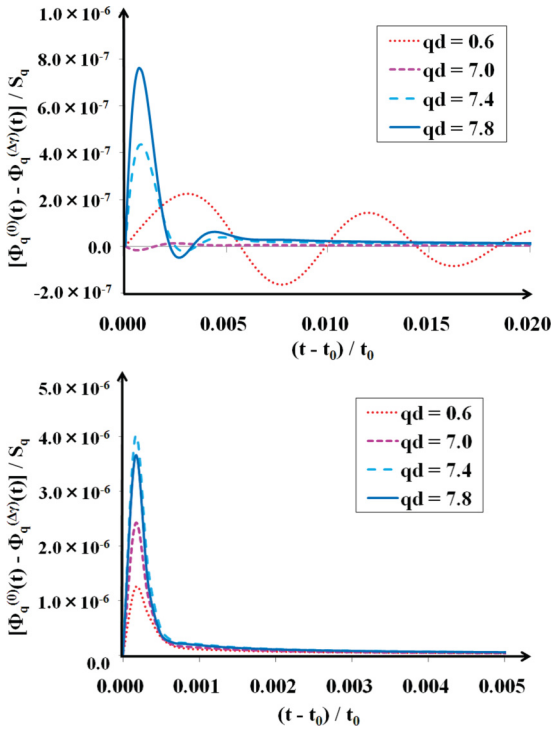

FIG. 9. (Color online) Response of the density time correlator. Top: Underdamped case. Bottom: Overdamped case. The four lines correspond to nondimensionalized wave numbers $qd = 0.6$, 7.0, 7.4, and 7.8.

The result for the response of the normalized density time-correlator, $-[\Phi_q^{(\Delta\dot{\gamma})}(t) - \Phi_q^{(0)}(t)]/S_q$, is shown in Fig. 9, for both the underdamped and the overdamped cases. Here, $\Phi_q^{(\Delta\dot{\gamma})}(t)$ and $\Phi_q^{(0)}(t)$ are the perturbed and the unperturbed density time correlators, respectively, and the sign convention is chosen simply for convenience. We can see that, in the underdamped case, there is a delay in the emergence of the response, and an oscillation of period typically of the order of $5 \times 10^{-3} t_0$ can be seen. This feature is due to the inertia effect of the underdamped system. On the other hand, in the overdamped case, the response emerges instantaneously and then decays with the relaxation time $10^{-3} t_0$. Hence, even though the density plateau coincides for the underdamped and overdamped cases, a clear difference can be observed in the response at this quasi–steady state.

The result of this subsection can be further applied to the response theory. The formulation and calculation of the response of the shear stress to a perturbation of the shear rate are presented in Appendix A.

VIII. DISCUSSION

In this section, we first compare our work with the previous works. To the best of our knowledge, the major representative works in sheared MCTs are Fuchs-Cates1 (FC1) [24,28], Fuchs-Cates2 (FC2) [30], Miyazaki *et al.* [25,41], CK [26], and HO [21]. Besides HO, which is formulated for inelastic granular systems, they are for sheared Brownian or thermostated systems. The relations among the above theories might be confusing, so we briefly review their basic setups and then discuss the resulting formulations.

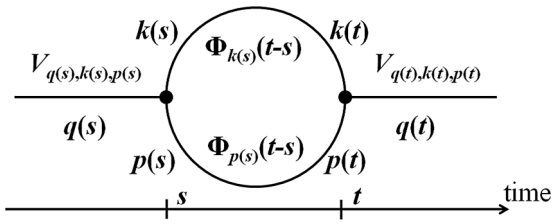

FIG. 10. Schematic of the structure of the memory kernel in our formulation. The kernels in the theories of Fuchs and Cates [30] and Miyazaki *et al.* [25,41] also have the same structure.

The FC theories, FC1 and FC2, are for overdamped systems whose dynamics is governed by the Smoluchowski operator. In FC1, the density time correlator is defined as $\Phi_{\boldsymbol{q}}^{(\mathrm{FC1})}(t) \equiv \langle n_{\boldsymbol{q}}(t) n^*_{\boldsymbol{q}(t)}(0)\rangle/N$, with $\boldsymbol{q}(t) \equiv \boldsymbol{q} + \boldsymbol{q}\cdot\boldsymbol{\kappa} t$. It is discussed in Ref. [30] that the application of MCT to the above time correlator leads to non-positive-definite "initial decay rates," which causes numerical instabilities. This has motivated the modification which leads to FC2. In FC2, the density time correlator is defined as $\Phi_{\boldsymbol{q}}^{(\mathrm{FC2})}(t) \equiv \langle n_{\boldsymbol{q}(t)}(t) n^*_{\boldsymbol{q}}(0)\rangle/N$, with $\boldsymbol{q}(t) \equiv \boldsymbol{q} - \boldsymbol{q}\cdot\boldsymbol{\kappa} t$, which is identical to our definition. Moreover, the resulting MCT equation is also formally correspondent if we neglect the transverse mode (or adopt the isotropic approximation) and take the overdamped limit (i.e., neglect the inertia term) in our framework; refer to Appendix B for this issue. Hence, our formulation can be regarded as an extension of that of FC2 to underdamped systems. To be more concrete, the initial decay rate $\Gamma_{\boldsymbol{q}}(t) \equiv \boldsymbol{q}(t)^2 v_T^2/S_{q(t)}$ is properly advected, and the memory kernel possesses the structure of wave-vector indices depicted schematically in Fig. 10; i.e., the memory kernel consists of vertex functions with wave-vector indices advected to time s, $V_{\boldsymbol{q}(s),\boldsymbol{k}(s),\boldsymbol{k}(s)}$, and time t, $V_{\boldsymbol{q}(t),\boldsymbol{k}(t),\boldsymbol{p}(t)}$, respectively, which are bridged by a projection-free propagator starting from time s with interval $t - s$, e.g., $\Phi_{\boldsymbol{k}(s)}(t - s)$. These features seem physically sensible, which manifests the alignment of the wave vectors which we adopt as a principle in Secs. III C and IV C. As discussed in Ref. [30], note that the application of the time-dependent projection operators enables the preservation of this principle.

The CK theory starts with a microscopic framework almost-identical to ours; i.e., an underdamped Sllod equation governed by a Liouvillian. The crucial difference at this level is that the dissipative coupling to the thermostat is a constant, while it contains current fluctuations in order to satisfy the isothermal condition in our framework. At the level of the Mori-type equations, another crucial difference is that the time correlators are defined as equivalent to FC1, e.g., $\Phi_{\boldsymbol{q}}^{(\mathrm{CK})}(t) = \Phi_{\boldsymbol{q}}^{(\mathrm{FC1})}(t)$ for the density time correlator, which are inequivalent to our definition. The conventional static projection operators are applied, and the resulting MCT equation differs from ours in two respects: (a) it breaks the alignment of the wave vectors, and (b) the memory kernel $L^{\lambda}_{\boldsymbol{q}}$ survives. The feature (a) can be seen in (i) the initial decay rate $\Gamma_{\boldsymbol{q}}^{(\mathrm{CK})} \equiv q^2 v_T^2/S_q$, which is not advected; (ii) the memory kernel, which has the structure of wave-vector indices depicted schematically in Fig. 11; and, probably most significantly, (iii)

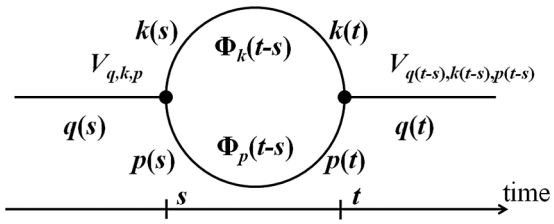

FIG. 11. Schematic of the structure of the memory kernel in the theory of Chong and Kim [26].

the wave-vector structure of the time integration, which reads

$$\int_0^t ds M_q(t-s)\frac{\partial}{\partial s}\Phi_{\bar{q}(t-s)}(s) \tag{135}$$

in the isotropic approximation. The advection of the wave-number index appears in the *time derivative* of the density time correlator, while it appears in the memory kernel in our framework [cf. Eq. (128)]. Numerically, the overshoot or undershoot found in the CK theory is a consequence of the term $\partial\Phi_{\bar{q}(t-s)}(s)/\partial s$, which shows a singular behavior when the advected wave number passes the first peak of the static structure factor. On the other hand, since the memory kernel includes only the density time correlator, not its time derivative, a singular behavior is not found in our result. As for feature (b), the memory kernel $L_{\boldsymbol{q}}^{\lambda}$ has been confirmed to be numerically negligible [26], at least for the situation of concern, which is compatible with our result, $L_{\boldsymbol{q}}^{\lambda}=0$.

In Miyazaki *et al.* [25,41], an alternative approach is adopted. They start with a generalized fluctuating hydrodynamics for the density and the velocity fields with a Gaussian noise. Aside from the drawbacks of this approach, which have been discussed [e.g., (i) the assumption of the fluctuation-dissipation theorem, which is known not to hold in sheared systems, and (ii) the formulation based on the steady-state fluctuations], the resulting MCT parallels that derived by the projection operator formalism. The time correlators are defined in accordance with our work and FC2, and it turns out that the MCT equation for the density time correlator in the overdamped limit coincides with that in FC2.

Next we discuss the novelties which result from our framework. First, a pronounced relaxation of the shear stress at the α-relaxation regime compared to the overdamped case is a genuine feature of our underdamped formulation. This result fills the gap between the MD simulation and the overdamped MCT reported in Ref. [35], where the overdamped MCT underestimates the "stress overshoot." In our underdamped fomulation, this gap is naturally interpreted as a result of the "cooling effect," which is accompanied by the growth of current fluctuations, which is not considered in the overdamped case. In the overdamped case, it might be possible to incorporate density fluctuations into the dissipative coupling $\alpha_{\rm od}$, but this does not lead to a relaxation of the shear stress discussed here.

Second, as demonstrated in Sec. VII C, we consider an application to the calculation of a response. In addition, in Appendix A we report the corresponding response of the stress tensor, which is formulated by the response of the density time correlator. From these results, it can be seen that although there is no difference in the plateau of the density time correlator for the underdamped and overdamped cases in the absence of a perturbation, there is a clear difference in the short-time response to a perturbation for the two cases. This is more clear evidence for the relevance of using the underdamped model even in glassy systems, where the dynamics is expected to be slow and neither the effects of current fluctuations nor those of inertia are believed to be irrelevant.

Another virtue of the present framework is that its extension to other systems, such as an assembly of granular particles, is relatively simple. One just has to replace the coupling to the thermostat [the term $-\alpha(\mathbf{\Gamma})\boldsymbol{p}_i(t)$ in Eq. (2)] with, e.g., interparticle viscous interactions of the Stokes' type. In fact, it is difficult to incorporate viscous interactions inherent in granular materials into the formulation of either FC [24,28,30] or Miyazaki *et al.* [25,41]. Dissipation has been introduced in the MCT by HO [21] and Kranz *et al.* [22], but they seem not to be satisfactory. As for HO, which deals with sheared granular systems, dissipation is introduced by the inelastic Boltzmann operator, i.e., the pseudo-Liouvillian [47]. The model considered by Kranz *et al.* [22] is for a driven granular system under a white-noise thermostat, which does not have any advected wave number. Moreover, the connection between the model of Kranz *et al.* and actual vibrating granular systems is unclear. The application of the MCT formulated here to sheared granular fluids is now in progress [23,37]. We have already found some remarkable features in the MCT for sheared granular fluids, where the projection onto the density-current mode plays an important role in destructing the plateau of the density time correlator [23]. Details will be reported elsewhere [37].

IX. SUMMARY AND CONCLUDING REMARKS

In this paper, we have constructed a nonequilibrium MCT for uniformly sheared *underdamped* systems. For such systems, the theory of CK [26] has been known, but the discrepancies with the theory of FC [30] in the overdamped limit have been left unresolved. We have figured out that the formulation of CK is physically not sensible; i.e., it does not satisfy the translational invariance in the sheared frame and leads to peculiar overshoot or undershoot of the density time correlator. We have performed a reformulation, starting from the redefinition of the time correlators to satisfy the alignment of the wave vectors, which is a consequence of the translational invariance. The resulting MCT equation preserves this alignment, coincides with that of FC in the overdamped limit, and avoids peculiar overshoot or undershoot in the density time correlator. Furthermore, motivated by the observation that the constant dissipative coupling to the thermostat does not lead to a steady-state kinetic temperature, we have implemented the isothermal condition at the level of the Mori-type equations. It is essential to incorporate current fluctuations in the dissipative coupling to satisfy the isothermal condition. Hence, it may well be said that we have nontrivially extended the FC theory to underdamped systems in a physically sensible way.

Although it has been believed that the equivalence of long-time dynamics in underdamped and overdamped systems (e.g., the NEP and the scaling properties of the density time

correlator at α relaxation) also holds for sheared systems, we have figured out two deviations of the underdamped from the overdamped case. These are the pronounced relaxation of the shear stress in the α-relaxation regime due to the "cooling effect," accompanied by the growth of current fluctuations in the dissipative coupling to the thermostat, and the short-time response to a perturbation of the shear rate. These findings are the genuine features of our underdamped formulation, which cannot be derived from the conventional overdamped framework. We also stress that our formulation provides a physically natural explanation to the discrepancy between MD and the overdamped MCT reported in Ref. [35].

An attractive feature of our formulation is that it is relatively simple to extend to granular systems. In these strongly nonequilibrium, nonlinear systems, genuine features of the underdamped dynamics are also expected to be observed. The construction of the theory and its numerical analysis is under investigation and will be published elsewhere [23,37].

ACKNOWLEDGMENTS

Numerical calculations in this work were carried out at the computer facilities at the Yukawa Institute and Canon Inc. The authors are grateful to S.-H. Chong, M. Otsuki, and G. Szamel for stimulating discussions and careful reading of the manuscript. They also thank K. Miyazaki for his kind advice and comments, M. Fuchs for his useful comments and provision of the information in Ref. [35] to the authors, and Canon Inc. for hosting of the collaboration. K.S. is also grateful to Mr. Shinjo, Mr. Nagane, and the members of the Analysis Technology Development Department 1 for their assistance.

APPENDIX A: APPLICATION TO THE RESPONSE THEORY

In this Appendix we apply the MCT to the calculation of the response formula for the stress tensor. We discuss a response to an instantaneous change in the shear rate $\dot\gamma$ at the quasi–steady state which corresponds to the plateau of the density time correlator at $t = t_0$, where t_0 is of the order of the early-β-relaxation time, τ_β. We consider a pulse-like perturbation identical to the one specified in Eq. (131) in Sec. VII C. For a time-reversible thermostated system, $\dot\gamma^{-1}$ is of the order of the α-relaxation time, $\dot\gamma\tau_\alpha \sim 1$. On the other hand, there is a large hierarchy between these two times in the weakly sheared case, $\tau_\beta \ll \tau_\alpha$, and hence $\dot\gamma t_0 \ll 1$ holds. In the remainder, we perform expansions with $\dot\gamma t_0$ and neglect terms with order $\mathcal{O}(\dot\gamma^2 t_0^2)$.

1. Formulation

We first formulate a response formula of the stress tensor. We consider a response of the stress tensor at $t > t_0 + \Delta t_{\dot\gamma}$,

$$\delta\sigma_{xy}(\mathbf{\Gamma}(t)) \equiv \sigma_{xy}^{(\Delta\dot\gamma)}(\mathbf{\Gamma}(t)) - \sigma_{xy}^{(0)}(\mathbf{\Gamma}(t)), \tag{A1}$$

where $\sigma_{xy}^{(\Delta\dot\gamma)}(\mathbf{\Gamma}(t))$ and $\sigma_{xy}^{(0)}(\mathbf{\Gamma}(t))$ are the perturbed and the unperturbed stress tensor, respectively. Our aim is to derive a formula for the statistical average of this quantity at the quasi–steady state. In the absence of perturbation, the average of a phase-space variable $A(\mathbf{\Gamma}(t))$ at the quasi–steady state is given by

$$\langle A(\mathbf{\Gamma}(t))\rangle_{\rm SS} = \int d\mathbf{\Gamma}(t_0)\rho_{\rm SS}(\mathbf{\Gamma},t_0)A(\mathbf{\Gamma}(t)) \tag{A2}$$

for $t > t_0$, where [27,48]

$$\rho_{\rm SS}(\mathbf{\Gamma},t_0) \equiv \rho_{\rm eq}(\mathbf{\Gamma})\exp\left[\int_0^{t_0} ds\,\Omega_0(\mathbf{\Gamma}(-s))\right] \tag{A3}$$

is the distribution function of the quasi–steady state, expressed in terms of the initial equilibrium distribution function $\rho_{\rm eq}(\mathbf{\Gamma})$ and the unperturbed work function $\Omega_0(\mathbf{\Gamma}(t))$. The unperturbed work function is given by

$$\Omega_0(\mathbf{\Gamma}) = -\beta\dot\gamma\sigma_{xy}^{(0)}(\mathbf{\Gamma}) - 2\beta\alpha(\mathbf{\Gamma})\delta K(\mathbf{\Gamma}), \tag{A4}$$

where we include only the conservative part, $-\beta\Delta\dot\gamma\sigma_{xy}^{(0)}(\mathbf{\Gamma})$, in the perturbation of the work function. While the conservative part of the work function is $\mathcal{O}(\dot\gamma)$, the dissipative part, $-2\beta\alpha(\mathbf{\Gamma})\delta K(\mathbf{\Gamma})$, is $\mathcal{O}(\dot\gamma^2 t)$. This can be seen from the fact that $\alpha(\mathbf{\Gamma})$ is accompanied by the time-evolution operator $U_R(t)$ given by Eq. (78), where $\lambda_\alpha(t)$ is given by Eq. (120), and the fact that the isotropic part of $k^x k^y$ is of the order of $\mathcal{O}(\dot\gamma t)$. Hence, the following equality holds:

$$\Omega_0(\mathbf{\Gamma}) = -\beta\dot\gamma\sigma_{xy}^{(0)}(\mathbf{\Gamma}) + \mathcal{O}(\dot\gamma^2 t), \tag{A5}$$

which validates the approximation mentioned above. We should note that $\dot\gamma t \ll 1$ holds, since $t \sim t_0$.

Then the average of the response of the stress tensor at the quasi–steady state is given by

$$\langle\delta\sigma_{xy}(\mathbf{\Gamma}(t))\rangle_{\rm SS} = \int d\mathbf{\Gamma}(t_0)\rho^{(\Delta\dot\gamma)}(\mathbf{\Gamma},t_0+\Delta t_{\dot\gamma})\delta\sigma_{xy}(\mathbf{\Gamma}(t)) + \mathcal{O}(\Delta\gamma^2) \tag{A6}$$

for $t > t_0 + \Delta t_{\dot\gamma}$, where

$$\rho^{(\Delta\dot\gamma)}(\mathbf{\Gamma},t_0+\Delta t_{\dot\gamma}) = \rho_{\rm SS}(\mathbf{\Gamma},t_0)\left\{1 - \beta\frac{\Delta\gamma}{\Delta t_{\dot\gamma}}\int_0^{\Delta t_{\dot\gamma}} ds\,\sigma_{xy}^{(0)}(\mathbf{\Gamma}(t_0-s))\right\} \tag{A7}$$

is the perturbed distribution function at $t = t_0 + \Delta t_{\dot\gamma}$. Here, $\Delta\gamma$ is the strain generated by the perturbation,

$$\Delta\gamma \equiv \Delta\dot\gamma\,\Delta t_{\dot\gamma}, \tag{A8}$$

which we fix at a small value $\Delta\gamma \ll 1$ and take the limit $\Delta t_{\dot\gamma} \to 0$ later.

The linear response of the stress tensor is given from Eq. (A6) by

$$\begin{aligned}
&\left[\frac{\partial}{\partial\Delta\gamma}\langle\delta\sigma_{xy}(\mathbf{\Gamma}(t))\rangle_{\rm SS}\right]_{\Delta\gamma=0} \\
&= -\frac{\beta}{\Delta t_{\dot\gamma}}\int d\mathbf{\Gamma}(t_0)\rho_{\rm SS}(\mathbf{\Gamma},t_0)\delta\sigma_{xy}(\mathbf{\Gamma}(t)) \\
&\quad\times\int_0^{\Delta t_{\dot\gamma}} ds\,\sigma_{xy}^{(0)}(\mathbf{\Gamma}(t_0-s)) \\
&= -\frac{\beta}{\Delta t_{\dot\gamma}}\int d\mathbf{\Gamma}(t_0)\int_0^{\Delta t_{\dot\gamma}} ds\,\rho_{\rm SS}(\mathbf{\Gamma},t_0-s) \\
&\quad\times\delta\sigma_{xy}(\mathbf{\Gamma}(t+s))\sigma_{xy}^{(0)}(\mathbf{\Gamma}(t_0)) \\
&\simeq -\beta\left\langle\delta\sigma_{xy}(\mathbf{\Gamma}(t))\sigma_{xy}^{(0)}(\mathbf{\Gamma}(t_0))\right\rangle_{\rm SS},
\end{aligned} \tag{A9}$$

where, in the final equality, we have utilized the fact that the pulse width is sufficiently small, $\Delta t_{\dot\gamma} \ll t_0$, which validates the following approximations: $\rho_{\rm SS}(\mathbf{\Gamma}, t_0 - s) \simeq \rho_{\rm SS}(\mathbf{\Gamma}, t_0)$ and $\delta\sigma_{xy}(\mathbf{\Gamma}(t+s)) \simeq \delta\sigma_{xy}(\mathbf{\Gamma}(t))$ $(0 \leqslant s \leqslant \Delta t_{\dot\gamma})$. Note that Eq. (A9) is equivalent to the conventional linear response formula [49] if the steady state is sufficiently close to equilibrium.

2. Steady-state distribution function

The response formula, Eq. (A9), is still merely a formal expression, and additional approximations are necessary to perform a concrete calculation. In this section we derive an approximate expression for the distribution function of the quasi–steady state, Eq. (A3), under a weakly sheared condition.

It is notable that $\rho_{\rm SS}(\mathbf{\Gamma}, t_0)$ can be rewritten as [48,50]

$$\rho_{\rm SS}(\mathbf{\Gamma}, t_0) = \rho_{\rm eq}(\mathbf{\Gamma}) \exp\left[\tfrac{1}{2}\left(\langle\Theta_-\rangle_{\boldsymbol{\gamma};0} + \langle\Theta_+\rangle_{\boldsymbol{\gamma};t_0}\right)\right] + \mathcal{O}\left(\dot\gamma^3 t_0^3\right), \tag{A10}$$

where $\Theta_\pm$ is defined as $\Theta_\pm \equiv \int_0^{t_0} dt\, \Omega_0(\mathbf{\Gamma}(\pm t))$, and $\langle\cdots\rangle_{\boldsymbol{\gamma};t_0}$, $\langle\cdots\rangle_{\boldsymbol{\gamma};0}$ are the "conditioned averages." Refer to Eqs. (3.2) and (3.3) of Ref. [48] for their definition. By expanding the Liouvillian as $i\mathcal{L} = i\mathcal{L}_0 + \mathcal{O}(\dot\gamma)$, $\mathbf{\Gamma}(t) = \mathbf{\Gamma}_0(t) + \mathcal{O}(\dot\gamma t)$ holds, where $\mathbf{\Gamma}_0(t) \equiv e^{i\mathcal{L}_0 t}\mathbf{\Gamma}(0)$. Then the two conditioned averages which appear in Eq. (A10) can be expanded in terms of $\dot\gamma$ as

$$\int_0^{t_0} ds\, \langle\Omega_0(\mathbf{\Gamma}(-s))\rangle_{\boldsymbol{\gamma};0} = \int_0^{t_0} ds\, \langle\Omega_0(\mathbf{\Gamma}_0(-s))\rangle_{\boldsymbol{\gamma};0} + \mathcal{O}\left(\dot\gamma^2 t_0^2\right), \tag{A11}$$

$$\int_0^{t_0} ds\, \langle\Omega_0(\mathbf{\Gamma}(s))\rangle_{\boldsymbol{\gamma};t_0} = \int_0^{t_0} ds\, \langle\Omega_0(\mathbf{\Gamma}_0(s))\rangle_{\boldsymbol{\gamma};t_0} + \mathcal{O}\left(\dot\gamma^2 t_0^2\right), \tag{A12}$$

where $\Omega_0 = \mathcal{O}(\dot\gamma)$ should be reminded. Note that the phase-space point which appears in the conditioned averages are $\mathbf{\Gamma}_0(0)$ and $\mathbf{\Gamma}_0(t_0)$ for $\langle\cdots\rangle_{\boldsymbol{\gamma};0}$ and $\langle\cdots\rangle_{\boldsymbol{\gamma};t_0}$, respectively. As in Ref. [48], we can show that

$$\int_0^{t_0} ds \langle\Omega_0(\mathbf{\Gamma}_0(-s))\rangle_{\boldsymbol{\gamma};0} = \int_0^{t_0} ds\, \langle\Omega_0(\mathbf{\Gamma}_0(s))\rangle_{\boldsymbol{\gamma};t_0}. \tag{A13}$$

From Eqs. (A11)–(A13), the following approximation holds:

$$\int_0^{t_0} ds\, \langle\Omega_0(\mathbf{\Gamma}(s))\rangle_{\boldsymbol{\gamma};t_0} = \int_0^{t_0} ds\, \langle\Omega_0(\mathbf{\Gamma}(-s))\rangle_{\boldsymbol{\gamma};0} + \mathcal{O}\left(\dot\gamma^2 t_0^2\right), \tag{A14}$$

and hence

$$\langle\Theta_-\rangle_{\boldsymbol{\gamma};0} + \langle\Theta_+\rangle_{\boldsymbol{\gamma};t_0} = 2\int_0^{t_0} ds\Omega_0(\boldsymbol{\gamma}(-s)) + \mathcal{O}\left(\dot\gamma^2 t_0^2\right), \tag{A15}$$

where $\langle\Omega_0(\mathbf{\Gamma}(-s))\rangle_{\boldsymbol{\gamma};0} = \Omega_0(\boldsymbol{\gamma}(-s))$ should be noted. From Eqs. (A10) and (A15), we obtain

$$\rho_{\rm SS}(\mathbf{\Gamma}, t_0) = \rho_{\rm eq}(\mathbf{\Gamma}) \exp\left[\int_0^{t_0} ds\Omega_0(\boldsymbol{\gamma}(-s))\right] + \mathcal{O}\left(\dot\gamma^2 t_0^2\right), \tag{A16}$$

where it should be remembered that $\int_0^{t_0} ds\Omega_0(\boldsymbol{\gamma}(-s))$ depends on the choice of the phase-space point $\boldsymbol{\gamma}$. Equation (A16) might seem similar to Eq. (A3), but actually it is not. The factor $\exp[\int_0^{t_0} ds\Omega_0(\boldsymbol{\gamma}(-s))]$ in Eq. (A16) is merely a number and factors out from the phase-space integral, which is not the case for the factor $\exp[\int_0^{t_0} ds\Omega_0(\mathbf{\Gamma}(-s))]$ in Eq. (A3).

The remaining task is to evaluate the factor $\exp[\int_0^{t_0} ds\Omega_0(\boldsymbol{\gamma}(-s))]$. One way to perform this is to expand $\Omega_0(\boldsymbol{\gamma}(-t))$ in terms of its *equilibrium* ensemble average and the correction terms. By introducing the Kawasaki transform $\boldsymbol{\gamma}^K$ [51] of $\boldsymbol{\gamma}$, and from the Kawasaki-transform property $\langle\Omega_0(\mathbf{\Gamma}(-t))\rangle_{\boldsymbol{\gamma};0} = -\langle\Omega_0(\mathbf{\Gamma}(t))\rangle_{\boldsymbol{\gamma}^K;0}$, $\Omega_0(\boldsymbol{\gamma}(-t))$ can be approximated as

$$\begin{aligned}\Omega_0(\boldsymbol{\gamma}(-t)) &\simeq -\langle\Omega_0(\mathbf{\Gamma}(t))\rangle_{\rm eq} \\ &\quad - \left(\langle\Omega_0(\mathbf{\Gamma}(t))\rangle^2_{\boldsymbol{\gamma}^K;0} - \langle\Omega_0(\mathbf{\Gamma}(t))^2\rangle_{\rm eq}\right)^{1/2} \\ &\simeq -\langle\Omega_0(\mathbf{\Gamma}(t))\rangle_{\rm eq},\end{aligned} \tag{A17}$$

where the correction term is expected to be negligible compared to the equilibrium average. Furthermore, by only retaining the conservative contribution to the work function as in Eq. (A5), $\Omega_0(\mathbf{\Gamma}) \simeq -\beta\dot\gamma\sigma^{(0)}_{xy}(\mathbf{\Gamma})$, the exponent of the factor is approximated as

$$\int_0^{t_0} ds\Omega_0(\boldsymbol{\gamma}(-s)) = \beta\dot\gamma\int_0^{t_0} ds\left\langle\sigma^{(0)}_{xy}(\mathbf{\Gamma}(s))\right\rangle_{\rm eq} + \mathcal{O}\left(\dot\gamma^2 t_0^2\right). \tag{A18}$$

From Eqs. (A16) and (A18), the distribution function for the quasi–steady state can be approximated as

$$\rho_{\rm SS}(\mathbf{\Gamma}, t_0) = \rho_{\rm eq}(\mathbf{\Gamma}) \exp\left[\beta\dot\gamma\int_0^{t_0} ds\langle\sigma^{(0)}_{xy}(\mathbf{\Gamma}(s))\rangle_{\rm eq}\right] + \mathcal{O}\left(\dot\gamma^2 t_0^2\right). \tag{A19}$$

Finally, from Eqs. (A9) and (A19), the approximate formula for the linear response is given by

$$\begin{aligned}&\left[\frac{\partial}{\partial\Delta\gamma}\left\langle\delta\sigma_{xy}(\mathbf{\Gamma}(t))\right\rangle_{\rm SS}\right]_{\Delta\gamma=0} \\ &\quad = -\beta\exp\left[\beta\dot\gamma\int_0^{t_0} ds\left\langle\sigma^{(0)}_{xy}(\mathbf{\Gamma}(s))\right\rangle_{\rm eq}\right] \\ &\qquad \times\left\langle\delta\sigma_{xy}(\mathbf{\Gamma}(t))\sigma^{(0)}_{xy}(\mathbf{\Gamma}(t_0))\right\rangle_{\rm eq} + \mathcal{O}\left(\dot\gamma^2 t_0^2\right).\end{aligned} \tag{A20}$$

3. Mode-coupling approximation

So far we have derived a response formula in terms of an *equilibrium* two-point function. One way to calculate this function is to apply the mode-coupling approximation, which we perform in this section.

From the definition of the response, Eq. (A1), the two-point function in Eq. (A20) consists of the following two terms:

$$\left\langle\sigma^{(\Delta\dot\gamma)}_{xy}(\mathbf{\Gamma}(t))\sigma^{(0)}_{xy}(\mathbf{\Gamma}(t_0))\right\rangle_{\rm eq} \tag{A21}$$

and

$$\left\langle\sigma^{(0)}_{xy}(\mathbf{\Gamma}(t))\sigma^{(0)}_{xy}(\mathbf{\Gamma}(t_0))\right\rangle_{\rm eq}. \tag{A22}$$

By inserting the "zero-mode" projection operator $\mathcal{P}^0_2(t)$ onto pair-density modes, the perturbed two-point function in

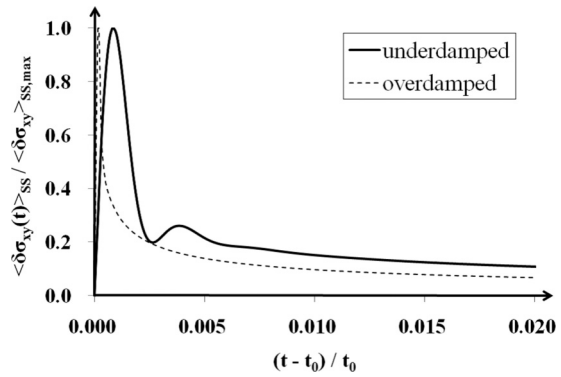

FIG. 12. Response of the stress tensor calculated from Eq. (A25), normalized by their maximum values.

Eq. (A21), for instance, can be approximated as

$$\left\langle \sigma_{xy}^{(\Delta\dot\gamma)}(\mathbf{\Gamma}(t))\sigma_{xy}^{(0)}(\mathbf{\Gamma}(t_0))\right\rangle_{\rm eq} \simeq \left\langle \left[\tilde U_0(t,t_0)\mathcal{P}_2^0(t)\sigma_{xy}^{(\Delta\dot\gamma)}(\mathbf{\Gamma}(t_0))\right]\mathcal{P}_2^0(t_0)\sigma_{xy}^{(0)}(\mathbf{\Gamma}(t_0))\right\rangle_{\rm eq}. \tag{A23}$$

Applying the factorization approximation, Eq. (A23) can be expressed in terms of the density time correlator $\Phi_{\boldsymbol q}(t)$ as

$$\left\langle \sigma_{xy}^{(\Delta\dot\gamma)}(\mathbf{\Gamma}(t))\sigma_{xy}^{(0)}(\mathbf{\Gamma}(t_0))\right\rangle_{\rm eq} \simeq \frac{1}{2}\frac{(k_BT_{\rm eq})^2}{V}\int\frac{d^3\boldsymbol k}{(2\pi)^3}\frac{W_{\boldsymbol k(t)}}{S_{k(t)}}\frac{W_{\boldsymbol k(t_0)}}{S_{k(t_0)}}\Phi_{\boldsymbol k(t_0)}^{(\Delta\dot\gamma)}(t)^2, \tag{A24}$$

where $\Phi_{\boldsymbol k(t_0)}^{(\Delta\dot\gamma)}(t)$ is the density time correlator in the presence of the perturbation. A similar approximation holds for the unperturbed two-point function, Eq. (A22), as well, with $\Phi_{\boldsymbol q}^{(\Delta\dot\gamma)}(t)$ replaced by its unperturbed counterpart, $\Phi_{\boldsymbol q}^{(0)}(t)$. The resulting expression reads

$$\left[\frac{\partial}{\partial\Delta\gamma}\langle\delta\sigma_{xy}(\mathbf{\Gamma}(t))\rangle_{\rm SS}\right]_{\Delta\gamma=0} \simeq -\frac{k_BT_{\rm eq}}{2}\exp\left[-\frac{\dot\gamma^2V}{2}\int_0^{t_0}ds\int_0^s ds'\times\int\frac{d^3\boldsymbol k}{(2\pi)^3}\frac{W_{\boldsymbol k(s')}}{S_{k(s')}}\frac{W_{\boldsymbol k}}{S_k}\Phi_{\boldsymbol k}^{(0)}(s')^2\right]\times\int\frac{d^3\boldsymbol k}{(2\pi)^3}\frac{W_{\boldsymbol k(t)}}{S_{k(t)}}\frac{W_{\boldsymbol k(t_0)}}{S_{k(t_0)}}\left\{\Phi_{\boldsymbol k(t_0)}^{(\Delta\dot\gamma)}(t)^2-\Phi_{\boldsymbol k(t_0)}^{(0)}(t)^2\right\}. \tag{A25}$$

Equation (A25) is our stress formula for the isothermal sheared thermostat system.

The result for the response formula, Eq. (A25), is shown in Fig. 12. In this calculation, the result for the response of the density time correlator, which is shown in Fig. 9, is utilized. As already shown by the result in Fig. 9, an oscillation can be observed for the underdamped case, while a monotonically decreasing behavior is seen for the overdamped case.

APPENDIX B: MORI-TYPE EQUATIONS FOR THE UNDERDAMPED AND OVERDAMPED CASES

In this Appendix, we discuss the relation between the Mori-type equations for the underdamped and overdamped [30] cases. In the underdamped case, the Mori-type equation consists of two equations, Eqs. (55) and (83). If we decompose $\boldsymbol H_{\boldsymbol q}(t)$ into the longitudinal and transverse components with respect to $\boldsymbol q(t)$,

$$\boldsymbol H_{\boldsymbol q}(t)=\boldsymbol H_{\boldsymbol q}^L(t)+\boldsymbol H_{\boldsymbol q}^T(t), \tag{B1}$$

the longitudinal component can be explicitly given from Eq. (55) as

$$\boldsymbol H_{\boldsymbol q}^L(t)=\frac{\boldsymbol q(t)}{q(t)^2}\frac{d}{dt}\Phi_{\boldsymbol q}(t). \tag{B2}$$

By differentiating Eq. (55) with time, and combining it with Eq. (83), we obtain

$$\begin{aligned}\frac{d^2}{dt^2}\Phi_{\boldsymbol q}(t)&=\dot{\boldsymbol q}(t)\cdot\boldsymbol H_{\boldsymbol q}(t)+\boldsymbol q(t)\cdot\frac{d}{dt}\boldsymbol H_{\boldsymbol q}(t)\\&=-v_T^2\frac{q(t)^2}{S_{q(t)}}\Phi_{\boldsymbol q}(t)-\alpha_{\boldsymbol q}(t)\frac{d}{dt}\Phi_{\boldsymbol q}(t)\\&\quad-2\boldsymbol q\cdot\boldsymbol\kappa\cdot\boldsymbol H_{\boldsymbol q}^T(t)-\int_0^t ds\,q(t)^\lambda L_{\boldsymbol q}^\lambda(t,s)\Phi_{\boldsymbol q}(s)\\&\quad-\int_0^t ds\,M_{\boldsymbol q}(t,s)\frac{d}{ds}\Phi_{\boldsymbol q}(s)\\&\quad-\int_0^t ds\,q(t)^\lambda M_{\boldsymbol q}^{\lambda\mu}(t,s)H_{\boldsymbol q}^{T\,\mu}(s),\end{aligned} \tag{B3}$$

where we have utilized Eq. (B2). Here, the effective friction coefficient $\alpha_{\boldsymbol q}(t)$ stands for

$$\alpha_{\boldsymbol q}(t)\equiv\lambda_\alpha(t)\alpha_0+2\frac{\boldsymbol q\cdot\boldsymbol\kappa\cdot\boldsymbol q(t)}{q(t)^2}, \tag{B4}$$

and the scalar memory kernel $M_{\boldsymbol q}(t,s)$ is defined as

$$M_{\boldsymbol q}(t,s)\equiv q(t)^\lambda M_{\boldsymbol q}^{\lambda\mu}(t,s)\frac{q(s)^\mu}{q(s)^2}. \tag{B5}$$

On the other hand, the Mori-type equation for the overdamped case reads

$$\frac{d}{dt}\Phi_{\boldsymbol q}(t)=-\Omega_{\boldsymbol q}^2(t)\Phi_{\boldsymbol q}(t)-\int_0^t ds\,m_{\boldsymbol q}(t,s)\frac{d}{ds}\Phi_{\boldsymbol q}(s), \tag{B6}$$

where $\Omega_{\boldsymbol q}^2(t)\equiv v_T^2q(t)^2/[\alpha_{\rm od}S_{q(t)}]$ and $m_{\boldsymbol q}(t,s)\equiv M_{\boldsymbol q}(t,s)/\alpha_{\rm od}$ [25,30,41]. Here, $\alpha_{\rm od}$ is the effective friction coefficient, which is related to the bare diffusion coefficient D_0 by $\alpha_{\rm od}=k_BT/(mD_0)$.

Aside from the inertia term, Eq. (B3) is not coincident with Eq. (B6) in three aspects: (i) the transverse component $\boldsymbol H_{\boldsymbol q}^T(t)$ does not decouple, (ii) there exists an additional memory kernel $L_{\boldsymbol q}^\lambda(t)$, and (iii) the effective friction coefficient $\alpha_{\boldsymbol q}(t)$ depends on $\boldsymbol q$ and t.

In situations where we can neglect $\boldsymbol H_{\boldsymbol q}^T(t)$ and $L_{\boldsymbol q}^\lambda(t)$, a concrete example of which is shown below, Eq. (B3) is reduced to

$$\frac{d^2}{dt^2}\Phi_{\boldsymbol q}(t)=-v_T^2\frac{q(t)^2}{S_{q(t)}}\Phi_{\boldsymbol q}(t)-\alpha_{\boldsymbol q}(t)\frac{d}{dt}\Phi_{\boldsymbol q}(t)-\int_0^t ds\,M_{\boldsymbol q}(t,s)\frac{d}{ds}\Phi_{\boldsymbol q}(s). \tag{B7}$$

Although Eq. (B7) is formally coincident with Eq. (B6) in the overdamped limit (i.e., upon neglection of the inertia term),

an exact correspondence is lacking due to the discrepancy between $\alpha_{\boldsymbol{q}}(t)$ and $\alpha_{\rm od}$. Still, however, it is tempting and meaningful to compare Eqs. (B7) and (B6) and their implications.

One way to neglect $\boldsymbol{H}^T_{\boldsymbol{q}}(t)$ and $L^{\lambda}_{\boldsymbol{q}}(t)$ is to resort to the isotropic approximation, which we adopt in this work (refer to Appendix D 1 for details). In this approximation, $\boldsymbol{H}^T_{\boldsymbol{q}}(t)$ is ignored by definition, and it is shown in Sec. V that the memory kernel $L^{\lambda}_{\boldsymbol{q}}(t)$ exactly vanishes in the mode-coupling approximation. The resulting equation for the underdamped case is given by Eq. (128), and that for the overdamped case is given as

$$\frac{d}{dt}\Phi_q(t) = -\Omega_q^2(t)\Phi_q(t) - \int_0^t ds \bar{m}_{\bar{q}(s)}(t-s)\frac{d}{ds}\Phi_q(s). \tag{B8}$$

Here, $\Omega_q^2(t) \equiv v_T^2\bar{q}(t)^2/[\alpha_{\rm od}S_{\bar{q}(t)}]$ and $\bar{m}_{\bar{q}(s)}(t-s) \equiv \bar{M}_{\bar{q}(s)}(t-s)/\alpha_{\rm od}$, where $\bar{M}_{\bar{q}(s)}(t-s)$ is given by Eq. (129). Comparison of the solutions of Eqs. (128) and (B8) is performed in this work.

APPENDIX C: DETAILS OF THE DERIVATIONS

Many of the details of the calculations can be found in previous papers, e.g., CK [26] and FC [30]. In this Appendix, we report some details which are specific to this work.

1. Steady-state formula

One of the goals of this study is to derive a formula for the statistical ensemble average of a phase-space variable at the nonequilibrium steady state. For this purpose, we derive an analog of the Green-Kubo formula which is valid for sheared thermostated systems.

To begin with, we adopt the "Heisenberg picture" for the statistical ensemble average of a phase-space variable $A(\boldsymbol{\Gamma})$, defined as

$$\langle A(\boldsymbol{\Gamma}(t))\rangle = \int d\boldsymbol{\Gamma}\rho_{\rm ini}(\boldsymbol{\Gamma})A(\boldsymbol{\Gamma}(t)). \tag{C1}$$

Here, $A(\boldsymbol{\Gamma})$ is time evolved, while the distribution function remains at its initial value, $\rho_{\rm ini}(\boldsymbol{\Gamma})$ [27]. Since the system is at equilibrium with temperature T at $t=0$, $\rho_{\rm ini}(\boldsymbol{\Gamma})$ is the Maxwell-Boltzmann distribution,

$$\rho_{\rm ini}(\boldsymbol{\Gamma}) \equiv \frac{e^{-\beta H_0(\boldsymbol{\Gamma})}}{\int d\boldsymbol{\Gamma} e^{-\beta H_0(\boldsymbol{\Gamma})}}, \tag{C2}$$

where $H_0(\boldsymbol{\Gamma}) \equiv K(\boldsymbol{\Gamma}) + U(\boldsymbol{\Gamma})$ is the Hamiltonian, $K(\boldsymbol{\Gamma}) \equiv \sum_i p_i^2/2m$ is the total kinetic energy, and $\beta \equiv 1/(k_BT)$.

The starting point to derive the analog of the Green-Kubo formula is the integral expression for the nonequilibrium distribution function $\rho(\boldsymbol{\Gamma},t)$,

$$\rho(\boldsymbol{\Gamma},t) = \rho_{\rm ini}(\boldsymbol{\Gamma}) - \beta\dot\gamma\int_0^t ds e^{-i\mathcal{L}^\dagger s}[\rho_{\rm ini}(\boldsymbol{\Gamma})\sigma_{xy}(\boldsymbol{\Gamma})] - 2\beta\int_0^t ds e^{-i\mathcal{L}^\dagger s}[\rho_{\rm ini}(\boldsymbol{\Gamma})\alpha(\boldsymbol{\Gamma})\delta K(\boldsymbol{\Gamma})]. \tag{C3}$$

Here,

$$\sigma_{xy}(\boldsymbol{\Gamma}) \equiv \sum_i\left(\frac{p_i^x p_i^y}{m} + y_i F_i^x\right), \tag{C4}$$

$$\delta K(\boldsymbol{\Gamma}) \equiv K(\boldsymbol{\Gamma}) - \frac{3}{2}Nk_BT \tag{C5}$$

are the zero-wave-vector limit of the shear stress and the fluctuation of the kinetic energy, respectively, which together constitute the work function

$$\Omega(\boldsymbol{\Gamma}) \equiv -\beta\dot\gamma\sigma_{xy}(\boldsymbol{\Gamma}) - 2\beta\alpha(\boldsymbol{\Gamma})\delta K(\boldsymbol{\Gamma}). \tag{C6}$$

As explained in Sec. IV D, note that the parameter $\alpha(\boldsymbol{\Gamma})$ depends on $\boldsymbol{\Gamma}$, whose specific choice in our work is shown in Eq. (112). From Eq. (C3), we obtain the following expression for the nonequilibrium ensemble average for a phase-space variable $A(\boldsymbol{\Gamma}(t))$:

$$\begin{aligned}\langle A(\boldsymbol{\Gamma}(t))\rangle &= \int d\boldsymbol{\Gamma}\rho_{\rm ini}(\boldsymbol{\Gamma})A(\boldsymbol{\Gamma}(t)) = \int d\boldsymbol{\Gamma}\rho(\boldsymbol{\Gamma},t)A(\boldsymbol{\Gamma}(0))\\ &= \langle A(\boldsymbol{\Gamma}(0))\rangle - \beta\dot\gamma\int_0^t ds\langle A(\boldsymbol{\Gamma}(t))\sigma_{xy}(\boldsymbol{\Gamma}(0))\rangle\\ &\quad - 2\beta\int_0^t ds\langle A(\boldsymbol{\Gamma}(t))\alpha(\boldsymbol{\Gamma})\delta K(\boldsymbol{\Gamma}(0))\rangle,\end{aligned} \tag{C7}$$

where the adjoint relation, Eq. (15), is utilized, and the integrations are assumed to converge uniformly. Differentiation of Eq. (C7) with time and the assumption of "mixing" results in the existence of a steady state in the limit $t\to\infty$, which leads to the following formula for the steady-state ensemble average:

$$\begin{aligned}\langle A\rangle_{\rm SS} &= \langle A(\boldsymbol{\Gamma})\rangle - \beta\dot\gamma\int_0^\infty ds\langle A(\boldsymbol{\Gamma}(t))\sigma_{xy}(\boldsymbol{\Gamma})\rangle\\ &\quad - 2\beta\int_0^\infty ds\langle A(\boldsymbol{\Gamma}(t))\alpha(\boldsymbol{\Gamma})\delta K(\boldsymbol{\Gamma})\rangle.\end{aligned} \tag{C8}$$

Here, the abbreviated notation $A(\boldsymbol{\Gamma}) \equiv A(\boldsymbol{\Gamma}(0))$ is adopted. This completes the derivation of Eq. (19).

2. Fourier transform in the sheared frame

The derivation of Eqs. (21), (22), and (24)–(26) is reported here. Since the phase-space variables are defined in terms of the phase-space coordinates, $\boldsymbol{\Gamma} = \{\boldsymbol{r}_i,\boldsymbol{p}_i\}_{i=1}^N$, we need to define "field variables" to consider the properties with respect to spatial transformations, e.g., translational invariance. A field variable for a phase-space variable $A(\boldsymbol{\Gamma})$ in the *experimental frame* is introduced as

$$A(\boldsymbol{r},t) = \sum_i A_i(\boldsymbol{\Gamma}(t))\delta(\boldsymbol{r}-\boldsymbol{r}_i(t)), \tag{C9}$$

where $A_i(\boldsymbol{\Gamma}(t))$ is a coefficient which depends only on the phase-space variables. Here, $\{\boldsymbol{r}\}$ is a coordinate fixed in space. Its equation of motion is

$$\begin{aligned}\frac{\partial}{\partial t}A(\boldsymbol{r},t) &= \sum_i\frac{\partial}{\partial t}A_i(\boldsymbol{\Gamma}(t))\delta(\boldsymbol{r}-\boldsymbol{r}_i(t))\\ &= \sum_i i\mathcal{L}A_i(\boldsymbol{\Gamma}(t))\delta(\boldsymbol{r}-\boldsymbol{r}_i(t)) = i\mathcal{L}A(\boldsymbol{r},t)\\ &= \left[i\mathcal{L}_0 + i\mathcal{L}_\alpha + i\mathcal{L}_{\dot\gamma_r} + i\mathcal{L}_{\dot\gamma_p}\right]A(\boldsymbol{r},t),\end{aligned} \tag{C10}$$

where the Liouvillians $i\mathcal{L}_0$, $i\mathcal{L}_\alpha$, $i\mathcal{L}_{\dot\gamma_r}$, and $i\mathcal{L}_{\dot\gamma_p}$ are given in Eqs. (11), (13), (27), and (26), respectively. Simple observation leads to

$$i\mathcal{L}_{\dot\gamma_r}A(\boldsymbol{r},t) = -\boldsymbol{r}\cdot\boldsymbol{\kappa}^T\cdot\frac{\partial}{\partial\boldsymbol{r}}A(\boldsymbol{r},t). \tag{C11}$$

From Eqs. (C10) and (C11), we obtain

$$\left[\frac{\partial}{\partial t}+\boldsymbol{r}\cdot\boldsymbol{\kappa}^T\cdot\frac{\partial}{\partial\boldsymbol{r}}\right]A(\boldsymbol{r},t) = i\tilde{\mathcal{L}}A(\boldsymbol{r},t), \tag{C12}$$

where

$$i\tilde{\mathcal{L}} \equiv i\mathcal{L}_0 + i\mathcal{L}_\alpha + i\mathcal{L}_{\dot\gamma_p} \tag{C13}$$

is the Liouvillian which is obtained by subtracting $i\mathcal{L}_{\dot\gamma_r}$ from $i\mathcal{L}$.

Next we move to the *sheared frame* $(\tilde{\boldsymbol{r}},\tilde{t})$, which is defined by the coordinate transformation,

$$\tilde{\boldsymbol{r}} \equiv \boldsymbol{r}-(\boldsymbol{\kappa}\cdot\boldsymbol{r})t = [\mathbf{1}-\boldsymbol{\kappa}t]\cdot\boldsymbol{r} = \begin{bmatrix} x-(\dot\gamma t)\,y \\ y \\ z\end{bmatrix},$$
$$\tilde{t} \equiv t. \tag{C14}$$

This is a comoving frame with the stretching of the wavelengths due to shearing. The value of a field variable is unaltered by the transformation, Eq. (C14), so

$$A(\boldsymbol{r},t) = A(\tilde{\boldsymbol{r}},\tilde{t}). \tag{C15}$$

Simple calculation leads to

$$\left[\frac{\partial}{\partial t}+\boldsymbol{r}\cdot\boldsymbol{\kappa}^T\cdot\frac{\partial}{\partial\boldsymbol{r}}\right]A(\boldsymbol{r},t) = \frac{\partial}{\partial\tilde{t}}A(\tilde{\boldsymbol{r}},\tilde{t}), \tag{C16}$$

which implies, together with Eq. (C12),

$$\frac{\partial}{\partial\tilde{t}}A(\tilde{\boldsymbol{r}},\tilde{t}) = i\tilde{\mathcal{L}}A(\tilde{\boldsymbol{r}},\tilde{t}). \tag{C17}$$

Hence, the time-evolution generator in the sheared frame is $i\tilde{\mathcal{L}}$, Eq. (C13).

Now we move on to the Fourier space. Fourier transform in the experimental frame is

$$A_{\boldsymbol{q}}(t) \equiv \int d^3\boldsymbol{r}\,A(\boldsymbol{r},t)e^{i\boldsymbol{q}\cdot\boldsymbol{r}} = \sum_i A_i(\boldsymbol{\Gamma}(t))e^{i\boldsymbol{q}\cdot\boldsymbol{r}_i(t)}, \tag{C18}$$

where $\boldsymbol{q}$ is some wave vector. It can easily be seen that $A_{\boldsymbol{q}}(t)$ satisfies Eq. (C10) as well:

$$\frac{\partial}{\partial t}A_{\boldsymbol{q}}(t) = i\mathcal{L}A_{\boldsymbol{q}}(t). \tag{C19}$$

Fourier transform in the sheared frame is

$$\begin{aligned} A_{\tilde{\boldsymbol{q}}}(\tilde{t}) &\equiv \int d^3\tilde{\boldsymbol{r}}\,A(\tilde{\boldsymbol{r}},\tilde{t})e^{i\tilde{\boldsymbol{q}}\cdot\tilde{\boldsymbol{r}}} \\ &= \int d^3\boldsymbol{r}\,\det\left(\frac{\partial\tilde{\boldsymbol{r}}}{\partial\boldsymbol{r}}\right)A(\boldsymbol{r},t)e^{i\tilde{\boldsymbol{q}}\cdot(\mathbf{1}-\boldsymbol{\kappa}t)\cdot\boldsymbol{r}} \\ &= \int d^3\boldsymbol{r}\,A(\boldsymbol{r},t)e^{i\tilde{\boldsymbol{q}}\cdot(\mathbf{1}-\boldsymbol{\kappa}t)\cdot\boldsymbol{r}}, \end{aligned} \tag{C20}$$

where Eqs. (C14) and (C15) are applied. Equation (C15) holds in the Fourier space as well, so comparing Eqs. (C18) and (C20), we obtain a relation between the wave vectors in both frames:

$$\boldsymbol{q} = \tilde{\boldsymbol{q}}\cdot(\mathbf{1}-\boldsymbol{\kappa}t). \tag{C21}$$

Inverting Eq. (C21),

$$\tilde{\boldsymbol{q}} = \boldsymbol{q}\cdot(\mathbf{1}+\boldsymbol{\kappa}t) = \boldsymbol{q}(-t), \tag{C22}$$

$$\boldsymbol{q}(t) \equiv \boldsymbol{q}-\boldsymbol{q}\cdot\boldsymbol{\kappa}t. \tag{C23}$$

We verify that the wave vector in the sheared frame is Affine deformed by the shear-rate tensor $\boldsymbol{\kappa}$. We choose the signature convention which is referred to as the "forward advection" by FC [30]. It can also easily be seen that $A_{\boldsymbol{q}(-t)}(\tilde{t})$ satisfies Eq. (C17):

$$\frac{\partial}{\partial\tilde{t}}A_{\boldsymbol{q}(-t)}(\tilde{t}) = i\tilde{\mathcal{L}}A_{\boldsymbol{q}(-t)}(\tilde{t}). \tag{C24}$$

3. The Mori-type equations

The derivation of Eqs. (67)–(72), i.e., the Mori-type equations without the isothermal condition, is reported here. Let us start with the basic properties, i.e., the action of the Liouvillians on the density and the current-density fluctuations, $n_{\boldsymbol{q}}$ and $j^\lambda_{\boldsymbol{q}}$. The following equalities can be verified by straightforward manipulations. First, for the density fluctuation,

$$i\tilde{\mathcal{L}}n_{\boldsymbol{q}} = \left[i\mathcal{L}_0+i\mathcal{L}_\alpha+i\mathcal{L}_{\dot\gamma_p}\right]\sum_i e^{i\boldsymbol{q}\cdot\boldsymbol{r}_i}, \tag{C25}$$

$$\begin{aligned} i\mathcal{L}_0 n_{\boldsymbol{q}} &= \sum_i\left(\frac{\boldsymbol{p}_i}{m}\cdot\frac{\partial}{\partial\boldsymbol{r}_i}+\boldsymbol{F}_i\cdot\frac{\partial}{\partial\boldsymbol{p}_i}\right)\sum_j e^{i\boldsymbol{q}\cdot\boldsymbol{r}_j} \\ &= \sum_i i\boldsymbol{q}\cdot\frac{\boldsymbol{p}_i}{m}e^{i\boldsymbol{q}\cdot\boldsymbol{r}_i} = i\boldsymbol{q}\cdot\boldsymbol{j}_{\boldsymbol{q}}; \end{aligned} \tag{C26}$$

$$i\mathcal{L}_\alpha n_{\boldsymbol{q}} = -\alpha(\boldsymbol{\Gamma})\sum_i\boldsymbol{p}_i\cdot\frac{\partial}{\partial\boldsymbol{p}_i}\sum_j e^{i\boldsymbol{q}\cdot\boldsymbol{r}_j} = 0; \tag{C27}$$

$$i\mathcal{L}_{\dot\gamma_p}n_{\boldsymbol{q}} = -\sum_i\boldsymbol{p}_i\cdot\boldsymbol{\kappa}^T\cdot\frac{\partial}{\partial\boldsymbol{p}_i}\sum_j e^{i\boldsymbol{q}\cdot\boldsymbol{r}_j} = 0. \tag{C28}$$

From Eqs. (C26)–(C28), the action of $i\tilde{\mathcal{L}}$ is obtained as

$$i\tilde{\mathcal{L}}n_{\boldsymbol{q}} = i\boldsymbol{q}\cdot\boldsymbol{j}_{\boldsymbol{q}}. \tag{C29}$$

Next, for the current-density fluctuation,

$$i\tilde{\mathcal{L}}j^\lambda_{\boldsymbol{q}} = \left[i\mathcal{L}_0+i\mathcal{L}_\alpha+i\mathcal{L}_{\dot\gamma_p}\right]\sum_i\frac{p^\lambda_i}{m}e^{i\boldsymbol{q}\cdot\boldsymbol{r}_i}; \tag{C30}$$

$$\begin{aligned} i\mathcal{L}_0 j^\lambda_{\boldsymbol{q}} &= \sum_i\left(\frac{\boldsymbol{p}_i}{m}\cdot\frac{\partial}{\partial\boldsymbol{r}_i}+\boldsymbol{F}_i\cdot\frac{\partial}{\partial\boldsymbol{p}_i}\right)\sum_j\frac{p^\lambda_j}{m}e^{i\boldsymbol{q}\cdot\boldsymbol{r}_j} \\ &= \sum_i\left(iq^\mu\frac{p^\mu_i p^\lambda_i}{m^2}+\frac{1}{m}\boldsymbol{F}^\lambda_i\right)e^{i\boldsymbol{q}\cdot\boldsymbol{r}_i}; \end{aligned} \tag{C31}$$

$$i\mathcal{L}_\alpha j^\lambda_{\boldsymbol{q}} = -\alpha(\boldsymbol{\Gamma})\sum_i\boldsymbol{p}_i\cdot\frac{\partial}{\partial\boldsymbol{p}_i}\sum_j\frac{p^\lambda_j}{m}e^{i\boldsymbol{q}\cdot\boldsymbol{r}_j} = -\alpha(\boldsymbol{\Gamma})j^\lambda_{\boldsymbol{q}}; \tag{C32}$$

$$\begin{aligned} i\mathcal{L}_{\dot\gamma_p}j^\lambda_{\boldsymbol{q}} &= -\sum_i\boldsymbol{p}_i\cdot\boldsymbol{\kappa}^T\cdot\frac{\partial}{\partial\boldsymbol{p}_i}\sum_j\frac{p^\lambda_j}{m}e^{i\boldsymbol{q}\cdot\boldsymbol{r}_j} \\ &= -\sum_i\frac{1}{m}(\boldsymbol{\kappa}\cdot\boldsymbol{p}_i)^\lambda e^{i\boldsymbol{q}\cdot\boldsymbol{r}_i} = -[\boldsymbol{\kappa}\cdot\boldsymbol{j}_{\boldsymbol{q}}]^\lambda. \end{aligned} \tag{C33}$$

Now we calculate the "correlated part," which is the first term on the r.h.s. of Eq. (66). It is projected by the rescaled projection operator, Eq. (61), as

$$\begin{aligned} U(t)\bar{\mathcal{P}}_t e^{i\mathcal{L}_{\dot\gamma_r}^\dagger t} i\tilde{\mathcal{L}} j^\lambda_{\boldsymbol{q}(t)} &= U(t)\sum_{\boldsymbol{k}} \left\{ \left\langle \left[e^{i\mathcal{L}_{\dot\gamma_r}^\dagger t} i\tilde{\mathcal{L}} j^\lambda_{\boldsymbol{q}(t)} \right] n^*_{\boldsymbol{k}} \right\rangle \frac{1}{NS_{k(t)}} n_{\boldsymbol{k}} + \left\langle \left[e^{i\mathcal{L}_{\dot\gamma_r}^\dagger t} i\tilde{\mathcal{L}} j^\lambda_{\boldsymbol{q}(t)} \right] j^{\mu *}_{\boldsymbol{k}} \right\rangle \frac{1}{Nv_T^2} j^\mu_{\boldsymbol{k}} \right\} \\ &= \sum_{\boldsymbol{k}} \left\{ \left\langle i\tilde{\mathcal{L}} j^\lambda_{\boldsymbol{q}(t)} \left[e^{-i\mathcal{L}_{\dot\gamma_r} t} n_{\boldsymbol{k}} \right]^* \right\rangle \frac{1}{NS_{k(t)}} n_{\boldsymbol{k}(t)}(t) + \left\langle i\tilde{\mathcal{L}} j^\lambda_{\boldsymbol{q}(t)} \left[e^{-i\mathcal{L}_{\dot\gamma_r} t} j^\mu_{\boldsymbol{k}} \right]^* \right\rangle \frac{1}{Nv_T^2} j^\mu_{\boldsymbol{k}(t)}(t) \right\} \\ &= \sum_{\boldsymbol{k}} \left\{ \left\langle \left[i\tilde{\mathcal{L}} j^\lambda_{\boldsymbol{q}(t)} \right] n^*_{\boldsymbol{k}(t)} \right\rangle \frac{1}{NS_{k(t)}} n_{\boldsymbol{k}(t)}(t) + \left\langle \left[i\tilde{\mathcal{L}} j^\lambda_{\boldsymbol{q}(t)} \right] j^{\mu *}_{\boldsymbol{k}(t)} \right\rangle \frac{1}{Nv_T^2} j^\mu_{\boldsymbol{k}(t)}(t) \right\}. \end{aligned} \tag{C34}$$

The two-point functions which appear in Eq. (C34) are obtained by explicit manipulations.

First,

$$\begin{aligned} \left\langle \left[i\tilde{\mathcal{L}} j^\lambda_{\boldsymbol{q}(t)} \right] n^*_{\boldsymbol{k}(t)} \right\rangle &= -\left\langle j^\lambda_{\boldsymbol{q}(t)} \left[i\tilde{\mathcal{L}} n_{\boldsymbol{k}(t)} \right]^* \right\rangle + \left\langle j^\lambda_{\boldsymbol{q}(t)} [n_{\boldsymbol{k}(t)} \tilde{\Omega}]^* \right\rangle \\ &= -\left\langle j^\lambda_{\boldsymbol{q}(t)} [i\boldsymbol{k}(t)\cdot \boldsymbol{j}_{\boldsymbol{k}(t)}]^* \right\rangle = ik(t)^\mu \left\langle j^\lambda_{\boldsymbol{q}(t)} j^{\mu *}_{\boldsymbol{k}(t)} \right\rangle = iNv_T^2 q(t)^\lambda \delta_{\boldsymbol{q},\boldsymbol{k}}, \end{aligned} \tag{C35}$$

where Eq. (C29) and the fact that terms with an odd number of momentum variables vanish are applied.

Next,

$$\left\langle \left[i\tilde{\mathcal{L}} j^\lambda_{\boldsymbol{q}(t)} \right] j^{\mu *}_{\boldsymbol{k}(t)} \right\rangle = \left\langle \left[i\mathcal{L}_\alpha j^\lambda_{\boldsymbol{q}(t)} \right] j^{\mu *}_{\boldsymbol{k}(t)} \right\rangle + \left\langle \left[i\mathcal{L}_{\dot\gamma_p} j^\lambda_{\boldsymbol{q}(t)} \right] j^{\mu *}_{\boldsymbol{k}(t)} \right\rangle, \tag{C36}$$

where the term with $i\mathcal{L}_0$ vanishes due to the odd number of momentum variables. In order to calculate the first term in Eq. (C36), it is necessary to specify the explicit form of $\alpha(\boldsymbol{\Gamma})$. As explained in Sec. VI B, we adopt the form of Eq. (112), which leads to

$$\begin{aligned} \left\langle \left[i\tilde{\mathcal{L}} j^\lambda_{\boldsymbol{q}(t)} \right] j^{\mu *}_{\boldsymbol{k}(t)} \right\rangle &= -Nv_T^2 \left\{ \alpha_0 \left(1 + \frac{2}{3N} \right) \delta^{\lambda\mu} + \boldsymbol{\kappa}^{\lambda\mu} \right\} \delta_{\boldsymbol{q},\boldsymbol{k}} \\ &\simeq -Nv_T^2 \{ \alpha_0 \delta^{\lambda\mu} + \boldsymbol{\kappa}^{\lambda\mu} \} \delta_{\boldsymbol{q},\boldsymbol{k}} \end{aligned} \tag{C37}$$

in the thermodynamic limit. From Eqs. (C34), (C35), and (C37), the result for the correlated part is

$$U(t)\bar{\mathcal{P}}_t e^{i\mathcal{L}_{\dot\gamma_r}^\dagger t} i\tilde{\mathcal{L}} j^\lambda_{\boldsymbol{q}(t)} = iv_T^2 \frac{q(t)^\lambda}{S_{q(t)}} n_{\boldsymbol{q}(t)}(t) - \alpha_0 j^\lambda_{\boldsymbol{q}(t)}(t) - [\boldsymbol{\kappa}\cdot \boldsymbol{j}_{\boldsymbol{q}(t)}(t)]^\lambda. \tag{C38}$$

This leads to the first three terms on the r.h.s. of Eq. (67).

Next, we calculate the uncorrelated part. The term without time integration is defined as the "random force" in Eqs. (68) and (69). This is nothing but the fourth term on the r.h.s. of Eq. (67). The part which requires some calculation is the one with memory kernels. Projection with the rescaled projection operator Eq. (61) is

$$\begin{aligned} \left[\frac{d}{dt} U(t) j^\lambda_{\boldsymbol{q}} \right]^{(\mathrm{mem})} &\equiv \int_0^t ds\, U(s)\bar{\mathcal{P}}_s e^{i\mathcal{L}_{\dot\gamma_r}^\dagger s} i\tilde{\mathcal{L}} e^{-i\mathcal{L}_{\dot\gamma_r} s} U_0(t,s) e^{i\mathcal{L}_{\dot\gamma_r} t} R^\lambda_{\boldsymbol{q}(t)} \\ &= \int_0^t ds\, U(s) \sum_{\boldsymbol{k}} \left\{ \left\langle \left[e^{i\mathcal{L}_{\dot\gamma_r}^\dagger s} i\tilde{\mathcal{L}} \tilde{U}_0(t,s) R^\lambda_{\boldsymbol{q}(t)} \right] n^*_{\boldsymbol{k}} \right\rangle \frac{1}{NS_{k(t)}} n_{\boldsymbol{k}} + \left\langle \left[e^{i\mathcal{L}_{\dot\gamma_r}^\dagger s} i\tilde{\mathcal{L}} \tilde{U}_0(t,s) R^\lambda_{\boldsymbol{q}(t)} \right] j^{\mu *}_{\boldsymbol{k}} \right\rangle \frac{1}{Nv_T^2} j^\mu_{\boldsymbol{k}} \right\} \\ &= \int_0^t ds \sum_{\boldsymbol{k}} \left\{ \left\langle \left[i\tilde{\mathcal{L}} \tilde{U}_0(t,s) R^\lambda_{\boldsymbol{q}(t)} \right] n^*_{\boldsymbol{k}(s)} \right\rangle \frac{1}{NS_{k(t)}} n_{\boldsymbol{k}(s)}(s) + \left\langle \left[i\tilde{\mathcal{L}} \tilde{U}_0(t,s) R^\lambda_{\boldsymbol{q}(t)} \right] j^{\mu *}_{\boldsymbol{k}(s)} \right\rangle \frac{1}{Nv_T^2} j^\mu_{\boldsymbol{k}(s)}(s) \right\}, \end{aligned} \tag{C39}$$

where we have introduced the abbreviated notation,

$$\tilde{U}_0(t,s) \equiv e^{-i\mathcal{L}_{\dot\gamma_r} s} U_0(t,s) e^{i\mathcal{L}_{\dot\gamma_r} t}. \tag{C40}$$

Substitution of Eq. (C39) into Eq. (56) yields

$$\begin{aligned} \frac{i}{N} \left\langle \left[\frac{d}{dt} U(t) j^\lambda_{\boldsymbol{q}} \right]^{(\mathrm{mem})} n^*_{\boldsymbol{q}} \right\rangle &= \int_0^t ds \left\{ \left\langle \left[i\tilde{\mathcal{L}} \tilde{U}_0(t,s) R^\lambda_{\boldsymbol{q}(t)} \right] n^*_{\boldsymbol{q}(s)} \right\rangle \frac{i}{NS_{q(t)}} \Phi_{\boldsymbol{q}}(s) + \left\langle \left[i\tilde{\mathcal{L}} \tilde{U}_0(t,s) R^\lambda_{\boldsymbol{q}(t)} \right] j^{\mu *}_{\boldsymbol{q}(s)} \right\rangle \frac{1}{Nv_T^2} H^\mu_{\boldsymbol{q}}(s) \right\} \\ &\equiv -\int_0^t ds L^\lambda_{\boldsymbol{q}}(t,s)\Phi_{\boldsymbol{q}}(s) - \int_0^t ds M^{\lambda\mu}_{\boldsymbol{q}}(t,s) H^\mu_{\boldsymbol{q}}(s), \end{aligned} \tag{C41}$$

where the memory kernels $L^\lambda_{\boldsymbol{q}}(t,s)$ and $M^{\lambda\mu}_{\boldsymbol{q}}(t,s)$ are the ones defined in Eqs. (70) and (71). These are the last two terms on the r.h.s. of Eq. (67).

4. Insertion of the projection operator $\mathcal{Q}$

The derivation of Eq. (88) is reported here. Let X be an arbitrary phase-space variable and consider the expression

$$U_0^\dagger(t,t')e^{i\mathcal{L}_{\dot\gamma r}t'}X^* = U_0^\dagger(t,t')e^{i\mathcal{L}_{\dot\gamma r}t'}[\mathcal{P}(t')+\mathcal{Q}(t')]X^*, \tag{C42}$$

where $U_0^\dagger(t,t')$ is the adjoint of $U_0(t,t')$:

$$U_0^\dagger(t,t') \equiv \exp_\leftarrow\left[-\int_{t'}^{t} ds e^{i\mathcal{L}_{\dot\gamma r}^\dagger s} i\tilde{\mathcal{L}}^\dagger \mathcal{Q}(s) e^{-i\mathcal{L}_{\dot\gamma r}^\dagger s}\right]. \tag{C43}$$

Here, the adjoint Liouvillians $i\tilde{\mathcal{L}}^\dagger$ and $i\mathcal{L}_{\dot\gamma r}^\dagger$ are defined in Eqs. (29) and (33), respectively. The correlated part of Eq. (C42) is

$$\begin{aligned} &U_0^\dagger(t,t')e^{i\mathcal{L}_{\dot\gamma r}t'}\mathcal{P}(t')X^* \\ &= U_0^\dagger(t,t')e^{i\mathcal{L}_{\dot\gamma r}t'}\sum_{\boldsymbol{k}}\left\{\frac{\langle X^* n_{\boldsymbol{k}(t')}\rangle}{NS_{k(t')}} n^*_{\boldsymbol{k}(t')} + \frac{\langle X^* j^\mu_{\boldsymbol{k}(t')}\rangle}{Nv_T^2} j^{\mu*}_{\boldsymbol{k}(t')}\right\} \\ &= \sum_{\boldsymbol{k}}\left\{\frac{\langle X^* n_{\boldsymbol{k}(t')}\rangle}{NS_{k(t')}} U_0^\dagger(t,t')n^*_{\boldsymbol{k}} + \frac{\langle X^* j^\mu_{\boldsymbol{k}(t')}\rangle}{Nv_T^2} U_0^\dagger(t,t')j^{\mu*}_{\boldsymbol{k}}\right\}. \end{aligned} \tag{C44}$$

The action of $U_0^\dagger(t,t')$ on $\xi = n$ and j is

$$\begin{aligned} &U_0^\dagger(t,t')\xi^*_{\boldsymbol{k}} \\ &= \exp_\leftarrow\left[-\int_{t'}^{t} ds e^{i\mathcal{L}_{\dot\gamma r}^\dagger s} i\tilde{\mathcal{L}}^\dagger \mathcal{Q}(s) e^{-i\mathcal{L}_{\dot\gamma r}^\dagger s}\right]\xi^*_{\boldsymbol{k}} \\ &= \exp_\leftarrow\left[-\int_{t'}^{t} ds e^{i\mathcal{L}_{\dot\gamma r}^\dagger s} i\tilde{\mathcal{L}}^\dagger \mathcal{Q}(s)\,[1+\Sigma(s)]\, e^{-i\mathcal{L}_{\dot\gamma r} s}\right]\xi^*_{\boldsymbol{k}} \\ &\simeq \exp_\leftarrow\left[-\int_{t'}^{t} ds e^{i\mathcal{L}_{\dot\gamma r}^\dagger s} i\tilde{\mathcal{L}}^\dagger \mathcal{Q}(s)\xi^*_{\boldsymbol{k}(s)}\right] = 0, \end{aligned} \tag{C45}$$

where we have neglected $\Sigma(s)$ in the last step, as explained following Eq. (86) in Sec. V.

From Eqs. (C44) and (C45), the correlated part vanishes, and hence

$$U_0^\dagger(t,t')e^{i\mathcal{L}_{\dot\gamma r}t'} = U_0^\dagger(t,t')e^{i\mathcal{L}_{\dot\gamma r}t'}\mathcal{Q}(t') \tag{C46}$$

or, taking the adjoint,

$$e^{-i\mathcal{L}_{\dot\gamma r}^\dagger t'}U_0(t,t') = \mathcal{Q}(t')e^{-i\mathcal{L}_{\dot\gamma r}^\dagger t'}U_0(t,t'). \tag{C47}$$

This is the desired equality.

5. The memory kernels

The derivation of Eqs. (91)–(94) is reported here. We start with the ensemble average of Eq. (70). From the adjoint relation, Eq. (28),

$$\begin{aligned} \left\langle\left[i\tilde{\mathcal{L}}\tilde{U}_0(t,s)R^\lambda_{\boldsymbol{q}(t)}\right]n^*_{\boldsymbol{q}(s)}\right\rangle &= -\left\langle\left[\tilde{U}_0(t,s)R^\lambda_{\boldsymbol{q}(t)}\right](i\tilde{\mathcal{L}}n_{\boldsymbol{q}(s)})^*\right\rangle \\ &\quad + \left\langle\left[\tilde{U}_0(t,s)R^\lambda_{\boldsymbol{q}(t)}\right]n^*_{\boldsymbol{q}(s)}\tilde{\Omega}\right\rangle. \end{aligned} \tag{C48}$$

Substituting Eq. (90) into the two terms of Eq. (C48),

$$\begin{aligned} &\left\langle\left[\tilde{U}_0(t,s)R^\lambda_{\boldsymbol{q}(t)}\right]X^*\right\rangle \\ &\simeq \left\langle\left[\mathcal{Q}(s)e^{-i\mathcal{L}_{\dot\gamma r}^\dagger s}U_0(t,s)e^{i\mathcal{L}_{\dot\gamma r}t}R^\lambda_{\boldsymbol{q}(t)}\right]X^*\right\rangle \\ &= \left\langle\left[\mathcal{Q}(s)\tilde{U}_0'(t,s)\mathcal{Q}(t)R^\lambda_{\boldsymbol{q}(t)}\right]\mathcal{Q}(s)X^*\right\rangle, \end{aligned} \tag{C49}$$

where $X = i\tilde{\mathcal{L}}n_{\boldsymbol{q}(s)},n_{\boldsymbol{q}(s)}\tilde{\Omega}$. Here, the idempotency and the Hermiticity of $\mathcal{Q}(s)$ and the abbreviated notation of Eq. (93) are used. From Eq. (C29), the first term in Eq. (C48) is projected out by $\mathcal{Q}(s)$, which leaves

$$\left\langle\left[\mathcal{Q}(s)\tilde{U}_0'(t,s)\mathcal{Q}(t)R^\lambda_{\boldsymbol{q}(t)}\right]\mathcal{Q}(s)[n_{\boldsymbol{q}(s)}\tilde{\Omega}]^*\right\rangle. \tag{C50}$$

Similar manipulation for Eq. (71) leads to

$$\left\langle\left[i\tilde{\mathcal{L}}\tilde{U}_0(t,s)R^\lambda_{\boldsymbol{q}(t)}\right]j^{\mu*}_{\boldsymbol{q}(s)}\right\rangle = -\left\langle\left[\mathcal{Q}(s)\tilde{U}_0'(t,s)\mathcal{Q}(t)R^\lambda_{\boldsymbol{q}(t)}\right]\Delta R^{\mu*}_{\boldsymbol{q}(s)}\right\rangle, \tag{C51}$$

where $\Delta R^{\mu*}_{\boldsymbol{q}(s)}$ is the modified random force defined in Eq. (94).

6. The vertex functions

The derivation of Eqs. (97)–(100) is reported here. We start with Eq. (97). From the definition of Eq. (69),

$$\begin{aligned} &\left\langle R^\lambda_{\boldsymbol{q}(t)}n^*_{\boldsymbol{k}(t)}n^*_{\boldsymbol{p}(t)}\right\rangle \\ &= \left\langle\left[\mathcal{Q}(t)i\tilde{\mathcal{L}}j^\lambda_{\boldsymbol{q}(t)}\right]n^*_{\boldsymbol{k}(t)}n^*_{\boldsymbol{p}(t)}\right\rangle \\ &= \left\langle\left[i\tilde{\mathcal{L}}j^\lambda_{\boldsymbol{q}(t)}\right]n^*_{\boldsymbol{k}(t)}n^*_{\boldsymbol{p}(t)}\right\rangle - \left\langle\left[\mathcal{P}(t)i\tilde{\mathcal{L}}j^\lambda_{\boldsymbol{q}(t)}\right]n^*_{\boldsymbol{k}(t)}n^*_{\boldsymbol{p}(t)}\right\rangle. \end{aligned} \tag{C52}$$

The first term in Eq. (C52) is evaluated, by the use of the adjoint relation Eq. (28) and Eq. (C29), as

$$\begin{aligned} &\left\langle\left[i\tilde{\mathcal{L}}j^\lambda_{\boldsymbol{q}(t)}\right]n^*_{\boldsymbol{k}(t)}n^*_{\boldsymbol{p}(t)}\right\rangle \\ &= -\left\langle j^\lambda_{\boldsymbol{q}(t)}[i\tilde{\mathcal{L}}n_{\boldsymbol{k}(t)}]^*n^*_{\boldsymbol{p}(t)}\right\rangle - \left\langle j^\lambda_{\boldsymbol{q}(t)}n^*_{\boldsymbol{k}(t)}[i\tilde{\mathcal{L}}n_{\boldsymbol{p}(t)}]^*\right\rangle \\ &= ik(t)^\mu\left\langle j^\lambda_{\boldsymbol{q}(t)}j^{\mu*}_{\boldsymbol{k}(t)}n^*_{\boldsymbol{p}(t)}\right\rangle + ip(t)^\mu\left\langle j^\lambda_{\boldsymbol{q}(t)}j^{\mu*}_{\boldsymbol{p}(t)}n^*_{\boldsymbol{k}(t)}\right\rangle. \end{aligned} \tag{C53}$$

The three-point function in Eq. (C53) can be calculated explicitly as

$$\begin{aligned} \left\langle j^\lambda_{\boldsymbol{q}}j^{\mu*}_{\boldsymbol{k}}n^*_{\boldsymbol{p}}\right\rangle &= \sum_{i,j}\left\langle\frac{p^\lambda_i}{m}e^{i\boldsymbol{q}\cdot\boldsymbol{r}_i}\frac{p^\mu_j}{m}e^{-i\boldsymbol{k}\cdot\boldsymbol{r}_j}n^*_{\boldsymbol{p}}\right\rangle \\ &= \delta^{\lambda\mu}\delta_{\boldsymbol{q}-\boldsymbol{k},\boldsymbol{p}}Nv_T^2S_p. \end{aligned} \tag{C54}$$

From Eqs. (C53) and (C54),

$$\left\langle\left[i\tilde{\mathcal{L}}j^\lambda_{\boldsymbol{q}(t)}\right]n^*_{\boldsymbol{k}(t)}n^*_{\boldsymbol{p}(t)}\right\rangle = i\delta_{\boldsymbol{q},\boldsymbol{k}+\boldsymbol{p}}Nv_T^2[k(t)^\lambda S_{p(t)} + p(t)^\lambda S_{k(t)}]. \tag{C55}$$

An explicit manipulation of the projection operator in the second term in Eq. (C52) leads to

$$\begin{aligned} &\left\langle\left[\mathcal{P}(t)i\tilde{\mathcal{L}}j^\lambda_{\boldsymbol{q}(t)}\right]n^*_{\boldsymbol{k}(t)}n^*_{\boldsymbol{p}(t)}\right\rangle \\ &= \sum_{\boldsymbol{q}'}\left\{\left\langle\left[i\tilde{\mathcal{L}}j^\lambda_{\boldsymbol{q}(t)}\right]n^*_{\boldsymbol{q}'(t)}\right\rangle\frac{1}{NS_{q'(t)}}\langle n_{\boldsymbol{q}'(t)}n^*_{\boldsymbol{k}(t)}n^*_{\boldsymbol{p}(t)}\rangle\right. \\ &\quad \left.+\left\langle\left[i\tilde{\mathcal{L}}j^\lambda_{\boldsymbol{q}(t)}\right]j^{\mu*}_{\boldsymbol{q}'(t)}\right\rangle\frac{1}{Nv_T^2}\left\langle j^\mu_{\boldsymbol{q}'(t)}n^*_{\boldsymbol{k}(t)}n^*_{\boldsymbol{p}(t)}\right\rangle\right\} \\ &= -\frac{1}{NS_{q'(t)}}\sum_{\boldsymbol{q}'}\left\langle j^\lambda_{\boldsymbol{q}(t)}\left[i\tilde{\mathcal{L}}n_{\boldsymbol{q}'(t)}\right]^*\right\rangle\langle n_{\boldsymbol{q}'(t)}n^*_{\boldsymbol{k}(t)}n^*_{\boldsymbol{p}(t)}\rangle \\ &= \frac{iq'(t)^\mu}{NS_{q'(t)}}\sum_{\boldsymbol{q}'}\left\langle j^\lambda_{\boldsymbol{q}(t)}j^{\mu*}_{\boldsymbol{q}'(t)}\right\rangle\langle n_{\boldsymbol{q}'(t)}n^*_{\boldsymbol{k}(t)}n^*_{\boldsymbol{p}(t)}\rangle \\ &= iv_T^2\frac{q(t)^\mu}{S_{q(t)}}\langle n_{\boldsymbol{q}(t)}n^*_{\boldsymbol{k}(t)}n^*_{\boldsymbol{p}(t)}\rangle. \end{aligned} \tag{C56}$$

The convolution approximation [36],

$$\langle n_{\boldsymbol{q}}n^*_{\boldsymbol{k}}n^*_{\boldsymbol{p}}\rangle \simeq \delta_{\boldsymbol{q},\boldsymbol{k}+\boldsymbol{p}}NS_qS_kS_p, \tag{C57}$$

is applied for the three-point function, which finally leads to the following expression:

$$\begin{aligned}
&\left\langle R^{\lambda}_{\boldsymbol{q}(t)} n^{*}_{\boldsymbol{k}(t)} n^{*}_{\boldsymbol{p}(t)} \right\rangle \\
&= i\delta_{\boldsymbol{q},\boldsymbol{k}+\boldsymbol{p}} N v_T^2 \left[k(t)^{\lambda} S_{p(t)} + p(t)^{\lambda} S_{k(t)} \right] \\
&\quad - i v_T^2 \frac{q(t)^{\lambda}}{S_{q(t)}} \delta_{\boldsymbol{q},\boldsymbol{k}+\boldsymbol{p}} N S_{q(t)} S_{k(t)} S_{p(t)} \\
&= i\delta_{\boldsymbol{q},\boldsymbol{k}+\boldsymbol{p}} N v_T^2 [k(t)^{\lambda} S_{p(t)} + p(t)^{\lambda} S_{k(t)} - q(t)^{\lambda} S_{k(t)} S_{p(t)}] \\
&= -i\delta_{\boldsymbol{q},\boldsymbol{k}+\boldsymbol{p}} N v_T^2 S_{k(t)} S_{p(t)} \\
&\quad \times \left(k(t)^{\lambda} + p(t)^{\lambda} - \frac{k(t)^{\lambda}}{S_{k(t)}} - \frac{p(t)^{\lambda}}{S_{p(t)}} \right) \\
&= -i\delta_{\boldsymbol{q},\boldsymbol{k}+\boldsymbol{p}} N v_T^2 S_{k(t)} S_{p(t)} n [k(t)^{\lambda} c_{k(t)} + p(t)^{\lambda} c_{p(t)}].
\end{aligned} \tag{C58}$$

Here, c_q is the direct correlation function [36], which is related to the static structure factor S_q as

$$n c_q = 1 - \frac{1}{S_q} \tag{C59}$$

by the Ornstein-Zernike relation [36]. From Eq. (C58), it is straightforward to verify Eqs. (97) and (99).

Next we deal with Eq. (98). From the definition of $\Delta R^{\lambda}_{\boldsymbol{q}}$,

$$\begin{aligned}
&\frac{\left\langle n_{\boldsymbol{k}(t)} n_{\boldsymbol{p}(t)} \Delta R^{\lambda *}_{\boldsymbol{q}(t)} \right\rangle}{N^2 S_{k(t)} S_{p(t)}} \\
&= \frac{\left\langle n_{\boldsymbol{k}(t)} n_{\boldsymbol{p}(t)} R^{\lambda *}_{\boldsymbol{q}(t)} \right\rangle}{N^2 S_{k(t)} S_{p(t)}} - \frac{\left\langle n_{\boldsymbol{k}(t)} n_{\boldsymbol{p}(t)} \mathcal{Q}(t) \left[j^{\lambda}_{\boldsymbol{q}(t)} \tilde{\Omega} \right]^{*} \right\rangle}{N^2 S_{k(t)} S_{p(t)}},
\end{aligned} \tag{C60}$$

where the first term in Eq. (C60) is the complex conjugate of Eq. (97). Hence, we only need to handle the second term. There are two terms in the modified work function, $\tilde{\Omega}(\boldsymbol{\Gamma}) = -\beta\dot{\gamma}\sigma^{(\mathrm{kin})}_{xy}(\boldsymbol{\Gamma}) - 2\beta\alpha(\boldsymbol{\Gamma})\delta K(\boldsymbol{\Gamma})$. For the first term,

$$\mathcal{Q}(t) \left[j^{\lambda}_{\boldsymbol{q}(t)} \sigma^{(\mathrm{kin})}_{xy} \right] = j^{\lambda}_{\boldsymbol{q}(t)} \sigma^{(\mathrm{kin})}_{xy} - \mathcal{P}(t) \left[j^{\lambda}_{\boldsymbol{q}(t)} \sigma^{(\mathrm{kin})}_{xy} \right], \tag{C61}$$

where $\sigma^{(\mathrm{kin})}_{xy} = \sum_i p_i^x p_i^y / 2m$ is the kinetic part of the shear stress. The projected term is

$$\begin{aligned}
\mathcal{P}(t) \left[j^{\lambda}_{\boldsymbol{q}(t)} \sigma^{(\mathrm{kin})}_{xy} \right] &= \sum_{\boldsymbol{k}} \frac{\left\langle \left[j^{\lambda}_{\boldsymbol{q}(t)} \sigma^{(\mathrm{kin})}_{xy} \right] n^{*}_{\boldsymbol{k}(t)} \right\rangle}{N S_{k(t)}} n_{\boldsymbol{k}(t)} \\
&\quad + \sum_{\boldsymbol{k}} \frac{\left\langle \left[j^{\lambda}_{\boldsymbol{q}(t)} \sigma^{(\mathrm{kin})}_{xy} \right] j^{\mu *}_{\boldsymbol{k}(t)} \right\rangle}{N v_T^2} j^{\mu}_{\boldsymbol{k}(t)} \\
&= m v_T^2 \left(\delta^{\lambda x} j^{y}_{\boldsymbol{q}(t)} + \delta^{\lambda y} j^{x}_{\boldsymbol{q}(t)} \right).
\end{aligned} \tag{C62}$$

From Eqs. (C61) and (C62), $\mathcal{Q}(t)[j^{\lambda}_{\boldsymbol{q}(t)} \sigma^{(\mathrm{kin})}_{xy}]$ is an odd function of the momentum variables and, hence, vanishes. For the second term,

$$\begin{aligned}
&\mathcal{Q}(t) \left[j^{\lambda}_{\boldsymbol{q}(t)} \alpha(\boldsymbol{\Gamma}) \delta K(\boldsymbol{\Gamma}) \right] \\
&= j^{\lambda}_{\boldsymbol{q}(t)} \alpha(\boldsymbol{\Gamma}) \delta K(\boldsymbol{\Gamma}) - \mathcal{P}(t) \left[j^{\lambda}_{\boldsymbol{q}(t)} \alpha(\boldsymbol{\Gamma}) \delta K(\boldsymbol{\Gamma}) \right],
\end{aligned} \tag{C63}$$

where $\delta K(\boldsymbol{\Gamma}) = \sum_i \boldsymbol{p}_i^2 / 2m - 3N k_B T / 2$ is the fluctuation of the kinetic energy, and $\alpha(\boldsymbol{\Gamma})$ is given in Eq. (112). The projected term is

$$\begin{aligned}
&\mathcal{P}(t) \left[j^{\lambda}_{\boldsymbol{q}(t)} \alpha(\boldsymbol{\Gamma}) \delta K(\boldsymbol{\Gamma}) \right] \\
&= \sum_{\boldsymbol{k}} \frac{\left\langle \left[j^{\lambda}_{\boldsymbol{q}(t)} \alpha(\boldsymbol{\Gamma}) \delta K(\boldsymbol{\Gamma}) \right] n^{*}_{\boldsymbol{k}(t)} \right\rangle}{N S_{k(t)}} n_{\boldsymbol{k}(t)} \\
&\quad + \sum_{\boldsymbol{k}} \frac{\left\langle \left[j^{\lambda}_{\boldsymbol{q}(t)} \alpha(\boldsymbol{\Gamma}) \delta K(\boldsymbol{\Gamma}) \right] j^{\mu *}_{\boldsymbol{k}(t)} \right\rangle}{N v_T^2} j^{\mu}_{\boldsymbol{k}(t)} \\
&\propto j^{\lambda}_{\boldsymbol{q}(t)}.
\end{aligned} \tag{C64}$$

From Eqs. (C63) and (C64), $\mathcal{Q}(t)[j^{\lambda}_{\boldsymbol{q}(t)} \alpha(\boldsymbol{\Gamma}) \delta K(\boldsymbol{\Gamma})]$ is an odd function of the momentum variables and, hence, vanishes as well. This completes the derivation of Eq. (98).

Finally, we show Eq. (100). The part which corresponds to the first term of the modified work function $\tilde{\Omega}(\boldsymbol{\Gamma})$ is

$$\mathcal{Q}(t) \left[n_{\boldsymbol{q}(t)} \sigma^{(\mathrm{kin})}_{xy} \right] = n_{\boldsymbol{q}(t)} \sigma^{(\mathrm{kin})}_{xy} - \mathcal{P}(t) \left[n_{\boldsymbol{q}(t)} \sigma^{(\mathrm{kin})}_{xy} \right], \tag{C65}$$

where the projected term vanishes,

$$\begin{aligned}
\mathcal{P}(t) \left[n_{\boldsymbol{q}(t)} \sigma^{(\mathrm{kin})}_{xy} \right] &= \sum_{\boldsymbol{k}} \frac{\left\langle \left[n_{\boldsymbol{q}(t)} \sigma^{(\mathrm{kin})}_{xy} \right] n^{*}_{\boldsymbol{k}(t)} \right\rangle}{N S_{k(t)}} n_{\boldsymbol{k}(t)} \\
&\quad + \sum_{\boldsymbol{k}} \frac{\left\langle \left[n_{\boldsymbol{q}(t)} \sigma^{(\mathrm{kin})}_{xy} \right] j^{\mu *}_{\boldsymbol{k}(t)} \right\rangle}{N v_T^2} j^{\mu}_{\boldsymbol{k}(t)} \\
&= 0,
\end{aligned} \tag{C66}$$

since $\langle p_i^x p_i^y \rangle_{\boldsymbol{p}} = 0$. Here, $\langle \cdots \rangle_{\boldsymbol{p}}$ is the ensemble average with only the momentum variables integrated. From Eqs. (C65) and (C66),

$$\left\langle n_{\boldsymbol{k}(t)} n_{\boldsymbol{p}(t)} \mathcal{Q}(t) \left[n^{*}_{\boldsymbol{q}(t)} \sigma^{(\mathrm{kin})}_{xy} \right] \right\rangle = \left\langle n_{\boldsymbol{k}(t)} n_{\boldsymbol{p}(t)} n^{*}_{\boldsymbol{q}(t)} \sigma^{(\mathrm{kin})}_{xy} \right\rangle, \tag{C67}$$

which again vanishes due to $\langle p_i^x p_i^y \rangle_{\boldsymbol{p}} = 0$. The second term is

$$\begin{aligned}
&\mathcal{Q}(t)[n_{\boldsymbol{q}(t)} \alpha(\boldsymbol{\Gamma}) \delta K(\boldsymbol{\Gamma})] \\
&= n_{\boldsymbol{q}(t)} \alpha(\boldsymbol{\Gamma}) \delta K(\boldsymbol{\Gamma}) - \mathcal{P}(t)[n_{\boldsymbol{q}(t)} \alpha(\boldsymbol{\Gamma}) \delta K(\boldsymbol{\Gamma})].
\end{aligned} \tag{C68}$$

Here, the projected term is

$$\begin{aligned}
&\mathcal{P}(t)[n_{\boldsymbol{q}(t)} \alpha(\boldsymbol{\Gamma}) \delta K(\boldsymbol{\Gamma})] \\
&= \sum_{\boldsymbol{k}} \frac{\langle [n_{\boldsymbol{q}(t)} \alpha(\boldsymbol{\Gamma}) \delta K(\boldsymbol{\Gamma})] n^{*}_{\boldsymbol{k}(t)} \rangle}{N S_{k(t)}} n_{\boldsymbol{k}(t)} \\
&\quad + \sum_{\boldsymbol{k}} \frac{\langle [n_{\boldsymbol{q}(t)} \alpha(\boldsymbol{\Gamma}) \delta K(\boldsymbol{\Gamma})] j^{\mu *}_{\boldsymbol{k}(t)} \rangle}{N v_T^2} j^{\mu}_{\boldsymbol{k}(t)} \\
&= \alpha_0 k_B T n_{\boldsymbol{q}(t)},
\end{aligned} \tag{C69}$$

where

$$\langle \alpha(\boldsymbol{\Gamma}) \delta K(\boldsymbol{\Gamma}) \rangle_{\boldsymbol{p}} = \alpha_0 k_B T \tag{C70}$$

is utilized. From Eqs. (C68) and (C69),

$$\begin{aligned}
&\langle n_{\boldsymbol{k}(t)} n_{\boldsymbol{p}(t)} \mathcal{Q}(t)[n^{*}_{\boldsymbol{q}(t)} \alpha(\boldsymbol{\Gamma}) \delta K(\boldsymbol{\Gamma})] \rangle \\
&= \langle n_{\boldsymbol{k}(t)} n_{\boldsymbol{p}(t)} n^{*}_{\boldsymbol{q}(t)} \alpha(\boldsymbol{\Gamma}) \delta K(\boldsymbol{\Gamma}) \rangle \\
&\quad - \alpha_0 k_B T \langle n_{\boldsymbol{k}(t)} n_{\boldsymbol{p}(t)} n^{*}_{\boldsymbol{q}(t)} \rangle,
\end{aligned} \tag{C71}$$

which again vanishes due to Eq. (C70).

7. Factorization approximations

The derivation of Eqs. (101) and (119) is shown here. From the definition, Eq. (93), the left-hand side (l.h.s.) of Eq. (101) can be expanded as

$$\begin{aligned}
&\frac{1}{N^2}\langle[\tilde{U}_0'(t,s)n_{\boldsymbol{k}(t)}n_{\boldsymbol{p}(t)}]n^*_{\boldsymbol{k}'(s)}n^*_{\boldsymbol{p}'(s)}\rangle \\
&\quad=\frac{1}{N^2}\langle[e^{-i\mathcal{L}^\dagger_{\dot\gamma r}s}U_0(t,s)e^{i\mathcal{L}_{\dot\gamma r}t}n_{\boldsymbol{k}(t)}n_{\boldsymbol{p}(t)}]n^*_{\boldsymbol{k}'(s)}n^*_{\boldsymbol{p}'(s)}\rangle \\
&\quad=\frac{1}{N^2}\langle[U_0(t,s)n_{\boldsymbol{k}}n_{\boldsymbol{p}}]n^*_{\boldsymbol{k}'}n^*_{\boldsymbol{p}'}\rangle, \qquad \text{(C72)}
\end{aligned}$$

where the property $e^{i\mathcal{L}_{\dot\gamma r}t}n_{\boldsymbol{k}(t)}n_{\boldsymbol{p}(t)}=n_{\boldsymbol{k}}n_{\boldsymbol{p}}$ is utilized. It is clear that this is the propagator for the pair-density fluctuations with respect to the projected time-evolution operator $U_0(t,s)$. As is familiar in the conventional MCT, Eq. (C72) is approximated by factorizing into a product of propagators for the density fluctuation with respect to the projection-free time-evolution operator $e^{i\mathcal{L}(t-s)}$:

$$\begin{aligned}
&\frac{1}{N^2}\langle[U_0(t,s)n_{\boldsymbol{k}}n_{\boldsymbol{p}}]n^*_{\boldsymbol{k}'}n^*_{\boldsymbol{p}'}\rangle \\
&\simeq\frac{1}{N^2}\langle[e^{i\mathcal{L}^\dagger_{\dot\gamma r}s}e^{i\mathcal{L}(t-s)}e^{-i\mathcal{L}_{\dot\gamma r}t}n_{\boldsymbol{k}}]n^*_{\boldsymbol{k}'}\rangle \\
&\quad\times\langle[e^{i\mathcal{L}^\dagger_{\dot\gamma r}s}e^{i\mathcal{L}(t-s)}e^{-i\mathcal{L}_{\dot\gamma r}t}n_{\boldsymbol{p}}]n^*_{\boldsymbol{p}'}\rangle \\
&=\frac{1}{N^2}\langle[e^{i\mathcal{L}(t-s)}e^{-i\mathcal{L}_{\dot\gamma r}(t-s)}n_{\boldsymbol{k}(s)}]n^*_{\boldsymbol{k}'(s)}\rangle \\
&\quad\times\langle[e^{i\mathcal{L}(t-s)}e^{-i\mathcal{L}_{\dot\gamma r}(t-s)}n_{\boldsymbol{p}(s)}]n^*_{\boldsymbol{p}'(s)}\rangle \\
&=\frac{1}{N^2}\langle[U(t-s)n_{\boldsymbol{k}(s)}]n^*_{\boldsymbol{k}'(s)}\rangle\langle[U(t-s)n_{\boldsymbol{p}(s)}]n^*_{\boldsymbol{p}'(s)}\rangle \\
&=\delta_{\boldsymbol{k}',\boldsymbol{k}}\delta_{\boldsymbol{p}',\boldsymbol{p}}\Phi_{\boldsymbol{k}(s)}(t-s)\Phi_{\boldsymbol{p}(s)}(t-s). \qquad \text{(C73)}
\end{aligned}$$

In the first step on the r.h.s. of Eq. (C73), the advection generators $e^{i\mathcal{L}^\dagger_{\dot\gamma r}s}$ and $e^{-i\mathcal{L}_{\dot\gamma r}t}$ are inserted to account for the time when the propagation starts, s, and ends, t. Hence Eq. (101) is shown.

Similarly, the l.h.s. of Eq. (119) is

$$\begin{aligned}
&\frac{1}{N^2}\langle[\tilde{U}_0(t,0)n_{\boldsymbol{k}(t)}n^*_{\boldsymbol{k}(t)}]n_{\boldsymbol{k}'}n^*_{\boldsymbol{k}'}\rangle \\
&\quad=\frac{1}{N^2}\langle[U_0(t,0)n_{\boldsymbol{k}}n^*_{\boldsymbol{k}}]n_{\boldsymbol{k}'}n^*_{\boldsymbol{k}'}\rangle, \qquad \text{(C74)}
\end{aligned}$$

which is approximated as

$$\begin{aligned}
&\frac{1}{N^2}\langle[U_0(t,0)n_{\boldsymbol{k}}n^*_{\boldsymbol{k}}]n_{\boldsymbol{k}'}n^*_{\boldsymbol{k}'}\rangle \\
&\simeq\frac{1}{N}\langle[e^{i\mathcal{L}t}e^{-i\mathcal{L}_{\dot\gamma r}t}n_{\boldsymbol{k}}]n^*_{\boldsymbol{k}'}\rangle\cdot\frac{1}{N}\langle[e^{i\mathcal{L}t}e^{-i\mathcal{L}_{\dot\gamma r}t}n^*_{\boldsymbol{k}}](n^*_{\boldsymbol{k}'})^*\rangle \\
&\quad+\frac{1}{N}\langle[e^{i\mathcal{L}t}e^{-i\mathcal{L}_{\dot\gamma r}t}n_{\boldsymbol{k}}](n^*_{\boldsymbol{k}'})^*\rangle\cdot\frac{1}{N}\langle[e^{i\mathcal{L}t}e^{-i\mathcal{L}_{\dot\gamma r}t}n^*_{\boldsymbol{k}}]n^*_{\boldsymbol{k}'}\rangle \\
&=\frac{1}{N}\langle[e^{i\mathcal{L}t}n_{\boldsymbol{k}(t)}]n^*_{\boldsymbol{k}'}\rangle\cdot\frac{1}{N}\langle[e^{i\mathcal{L}t}n^*_{\boldsymbol{k}(t)}](n^*_{\boldsymbol{k}'})^*\rangle \\
&\quad+\frac{1}{N}\langle[e^{i\mathcal{L}t}n_{\boldsymbol{k}(t)}](n^*_{\boldsymbol{k}'})^*\rangle\cdot\frac{1}{N}\langle[e^{i\mathcal{L}t}n^*_{\boldsymbol{k}(t)}]n^*_{\boldsymbol{k}'}\rangle \\
&=\delta_{\boldsymbol{k}',\boldsymbol{k}}\Phi_{\boldsymbol{k}}(t)\cdot\delta_{\boldsymbol{k}',\boldsymbol{k}}\Phi_{-\boldsymbol{k}}(t)+\delta_{-\boldsymbol{k}',\boldsymbol{k}}\Phi_{\boldsymbol{k}}(t)\cdot\delta_{\boldsymbol{k}',-\boldsymbol{k}}\Phi_{-\boldsymbol{k}}(t) \\
&=[\delta_{\boldsymbol{k}',\boldsymbol{k}}+\delta_{\boldsymbol{k}',-\boldsymbol{k}}]\Phi_{\boldsymbol{k}}(t)^2. \qquad \text{(C75)}
\end{aligned}$$

Hence Eq. (119) is shown. Note that Eq. (C75) is a special case of Eq. (C73) with $s=0$, aside from the possible pairings of the density fluctuations.

8. The projected time correlator

The derivation of Eq. (106) is reported here. From Eq. (64), it holds that

$$\begin{aligned}
U(t)A(\boldsymbol{\Gamma})=U_0(t,0)A(\boldsymbol{\Gamma})+\int_0^t dsU(s)\bar{\mathcal{P}}_s e^{i\mathcal{L}^\dagger_{\dot\gamma r}s} \\
\times i\tilde{\mathcal{L}}e^{-i\mathcal{L}_{\dot\gamma r}s}U_0(t,s)A(\boldsymbol{\Gamma}). \qquad \text{(C76)}
\end{aligned}$$

For the second term, the application of the rescaled projection operator, Eq. (61), leads to the form

$$\int_0^t ds\sum_{\boldsymbol{k}}\left\{\frac{C^{(n)}_{\boldsymbol{k}}}{S_{k(t)}}n_{\boldsymbol{k}(s)}(s)+\frac{C^{(j)\lambda}_{\boldsymbol{k}}}{S_{k(t)}}j^\lambda_{\boldsymbol{k}(s)}(s)\right\}, \qquad \text{(C77)}$$

where $C^{(\xi)}_{\boldsymbol{k}}$ $(\xi=n,j)$ is a correlator whose detailed expression is not important for our purpose. The time correlators of the density and the current-density fluctuations with zero-wave-vector variables $B(\boldsymbol{\Gamma})$ vanish,

$$\begin{aligned}
\langle n_{\boldsymbol{k}(s)}(s)B(\boldsymbol{\Gamma})\rangle&=\delta_{\boldsymbol{k},0}\langle n_{\boldsymbol{k}=0}(s)B(\boldsymbol{\Gamma})\rangle=0, \\
\langle j^\lambda_{\boldsymbol{k}(s)}(s)B(\boldsymbol{\Gamma})\rangle&=\delta_{\boldsymbol{k},0}\langle j^\lambda_{\boldsymbol{k}=0}(s)B(\boldsymbol{\Gamma})\rangle=0, \qquad \text{(C78)}
\end{aligned}$$

since $n_{\boldsymbol{k}=0}=0$ holds by definition, and

$$j^\lambda_{\boldsymbol{k}=0}(s)=e^{i\mathcal{L}s}\sum_i\frac{p^\lambda_i}{m}=0 \qquad \text{(C79)}$$

from the definition of the peculiar momentum, $\boldsymbol{p}_i\equiv m(\dot{\boldsymbol{r}}_i-\boldsymbol{\kappa}\cdot\boldsymbol{r}_i)$. This completes the derivation.

9. The projected shear stress

The derivation of Eq. (115) is reported here. The shear stress is projected by the second projection operator as

$$\mathcal{P}^0_2(t)\sigma_{xy}=\sum_{\boldsymbol{k}>0}\frac{\langle\sigma_{xy}n^*_{\boldsymbol{k}(t)}n_{\boldsymbol{k}(t)}\rangle}{N^2S^2_{k(t)}}n_{\boldsymbol{k}(t)}n^*_{\boldsymbol{k}(t)}. \qquad \text{(C80)}$$

Only the potential part of the shear stress $\sigma^{(\mathrm{pot})}_{xy}$ survives in the correlator of Eq. (C80), since the kinetic part vanishes due to $\langle p^x_i p^y_i\rangle_{\boldsymbol{p}}=0$. The remaining part is

$$\langle\sigma^{(\mathrm{pot})}_{xy}n^*_{\boldsymbol{k}(t)}n_{\boldsymbol{k}(t)}\rangle=\sum_i\langle x_iF^{(el)y}_i n_{\boldsymbol{k}(t)}n^*_{\boldsymbol{k}(t)}\rangle. \qquad \text{(C81)}$$

We utilize the relation well known in equilibrium statistical mechanics [36],

$$\langle AF^\lambda_i\rangle=-\left\langle A\frac{\partial U}{\partial r^\lambda_i}\right\rangle=-k_BT\left\langle\frac{\partial A}{\partial r^\lambda_i}\right\rangle, \qquad \text{(C82)}$$

which also holds in our formulation since the ensemble average $\langle\cdots\rangle$ is defined by an averaging with the Maxwell-Boltzmann

distribution, Eq. (C2). Then it is straightforward to show

$$\begin{aligned}
&\left\langle \sigma_{xy}^{(\mathrm{pot})} n^*_{\boldsymbol{k}(t)} n_{\boldsymbol{k}(t)} \right\rangle \\
&= -k_B T \sum_i \left\langle x_i \frac{\partial}{\partial y_i} [n_{\boldsymbol{k}(t)} n^*_{\boldsymbol{k}(t)}] \right\rangle \\
&= -k_B T k(t)^y \sum_i \left\langle i x_i e^{i\boldsymbol{k}(t)\cdot \boldsymbol{r}_i} n^*_{\boldsymbol{k}(t)} - i x_i e^{-i\boldsymbol{k}(t)\cdot \boldsymbol{r}_i} n_{\boldsymbol{k}(t)} \right\rangle \\
&= -k_B T k(t)^y \left\langle \frac{\partial n_{\boldsymbol{k}(t)}}{\partial k(t)^x} n^*_{\boldsymbol{k}(t)} + \frac{\partial n^*_{\boldsymbol{k}(t)}}{\partial k(t)^x} n_{\boldsymbol{k}(t)} \right\rangle \\
&= -k_B T k(t)^y \frac{\partial}{\partial k(t)^x} \left\langle n_{\boldsymbol{k}(t)} n^*_{\boldsymbol{k}(t)} \right\rangle \\
&= -N k_B T k(t)^y \frac{\partial S_{k(t)}}{\partial k(t)^x} \\
&= -N k_B T \frac{k(t)^x k(t)^y}{k(t)} \frac{\partial S_{k(t)}}{\partial k(t)}. \qquad \text{(C83)}
\end{aligned}$$

This, together with Eq. (C80), proves Eq. (115).

APPENDIX D: MISCELLANEOUS DETAILS ON THE NUMERICAL ANALYSIS

1. The isotropic approximation

The basics of the isotropic approximation and the derivation of its resulting equations, Eqs. (128) and (129), are reported here. Refer to CK [26] for further details.

The fundamental idea of the isotropic approximation is to reduce the dependence of the three-dimensional wave vector to its modulus. This is accomplished for the time correlators by the assumption of

$$\Phi_{\boldsymbol{q}}(t) \simeq \Phi_q(t), \qquad \text{(D1)}$$

$$\boldsymbol{H}_{\boldsymbol{q}}(t) \simeq \frac{\boldsymbol{q}(t)}{q(t)^2} \frac{d}{dt} \Phi_q(t). \qquad \text{(D2)}$$

In addition, there are polynomials of the wave vectors to be handled. They are approximated by their mean values with respect to the solid angles. For instance,

$$\begin{aligned}
\boldsymbol{q}(t)\cdot\boldsymbol{k}(t) &= \boldsymbol{q}\cdot\boldsymbol{k} - (\dot\gamma t)(q_x k_y + q_y k_x) + (\dot\gamma t)^2 q_x k_x \\
&\simeq (\boldsymbol{q}\cdot\boldsymbol{k})\left[1 + \tfrac{1}{3}(\dot\gamma t)^2\right], \qquad \text{(D3)}
\end{aligned}$$

$$k_x(t) k_y(t) = k_x[k_y - (\dot\gamma t) k_x] \simeq -\tfrac{1}{3}(\dot\gamma t) k^2. \qquad \text{(D4)}$$

Note that the anisotropic terms are neglected in the above approximations, which are the leading terms in the shear rate for the case $\dot\gamma t \ll 1$.

The modulus of the advected wave vector is approximated as

$$q(t)^2 = q^2 - 2(\dot\gamma t) q_x q_y + (\dot\gamma t)^2 q_x^2 \simeq \bar q(t)^2, \qquad \text{(D5)}$$

where $\bar q(t)$ is defined as

$$\bar q(t) \equiv q\sqrt{1 + \tfrac{1}{3}(\dot\gamma t)^2}. \qquad \text{(D6)}$$

Combining Eqs. (55) and (83), with the application of Eqs. (D1) and (D2), leads to

$$\frac{d^2}{dt^2}\Phi_q(t) = -\dot\gamma \frac{q_x q_y(t)}{q(t)^2}\frac{d}{dt}\Phi_q(t) - v_T^2 \frac{q(t)^2}{S_{q(t)}}\Phi_q(t) - \lambda_\alpha(t)\alpha_0 \frac{d}{dt}\Phi_q(t) - \dot\gamma \frac{q_x(t) q_y(t)}{q(t)^2}\frac{d}{dt}\Phi_q(t) - \int_0^t ds\, M_{\boldsymbol{q}}(t,s)\frac{d}{ds}\Phi_q(s). \qquad \text{(D7)}$$

The scalar memory kernel $M_{\boldsymbol{q}}(t,s)$, which is defined in Eq. (B5), reads

$$M_{\boldsymbol{q}}(t,s) = \frac{n v_T^2}{2q(s)^2}\int \frac{d^3\boldsymbol{k}}{(2\pi)^3}[(\boldsymbol{q}(t)\cdot\boldsymbol{k}(t))c_{k(t)} + (\boldsymbol{q}(t)\cdot\boldsymbol{p}(t))c_{p(t)}][(\boldsymbol{q}(s)\cdot\boldsymbol{k}(s))c_{k(s)} + (\boldsymbol{q}(s)\cdot\boldsymbol{p}(s))c_{p(s)}]\Phi_{k(s)}(t-s)\Phi_{p(s)}(t-s), \qquad \text{(D8)}$$

where Eqs. (103) and (99) are utilized. It is convenient to shift the integration variable in Eq. (D8) as $\boldsymbol{k} \to \boldsymbol{k}' \equiv \boldsymbol{k}(s)$, which leads to

$$M_{\boldsymbol{q}}(t,s) = \bar M_{\boldsymbol{q}(s)}(t-s), \qquad \text{(D9)}$$

where

$$\bar M_{\boldsymbol{q}}(\tau) \equiv \frac{n v_T^2}{2q^2}\int \frac{d^3\boldsymbol{k}}{(2\pi)^3}[(\boldsymbol{q}\cdot\boldsymbol{k})c_k + (\boldsymbol{q}\cdot\boldsymbol{p})c_p][(\boldsymbol{q}(\tau)\cdot\boldsymbol{k}(\tau))c_{k(\tau)} + (\boldsymbol{q}(\tau)\cdot\boldsymbol{p}(\tau))c_{p(\tau)}]\Phi_k(\tau)\Phi_p(\tau). \qquad \text{(D10)}$$

Application of Eqs. (D3), (D4), and (D5) to Eq. (D7) leads to Eq. (128), and application to Eq. (D10) leads to Eq. (129).

2. Discretization

The discretized form of the memory kernel on the one-dimensional spatial grid is given by

$$\begin{aligned}
\bar M_q(\tau) &= \frac{1}{32\pi^2}\frac{n v_T^2}{q^3}\left[1 + \frac{1}{3}(\dot\gamma\tau)^2\right]\int_0^\infty dk \int_{|q-k|}^{q+k} dp[(q^2+k^2-p^2)c_{\bar k(\tau)} + (q^2-k^2+p^2)c_{\bar p(\tau)}] \\
&\quad \times [(q^2+k^2-p^2)c_k + (q^2-k^2+p^2)c_p] k p \Phi_k(\tau)\Phi_p(\tau) \\
&\simeq \frac{n v_T^2}{32\pi^2}\frac{\Delta^5}{d^5}\frac{1}{\hat q^3}\left[1 + \frac{1}{3}(\dot\gamma\tau)^2\right]\sum_{\hat k}\hat k \Phi_k(\tau) {\sum_{\hat p}}' [(\hat q^2 + \hat k^2 - \hat p^2)c_{\bar k(\tau)} + (\hat q^2 - \hat k^2 + \hat p^2)c_{\bar p(\tau) a}] \\
&\quad \times [(\hat q^2 + \hat k^2 - \hat p^2)c_k + (\hat q^2 - \hat k^2 + \hat p^2)c_p]\hat p \Phi_p(\tau). \qquad \text{(D11)}
\end{aligned}$$

In the last step, the wave number is discretized as $qd = \Delta\hat{q}$, where Δ is the grid spacing and $\hat{q}$ is the discretized index of the wave number, $\hat{q} = (2m-1)/2$ ($m = 1,2,\ldots,M$), M being the number of grids. The summation with respect to $\hat{p}$ is restricted to those which satisfy the triangle inequality, i.e.,

$$\sum_{\hat{p}}{}' = \sum_{\hat{p}=|\hat{q}-\hat{k}|+1/2}^{\hat{p}=\hat{q}+\hat{k}-1/2}.$$

[1] W. Götze and L. Sjogren, Rep. Prog. Phys. **55**, 241 (1992).
[2] W. Götze, *Complex Dynamics of Glass-Forming Liquids. A Mode Coupling Theory* (Oxford, New York, 2009).
[3] K. Miyazaki, Bussei Kenkyu **88**, 621 (2007), in Japanese.
[4] W. van Megen and S. M. Underwood, Phys. Rev. Lett. **70**, 2766 (1993).
[5] W. van Megen and S. M. Underwood, Phys. Rev. E **49**, 4206 (1994).
[6] Y. Yang and K. A. Nelson, J. Chem. Phys. **104**, 5429 (1996).
[7] A. Meyer, J. Wuttke, W. Petry, O. G. Randl, and H. Schober, Phys. Rev. Lett. **80**, 4454 (1998).
[8] J. Wuttke, M. Ohl, M. Goldammer, S. Roth, U. Schneider, P. Lunkenheimer, R. Kahn, B. Ruffle, R. Lechner, and M. A. Berg, Phys. Rev. E **61**, 2730 (2000).
[9] J. Horbach and W. Kob, Phys. Rev. E **64**, 041503 (2001).
[10] G. Foffi, W. Götze, F. Sciortino, P. Tartaglia, and T. Voigtmann, Phys. Rev. E **69**, 011505 (2004).
[11] W. Kob and H. C. Andersen, Phys. Rev. Lett. **73**, 1376 (1994).
[12] A. Andreanov, G. Biroli, and A. Lefevre, J. Stat. Mech. (2006) P07008.
[13] B. Kim and K. Kawasaki, J. Phys. A **40**, F33 (2007).
[14] B. Kim and K. Kawasaki, J. Stat. Mech. (2008) P02004.
[15] T. H. Nishino and H. Hayakawa, Phys. Rev. E **78**, 061502 (2008).
[16] H. Jacquin and F. van Wijland, Phys. Rev. Lett. **106**, 210602 (2011).
[17] G. Szamel, Phys. Rev. Lett. **90**, 228301 (2003).
[18] G. Szamel, Prog. Theor. Exp. Phys. **2013**, 012J01 (2013).
[19] P. Mayer, K. Miyazaki, and D. R. Reichman, Phys. Rev. Lett. **97**, 095702 (2006).
[20] G. Biroli, J. P. Bouchaud, K. Miyazaki, and D. R. Reichman, Phys. Rev. Lett. **97**, 195701 (2006).
[21] H. Hayakawa and M. Otsuki, Prog. Theor. Phys. **119**, 381 (2008).
[22] W. T. Kranz, M. Sperl, and A. Zippelius, Phys. Rev. Lett. **104**, 225701 (2010).
[23] K. Suzuki and H. Hayakawa, submitted for publication (2013).
[24] M. Fuchs and M. E. Cates, Phys. Rev. Lett. **89**, 248304 (2002).
[25] K. Miyazaki and D. R. Reichman, Phys. Rev. E **66**, 050501(R) (2002).
[26] S.-H. Chong and B. Kim, Phys. Rev. E **79**, 021203 (2009).
[27] D. J. Evans and G. P. Morriss, *Statistical Mechanics of Nonequilibrium Liquids*, 2nd ed. (Cambridge University Press, Cambridge, 2008).
[28] M. Fuchs and M. E. Cates, J. Phys.: Condens. Matter **17**, S1681 (2005).
[29] P. J. Daivis and B. D. Todd, J. Chem. Phys. **124**, 194103 (2006).
[30] M. Fuchs and M. E. Cates, J. Rheol. **53**, 957 (2009).
[31] G. Szamel and H. Löwen, Phys. Rev. A **44**, 8215 (1991).
[32] T. Gleim, W. Kob, and K. Binder, Phys. Rev. Lett. **81**, 4404 (1998).
[33] G. Szamel and E. Flenner, Euro. Phys. Lett. **67**, 779 (2004).
[34] There is a subtle problem in defining the "random force" in the present formulation, as also pointed out in Ref. [30]. This issue is discussed in Sec. V.
[35] J. Zausch, J. Horbach, M. Laurati, S. U. Egelhaaf, J. M. Brader, T. Voigtmann, and M. Fuchs, J. Phys.: Condens. Matter **20**, 404210 (2008).
[36] J. P. Hansen and I. R. McDonald, *Theory of Simple Liquids*, 3rd ed. (Academic Press, London, 2006).
[37] S.-H. Chong, K. Suzuki, M. Otsuki, and H. Hayakawa, in preparation.
[38] K. Suzuki and H. Hayakawa, in *Slow Dynamics in Complex Systems*, edited by M. Tokuyama (AIP, New York, 2013).
[39] The problem discussed here for the "uncorrelated part" is avoided for the "correlated part" by the introduction of the rescaled static projection operator $\bar{\mathcal{P}}_t$ defined in Eq. (61).
[40] The resulting kinetic temperature is not divergent, since the density time correlator decays to 0 around $t \sim \dot{\gamma}^{-1}$ but is independent of α_0, i.e., unaffected by the strength of dissipation.
[41] K. Miyazaki, D. R. Reichman, and R. Yamamoto, Phys. Rev. E **70**, 011501 (2004).
[42] O. Henrich, F. Weysser, M. E. Cates, and M. Fuchs, Philos. Trans. R. Soc. A **367**, 5033 (2009).
[43] At the quantitative level, it is known that the isotropic approximation underestimates the effect of shearing. Hence, a more accurate approximation scheme is desirable for three-dimensional calculations.
[44] M. Fuchs, W. Götze, I. Hofacker, and A. Latz, J. Phys.: Condens. Matter **3**, 5047 (1991).
[45] T. Franosch, M. Fuchs, W. Götze, M. R. Mayr, and A. P. Singh, Phys. Rev. E **55**, 7153 (1997).
[46] N. K. Ailawadi, Phys. Rev. A **7**, 2200 (1973).
[47] N. V. Brilliantov and T. Pöschel, *Kinetic Theory of Granular Gases* (Oxford University Press, New York, 2010).
[48] S.-H. Chong, M. Otsuki, and H. Hayakawa, Prog. Theor. Phys. Suppl. **184**, 72 (2010).
[49] R. Kubo, M. Toda, and N. Hashitsume, *Statistical Physics II: Nonequilibrium Statistical Mechanics* (Springer, Berlin, 1995).
[50] T. S. Komatsu and N. Nakagawa, Phys. Rev. Lett. **100**, 030601 (2008).
[51] G. P. Morriss and D. J. Evans, Phys. Rev. A **39**, 6335 (1989).